SEISMIC ATTRIBUTES OF THE CLINTON INTERVAL RESERVOIR IN THE DOMINION EAST OHIO GABOR GAS STORAGE FIELD NEAR NORTH CANTON, OHIO

A thesis submitted in partial fulfillment of the requirements for the degree of Master of Science

By

DOMINIQUE HANEBERG-DIGGS

B.S., University of Cincinnati, 2012

2014

Wright State University

WRIGHT STATE UNIVERSITY
GRADUATE SCHOOL

December 11, 2014

I HEREBY RECOMMEND THAT THE THESIS PREPARED UNDER MY SUPERVISION BY Dominique Miguel Haneberg-Diggs ENTITLED Seismic attributes of the Clinton interval reservoir in the Dominion East Ohio Gabor gas storage field near North Canton, Ohio BE ACCEPTED IN PARTIAL FULFILLMENT OF THE REQUIREMENTS FOR THE DEGREE OF Master of Science.

Doyle R. Watts, Ph.D.
Thesis Director

David F. Dominic, Ph.D.
Chair, Department of Earth & Environmental Sciences

Committee on
Final Examination

Doyle R. Watts, Ph.D.

Ernest C. Hauser, Ph.D.

David F. Dominic, Ph.D.

Robert E. W. Fyffe, Ph.D.
Vice President for Research and
Dean of the Graduate School

ABSTRACT

Haneberg-Diggs, Dominique. M.S. Department of Earth & Environmental Sciences, Wright State University, 2014. Seismic Attributes of the Clinton interval Reservoir in the Dominion East Ohio Gabor Gas Storage Field near North Canton, Ohio.

Wright State University acquired two vibroseis-sourced seismic reflection lines over the Dominion East Ohio Gabor Gas Storage field near Canton, Ohio. The data were gathered over a fully charged reservoir within the Clinton interval. Seismic attributes were applied to the seismic data for interpretation. The seismic response of nearby wells was modeled for comparison with the seismic lines. Within the seismic data a gas shadow was observed. The gas shadow coincides with an area of high initial production of wells targeting the Clinton interval for production. The gas shadow is also associated with broadening of the Packer Shell sidelobe. Modelling of the seismic response of well API# 3416925010000 shows a broadening effect of the Packer Shell sidelobe similar to that seen in the seismic data. This broadening is also associated with low porosity, implying that broadening of the Packer Shell sidelobe is indicative of a poor hydrocarbon reservoir.

Table of Contents

Chapter 1: Introduction 1

1.1 Gas Shadows 5

1.2 Seismic Attributes 5

Chapter 2: Geology 7

2.1 Clinton interval 7

2.2 Stratigraphy and Depositional History 7

Chapter 3: Methods 10

3.1 Seismic Reflection 10

3.2 Attribute Analysis 11

3.3 Wavelet Extraction 12

3.4 Well Log Analysis 12

Chapter 4: Results 14

4.1 Amplitude 14

4.2 Average Frequency 24

4.3 Instantaneous Frequency 27

4.4 Wavelet Packet Transform 31

4.5 Well Log Modeling 35

4.5.1 Well API# 3407525308 35

4.5.2 Well API# 3415125102 42

4.5.3 Well API# 3416925010 48

4.5.4 Well API# 3415123662 55

4.5.5 Well API # 3416923438 59

4.5.6 Well API# 3416923437 63

4.5.7 Well API# 3416923352 67

4.5.8 Well API # 3416924931 71

4.6 Velocity Transition Zones 76

Chapter 5: Conclusions 77

References 80

Table of Figures

Figure 1. Location map of the study area showing the location of the wells used in relation to the seismic survey. 3

Figure 2. Initial gas production map of the area of the seismic survey. Note numbered receiver locations near the red (high initial production) portions of the map. After Bey (2012). 4

Figure 3. The extracted wavelet response from the east-west line. Note the wavelet is zero phase, so it has positive and negative time sidelobes. 15

Figure 4. Above is a selection of the east-west trending seismic section. The basal Packer Shell reflection is highlighted just above 500 ms. The primary positive time

sidelobe has been enclosed by a box at about 500 ms. The amplitude and shape of the sidelobe varies within the section. Note the broadening around CDP 4176 and CDP 4140.....18

Figure 5. Above is a selection of the north-south trending seismic section. The basal Packer Shell reflection is highlighted just above 500 ms. The primary positive time sidelobe has been enclosed by a box at about 500 ms. The amplitude and shape of the sidelobe varies within the section. Note the broadening of the sidelobe around CDP 2115 and CDP 2163. 19

Figure 6. Above is a selection of the east-west trending seismic section. The basal Packer Shell reflection is highlighted just above 500 ms as well as the top of the Cincinnati Group at about 575 ms. Attenuation due to the gas shadow effect can be seen within the box centered at CDP 4208. The gas is attenuating the Cincinnati Group in addition to its sidelobes. Note the lack of broadening of the positive time sidelobe of the Packer Shell within the highlighted area. 20

Figure 7. Above is a portion of the north-south trending seismic section. The basal Packer Shell reflection is highlighted just above 500 ms as well as the top of the Cincinnati Group at about 575 ms. Attenuation due to the gas shadow effect can be seen within the box centered at CDP 2133. The gas is attenuating the Cincinnati Group in addition to its sidelobes. Note the lack of broadening of the positive time sidelobe of the Packer Shell within the highlighted area. 21

Figure 8. Above is a portion of the north-south trending seismic line. Highlighted at about 585 ms is an event within the Cincinnati Group that shows downward bowing structure. This structure appears nearly directly below the area of attenuation due to gas

at CDP 2133. Gas effects are likely not the cause of this structure as underlying events would be clearly affected. 22
Figure 9. Above is a portion of the east-west trending seismic line. Highlighted at about 585 ms is an event within the Cincinnati Group that shows downward bowing structure. This structure does not show any indication of being associated with a gas reservoir and is likely true structure.....23
Figure 10. Above is a portion of the average frequency plot of the east-west trending seismic section. Highlighted is an area of low average frequency centered at CDP 4208. This area of low frequency is caused by attenuation from the Clinton interval gas reservoir, located just beneath the Packer Shell at about 500 ms. 25
Figure 11. Above is a portion of the average frequency plot of the east-west trending seismic section. Highlighted are areas of low average frequency. The area around CDP 2149 is very close to an area of attenuation believed to be caused by gas within the Clinton interval. The other areas of low frequency have fewer indications of the presence of gas. 26
Figure 12. . Above is a portion of the instantaneous frequency plot of the east-west trending seismic section. Highlighted is an area where coherency is interrupted within the Clinton interval. This along with the complex behavior below is associated with the effects of gas. 29
Figure 13. Above is a portion of the instantaneous frequency plot of the north-south trending seismic section. Highlighted is an area where coherency is interrupted within the Clinton interval. This along with the complex behavior below is associated with the effects of gas. 30

Figure 14. Frequency content of the second wavelet packet transform scale.....31

Figure 15. Above is a portion of the wavelet packet transform of the east-west trending line. The removal of frequencies centered around 70 Hz associated with a gas reservoir within the Clinton interval is highlighted. 33

Figure 16. Above is a portion of the wavelet packet transform of the north-south trending line. The removal of frequencies centered around 70 Hz associated with a gas reservoir within the Clinton interval is highlighted. 34

Figure 17. Above is a section of well API# 3407525308. The synthetic trace is unreliable due to the poor quality of the desnity log within the Queenston. 38

Figure 18. Above is a section of well API# 3407525308 with synthetic traces, gamma ray log, density log, and caliper log. Variablility in the caliper log within the Queenston indicates washouts from drilling. These washouts correlate with low spikes in the density log that are skewing the synthetic traces.....39

Figure 19. Above is the Packer Shell through the Medina in well API# 3407525308. Shown from left to right are the synthetic traces, gamma ray log, seismic velocity log, and density log. 40

Figure 20. Isolation model of the Packer Shell in well API# 3407525308. The high amplitude through from the basal Packer Shell is present along with the sidelobe.....41

Figure 21. Isolation model of the Upper Cabot Head through Medina Sandstone in well API# 3407525308. A trough is made in the upper portion of this interval and a peak is made in the lower portion. 42

Figure 22. Above is a section of well API# 3415125102 with synthetic traces, gamma ray log, density log, and velocity log. There is no sign of broadening of the positive time basal Packer Shell sidelobe. 45

Figure 23. Above is the Packer Shell through the Medina sandstone in well API# 3415125102. Shown from left to right are the synthetic traces, gamma ray log, seismic velocity log, and density log. 46

Figure 24. Isolation model of the Packer Shell in well API# 3415125102. The high amplitude through from the basal Packer Shell is present along with the sidelobe. 47

Figure 25. Isolation model of the Upper Cabot Head through Medina Sandstone in well API# 3415125102. A trough is made in the upper portion of this interval and a peak is made in the lower portion. 48

Figure 26. Above is a section of well API# 3416925010 with synthetic traces, gamma ray log, density log, and velocity log. This log does show broadening of the positive time basal Packer Shell Sidelobe possibly caused by the Clinton interval. 50

Figure 27. Above is a section of well API# 3416925010 with synthetic traces and gamma ray, density, and caliper logs. Variablility in the caliper log within the Queenston indicates washouts from drilling. These washouts correlate with low spikes in the density and velocity logs that are skewing the synthetic traces. 51

Figure 28. Above is the Packer Shell through the Medina Sandstone in well API# 3416925010. Shown from left to right are the synthetic traces, gamma ray log, seismic velocity log, and density log. Broadening of the Packer Shell sidelobe can be seen extending past the surface of the Lower Cabot Head. 52

Figure 29. Isolation model of the Packer Shell in well API# 3416925010. The high amplitude through from the basal Packer Shell is present along with the sidelobe.....53
Figure 30. Isolation model of the Upper Cabot Head through Medina Sandstone in well API# 3416925010. This interval creates a trough in the middle with positive events at the top and bottom. 54
Figure 31. Isolation model of the Packer Shell through Medina Sandstone in well API# 3416925010. This interval creates a trough in the middle with positive events at the top and bottom. 55
Figure 32. Above is a portion of the synthetic traces and gamma ray, density and velocity logs from well API# 3415123662. This well does not extend deep enough to reveal the effects of the Cincinnati Group. This well does not show signs of broadening in the positive time Packer Shell sidelobe. 57
Figure 33. Isolation model of the Packer Shell in well API# 3415123662. The high amplitude through from the basal Packer Shell is present along with the sidelobe.....58
Figure 34. Isolation model of the Upper Cabot Head through Medina Sandstone in well API# 3415123662. This interval creates a trough in the middle with positive events at the top and bottom. 59
Figure 35. Above is a portion of the synthetic traces and gamma ray, density and velocity logs from well API # 3416923438. This well does not extend deep enough to reveal the effects of the Cincinnati Group. This well does not show signs of broadening in the positive time Packer Shell sidelobe. 61
Figure 36. Isolation model of the Packer Shell in well API# 3416923438. The high amplitude through from the basal Packer Shell is present along with the sidelobe.....62

Figure 37. Isolation model of the Upper Cabot Head through Medina Sandstone in well API# 3416923438. This interval creates a trough in the middle with positive events at the top and bottom. 63

Figure 38. Above is a portion of the synthetic traces and gamma ray, density and velocity logs from well API# 3416923437. This well does not extend deep enough to reveal the effects of the Cincinnati Group. This well does not show signs of broadening in the positive time Packer Shell sidelobe. 65

Figure 39. Isolation model of the Packer Shell in well API# 3416923437. The high amplitude through from the basal Packer Shell is present along with the sidelobe.....66

Figure 40. Isolation model of the Upper Cabot Head through Medina Sandstone in well API# 3416923437. This interval creates a trough in the middle with positive events at the top and bottom. 67

Figure 41. Above is a portion of the synthetic traces and gamma ray, density and velocity logs from well API# 3416923352. This well does not extend deep enough to reveal the effects of the Cincinnati Group. This well does not show signs of broadening in the positive time Packer Shell sidelobe. 69

Figure 42. Isolation model of the Packer Shell in well API# 3416923352. The high amplitude through from the basal Packer Shell is present along with the sidelobe.....70

Figure 43. Isolation model of the Upper Cabot Head through Medina Sandstone in well API# 3416923352. This interval creates a trough in the middle with positive events at the top and bottom. 71

Figure 44. Above is a section of the synthetic traces and gamma ray, density and velocity logs from well API # 3416924931. The synthetic traces show unusual behavior in the Packer Shell-Clinton interval. 73

Figure 45. Above is a section of the synthetic traces and gamma ray, density and caliper logs from well API # 3416924931. Variability in the caliper log indicates washouts. Washouts cause bad readings in the density and velocity logs. This is likely causing the unusual behavior in the synthetic trace from the Packer Shell-Clinton interval. 74

Figure 46. Above is the Packer Shell through the Medina Sandstone in well API# 3416925010. Shown from left to right are the synthetic traces, gamma ray log, seismic velocity log, and density log. 75

Acknowledgements

I thank Precision Geophysical for data acquisition, seismic Earth Resources Technology for processing the data, CGG Veritas for the donation of the Hampson-Russell software, and the Ohio Geological Survey for the donation of well logs and support.

Chapter 1: Introduction

In the late 1800s oil and gas exploration began taking place in northeastern Ohio. One of the oil and gas targets became known by drillers as the "Clinton interval." The Clinton interval is a Lower Silurian deltaic deposit consisting of interbedded sandstones and shales. Over the past century, since the exploration began, many wells were abandoned as reservoirs were depleted. Some of these depleted reservoirs have been converted into gas storage fields by the Dominion East Ohio gas company. Dominion East Ohio has a gas storage field, near North Canton, Ohio, called the Gabor gas storage field (Figure 1). This gas storage field is being studied by Wright State University for possible natural microtremor events associated with the presence of hydrocarbon (Goertz et. al. 2011). To acquire velocity information in the vicinity of the reservoir, Wright State University collected two vibroseis, 2D seismic reflection surveys. The lines collected were oriented roughly east-west and north-south (Figure 1). My interpretation of the lines is accomplished using logs from nearby wells.

A past study (Bey, 2012) of the seismic reflection data collected by Wright State University identified attenuation of reflectors beneath the Clinton interval, attributed to gas shadows. As further evidence of association with reservoir properties, the features were compared to a map of initial production (Figure 2). In addition the study identified complex behavior of seismic reflection wavelets at the Clinton interval. The cause of the complex behavior remains largely speculative. With the aid of seismic attributes and

nearby well logs, I investigate the possibility of further effects of the presence of gas within the Clinton interval, as well as the potential cause of the complex behavior at the Clinton interval.

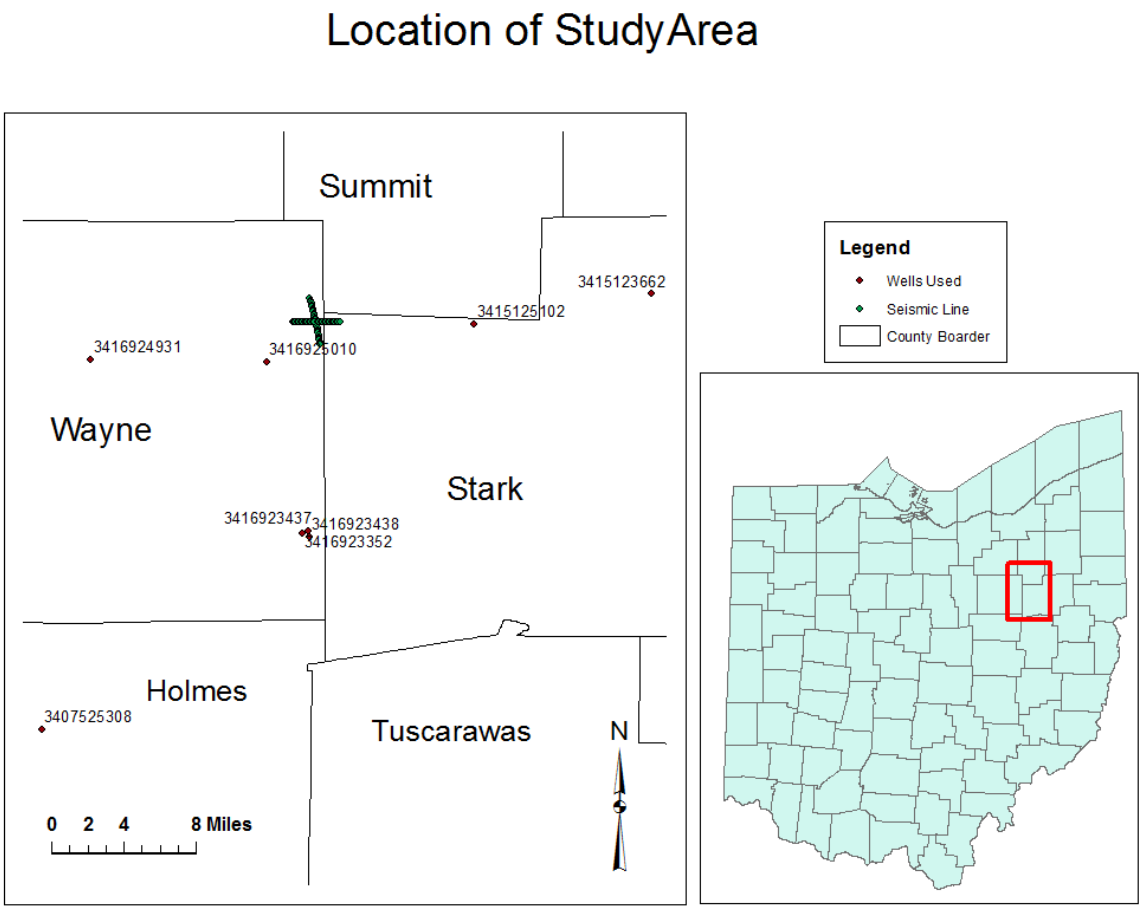

Figure 1. Location map of the study area showing the location of the wells used in relation to the seismic survey.

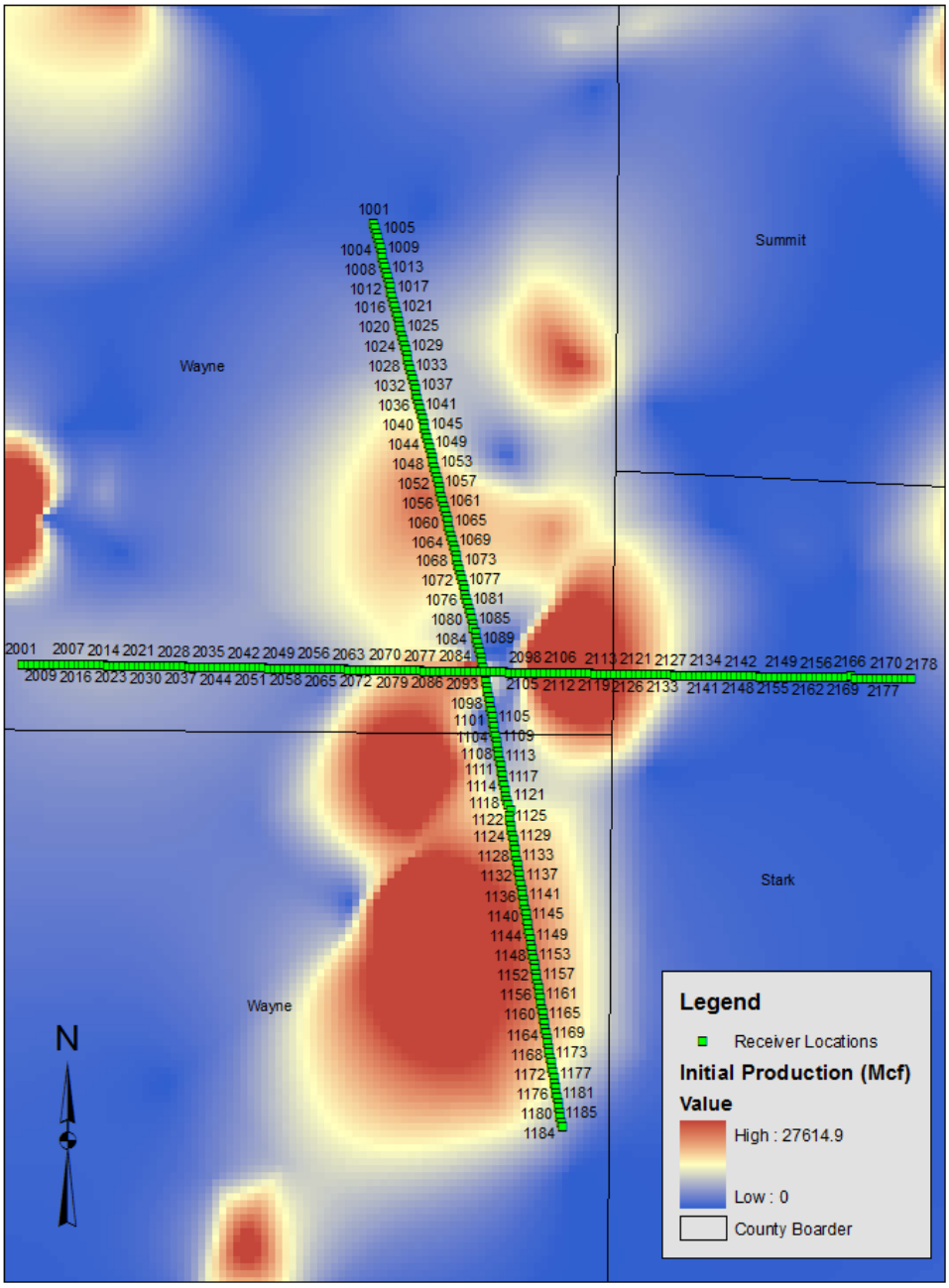

Figure 2. Initial gas production map of the area of the seismic survey. Note numbered receiver locations near the red (high initial production) portions of the map. After Bey (2012).

1.1 Gas Shadows

A gas shadow, also known as a low-frequency shadow, represents attenuation of high frequency energy occurring directly beneath a gas accumulation (Tanner *et. al*., 1979). In the seismic sections considered here, I find laterally continuous events whose coherency is being interrupted by this attenuation. The mechanism for attenuation by gas filled reservoirs remains unclear. It has been proposed that gas shadows could be caused by stacking or data processing issues, and/or intrinsic attenuation by the reservoir and surrounding geology (Ebrom, 2004). Stacking can be made difficult by gas accumulations because gas modifies the velocity at which seismic energy propagates through a formation. Stacks are dependent upon velocity corrections that cannot compensate for this abrupt local change in velocity. Stacking issues may not be the only cause of the attenuation. There is likely intrinsic attenuation by gas filled reservoirs analogous to the absorption of sound by foam. In addition to the attenuation of high frequencies, there may be amplification and/or addition of low frequencies (Castagna, 2003). Despite uncertainties as to the physical cause of the gas shadow, the empirical relationship between them and gas accumulations remains solid.

1.2 Seismic Attributes

Seismic attributes are quantities derived from basic seismic reflection data, including time, amplitude, frequency, and attenuation, as examples that allow for additional methods for presenting the data (Brown, 1996). There are limitless ways to mathematically derive values from seismic data, but some attributes are more useful than others. Not only does utility vary but seemingly different attributes can even be exactly identical to others in the sense that they convey exactly the same information (Brown,

2007). Correlations can be made between seismic attributes and phenomena in the subsurface, however in many cases, their geologic causes remain unknown (Sheriff, 2002). Assuming an attribute has any physically meaningful applications may lead an interpreter astray. Increasingly, as more trends are identified, combinations of attributes can overcome this glaring pitfall (Tanner, 2001). Hundreds of attributes have been defined that highlight features and anomalies that otherwise may be difficult to identify, like gas shadows (Chen and Sidney, 1997).

Chapter 2: Geology

2.1 Clinton interval

The Clinton interval is a Silurian deltaic deposit in the subsurface of northeastern Ohio. The interval was originally miscorrelated with the Clinton Group of New York, but was later found to be stratigraphically equivalent to the Medina Group sandstones of western New York (Brett et al, 1990; Castle, 1998). In Ohio, it has been traditionally divided by drillers into three units, the Stray, Red, and White Clinton since 1887 (Pepper, 1953). The names given by drillers were arbitrarily based on appearance and occurrence to drillers (Knight, 1969). The distinction is important because the Stray Clinton is not known to contain hydrocarbons, whereas the Red and White Clinton potentially are gas and oil reservoirs. These units can be identified in well logs by examining gamma ray responses at the depths of the Clinton interval. In the gamma ray log the White Clinton is coarsening upward, the Red Clinton is coarsening upward, and the Stray Clinton is fining upward (Ryder, 2004).

2.2 Stratigraphy and Depositional History

The units of interest in this study range from Ordovician to Lower Silurian. The Cincinnati Group is the lowermost formation considered in this study. The Cincinnati Group overlies the Utica Formation directly (Ryder et al, 2012). The formation consists of light gray shales predominantly with some interbedded siltstones and limestones.

These sediments represent shallow marine and intertidal environments as the Taconic foreland basin was filling with a prograding wedge of sediment sourced by the concurrently forming Taconic Mountains (Castle, 2001). The older portion of the formation is almost exclusively shale. As the basin filled, conditions became favorable for the siltstones and limestones to be included with the shales (Coogan, 1996).

The youngest formation of the Ordovician sourced by the Taconic Mountains is the Queenston Shale. This unit is predominantly shale within the clastic wedge sourced by the Taconic orogeny. By the late Ordovician, the clastic wedge had prograded and thickened, making the environment shallower. This shallow environment allowed for the iron within the Queenston to be oxidized leaving the shale red in appearance. The Queenston is separated from the Lower Silurian units by the Cherokee Unconformity.

Marking the beginning of the Silurian Period the Queenston is overlain unconformably by more clastic deposits sourced by the Taconic Orogeny. The Medina Sandstone was the first unit to be deposited, representing the transgressing shoreline. As relative sea level rose further, the lower tongue of the Cabot Head Shale was deposited. Next there was a series of smaller scale regressions and transgressions evident in the stratigraphy of the Clinton interval.

The oldest unit within the Clinton interval is the White Clinton. The White Clinton shows a gradual regression from the high stand associated with the Cabot Head. As a result of this regression it can be characterized by a coarsening upward sequence. Abruptly above the White Clinton, the initial shale of the Red Clinton indicates a rapid transgression. This transgression is the beginning of two coarsening upward sequences

within the Red Clinton. Above the Red Clinton, the Stray Clinton is characterized by a fining upward sequence grading into the upper tongue of the Cabot Head Shale.

All of the aforementioned units are part of the Queenston Delta clastic wedge. The Stray Clinton grading into the Upper Cabot Head shows the beginning of a transgressive sequence. The Dayton Limestone, the uppermost unit in this study, is evidence for further transgression. It is deposited directly on the Upper Cabot Head with some interbedding. Drillers refer to the more formal Dayton Limestone as the Packer Shell.

Chapter 3: Methods

3.1 Seismic Reflection

Wright State University acquired two, 2D, seismic reflection surveys atop Dominion East Ohio's Gabor gas storage field (Figure 2). The field is located about 38 miles due south of Cleveland, Ohio (Figure 1). The two lines were oriented nearly north-south and east-west, containing 185 and 178 recording stations respectively. Each station, spaced 82.5 feet apart, contained a geophone array. Each geophone array comprised six individual geophones, spaced about 15 feet, along the line, in an effort to reduce the influence of surface waves. The survey was sourced by a vibroseis truck supplied by Precision Geophysical performing two sweeps from 8-128 Hz. The first sweep acts to compact underlying soil to enhance the coupling of the vibroseis truck to the soil. The second sweep was recorded for 12 seconds by an Aram Aries recording system at a 2 ms sample rate. The data were professionally processed by Tom McGovern of Seismic Earth Resources Technology. Both pre-stack and post-stack migrated data were supplied for analysis. The data were analyzed using Hampson-Russell. Color plots are widely used for interpretation of amplitude data however; in this case the variable area, solid black fill of positive amplitudes was also used to display the data as it accentuates subtle features.

3.2 Attribute Analysis

Hampson-Russell was the primary software package used for attribute calculation, analysis and display. Bey (2012) used Hampson-Russell to specifically apply instantaneous frequency and phase, and average frequency to the interpretation of the data. These attributes were additionally used to compare the gas shadow to the broadening of the Packer Shell sidelobe.

The other program used for attribute application and analysis is the seismic processing package, ProMAX. ProMAX was used to apply a wavelet packet transform (Deighan, 1997) to the data. This process transforms the data to show frequency dependence at points in time. The specific wavelet applied was a coiflet (Coifman et al., 1989). Coiflets only bear a superficial resemblance to a seismic pulse, but they facilitate a transform which isolates the data simultaneously in time and frequency. The time section is divided into four scales, each condensing the full seismic section to 512 samples. The first scale is where low frequencies are present, and each subsequent scale contains higher frequencies. The frequencies in the second scale are centered around 70 Hz. After this scale the frequencies are too high for the scales to yield data meaningful to this study. These data were kept in ProMAX for analysis.

These attributes were chosen for their ability to indicate a relationship to a gas filled reservoir. The attribute data were then compared to a map of initial production from Bey, 2012. Initial production data from wells the produced from only the Clinton interval were plotted in ArcGIS. Then the nearest neighbor function was used to interpolate between wells filling the map. The map was then compared to the seismic

line locations. This comparison supplied and additional line of evidence of the presence of gas at the locations where the attributes were affected.

3.3 Wavelet Extraction

ProMAX was also used to extract an appropriate source wavelet for modeling. As the source signature propagates deeper into the earth, its representative wavelet changes as a result of general increases in velocity with depth and absorption of high frequencies. ProMAX is able to extract an average wavelet from any given trace, or collection of traces. To attain an improved average, the option is given to use the minimum entropy deconvolution (MED) method. This method transforms spectral data from the average wavelet within a specific two way travel time window. The time of this investigation is centered on 500 ms. Consequently the wavelet most appropriate for synthetic trace modeling was extracted from 400 to 600 ms on both the north-south and east-west seismic lines.

3.4 Well Log Analysis

Well logs from the vicinity of the seismic reflection survey were supplied by the Ohio Geological Survey. To quantify proximity to the seismic lines, both the lines and the wells were mapped in ArcGIS. Wells were selected that fully penetrate the Clinton interval and have both sonic and density logs. All of the logs selected were digitized using NeuraLog and were loaded into Hampson-Russell for analysis.

Driller's logs were used to find approximate depths of formations. Digitized gamma ray logs were used to refine the driller's formation picks. The Clinton interval has traditionally been divided into three subintervals, the Stray, Red, and White. Kelch (1985) first observed the gamma ray signature reflecting the sequence stratigraphic

interpretation of the units. The White Clinton was found to be a coarsening upward sequence, followed by the Red Clinton as another coarsening upward sequence, and lastly the Stray Clinton is characterized by a fining upward sequence. Interpreted with gamma ray logs, the White Clinton is seen, from bottom to top, as a generally lowering response, followed by the Red Clinton as another generally lowering response, and that is capped with the Stray Clinton as a generally rising response. The gamma ray logs respond to the amount of clay minerals in the formation. The more clay, the finer grained the formation, and the higher the gamma ray response.

Sonic and density logs, additionally, were used to calculate the acoustic impedance. The acoustic impedance was used to calculate the reflection coefficients of the borehole. These reflection coefficients were convolved with the extracted wavelet creating a synthetic trace, representing a model of the seismic response of the strata in the well. This model is most accurate from 400 to 600ms as this is the interval where the wavelet was extracted. Within this time window, the synthetic traces were used to identify reflectors in the seismic sections.

Additional models were made with logs that were manually edited to isolate intervals of interest. Henceforth these models will be described as isolation models. The top and bottom of the intervals of interest were selected. Then the values at those points in the sonic and density logs were used to fill to the top and bottom of the logs. The sonic and density logs were edited such that when the reflection coefficients were convolved with the extracted wavelet, the only response is from the interval of interest. The intervals isolated were the Packer Shell, and the Upper Cabot Head through the Medina.

Chapter 4: Results

4.1 Amplitude

The wavelet extracted from the east-west trending seismic section is zero phase, as it was sourced by Vibroseis (Figure 3). The wavelet extracted from the north-south line is also zero phase and indistinguishable from the east-west line.

Both of the seismic lines show the basal Packer Shell reflection as a strong negative signal at about 490 ms (Figures 4 & 5). The Packer Shell reflection is very continuous, and exhibits little variation. Although the amplitude does vary slightly throughout, it does have lower amplitude above the gas shadow of Bey (2012). The primary positive sidelobe of the Packer Shell reflection is seen centered around 500 ms (Figures 4 & 5).

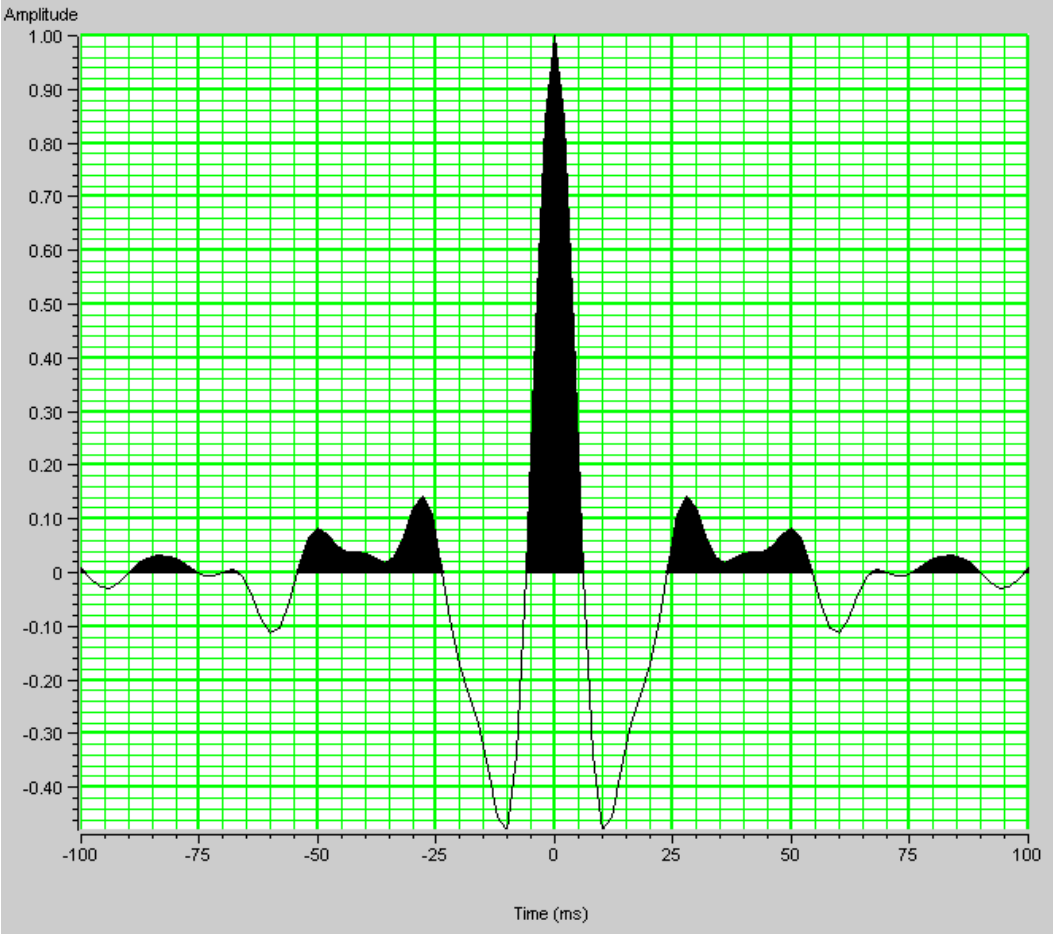

Figure 3. The extracted wavelet response from the east-west line. Note the wavelet is zero phase, so it has positive and negative time sidelobes.

In some areas, the sidelobe of the Packer Shell shows modification in the form of broadening toward greater times. This modification is seen at various CDP's on both sections at about 505 ms. The sidelobe appears to be broadening, or lengthening up to 15 ms extra, past 510 ms. The most notable occurrence of this is in the east-west line is between CDPs 4162 and 4194 (Figure 4). This broadening effect can also be seen in the north-south line between CDPs 2156 and 2189, as well as CDPs 2112 to 2122 (Figure 5).

The first reflection event, below the basal Packer Shell reflector, is from the top of the Cincinnati Group. Here, there are limestones interbedded with calcareous shales and

siltstones. The top of the Cincinnati Group creates a small positive amplitude event at about 575ms (Figures 4 & 5). The event is traceable throughout the section. The negative time sidelobes of the Cincinnati Group along with parts of the positive time sidelobes of the Packer Shell are attenuated in the east-west section between CDPs 4200 and 4217 at between 500 and 600 ms (Figure 4).

Although somewhat less apparent than attenuation in the east-west line, attenuation is present in the north-south line between CDPs 2124 and 2141, at the same time window (Figure 7). In addition, more attenuation can be seen between CDPs 2086 to 2108 although much less apparent than the other location in the north-south line.

There appears to be a relationship between gas shadows and broadening of the Packer Shell side lobe. Broadening only occurs above the flanks of the gas shadows, but never directly above the gas shadow. Broadening could be geologic in nature, or it could be a related to the presence or absence of gas. I expect that if a new seismic line were to be recorded over the reservoir after depletion, broadening of the positive time sidelobe of the basal Packer Shell would not be present where I currently observe the effects of gas. This implies broadening is a result of geology that indicates favorable conditions for a gas reservoir.

In both sections, attenuation of high frequency content of reflection events immediately beneath the Clinton interval is interpreted to be the result of gas shadows. Examples of this can be seen centered around CDP 4208 in Figure 6, and around CDP 2133 in Figure 7. This attenuation immediately beneath the Clinton interval is likely the result of gas accumulation. I not only know the Clinton interval is used as the gas storage

reservoir, but also that the reservoir was fully charged at the time of data acquisition. I find that in comparison to the map of initial production, the gas shadows correlate with regions of high initial gas production in the Clinton interval. This association adds confidence to the interpretation of gas causing the observed attenuation.

Another response that I find in the north-south section is at about 585 ms. Here between CDPs 2066 and 2166, the reflector from the top of the Cincinnati Group has subtle depressions or sags up to 20 ms deeper than usual (Figure 8). At the affected CDPs, the Packer Shell reflection is coherent, but it's negative time sidelobes, along with the positive sidelobes of the Cincinnati Group are attenuated.

The CDP range that the subtle depressions at the top of the Cincinnati Group occurs makes it tempting to interpret this as an effect of a gas filled reservoir. The depression in at the top of the Cincinnati Group shown in the north-south line (Figure 8) occurs directly beneath the attenuation from the gas reservoir. Sandstones whose pores contain high amounts of gas will have a lower density and also a lower seismic velocity because gas has a lower density and a lower seismic velocity than that of the water or oil that would otherwise be there. The lower velocity can distort an image by shifting a reflection to a later time, known as a velocity pull down. In order for this to actually be a velocity effect, the underlying events would also need to be effected. This is why the temptation to link this apparent effect to the gas shadow is likely wrong. There is no indication of underlying reflections being altered. Additionally, there is a similar structure in the east-west line that has no indication of the presence of gas (Figure 9).

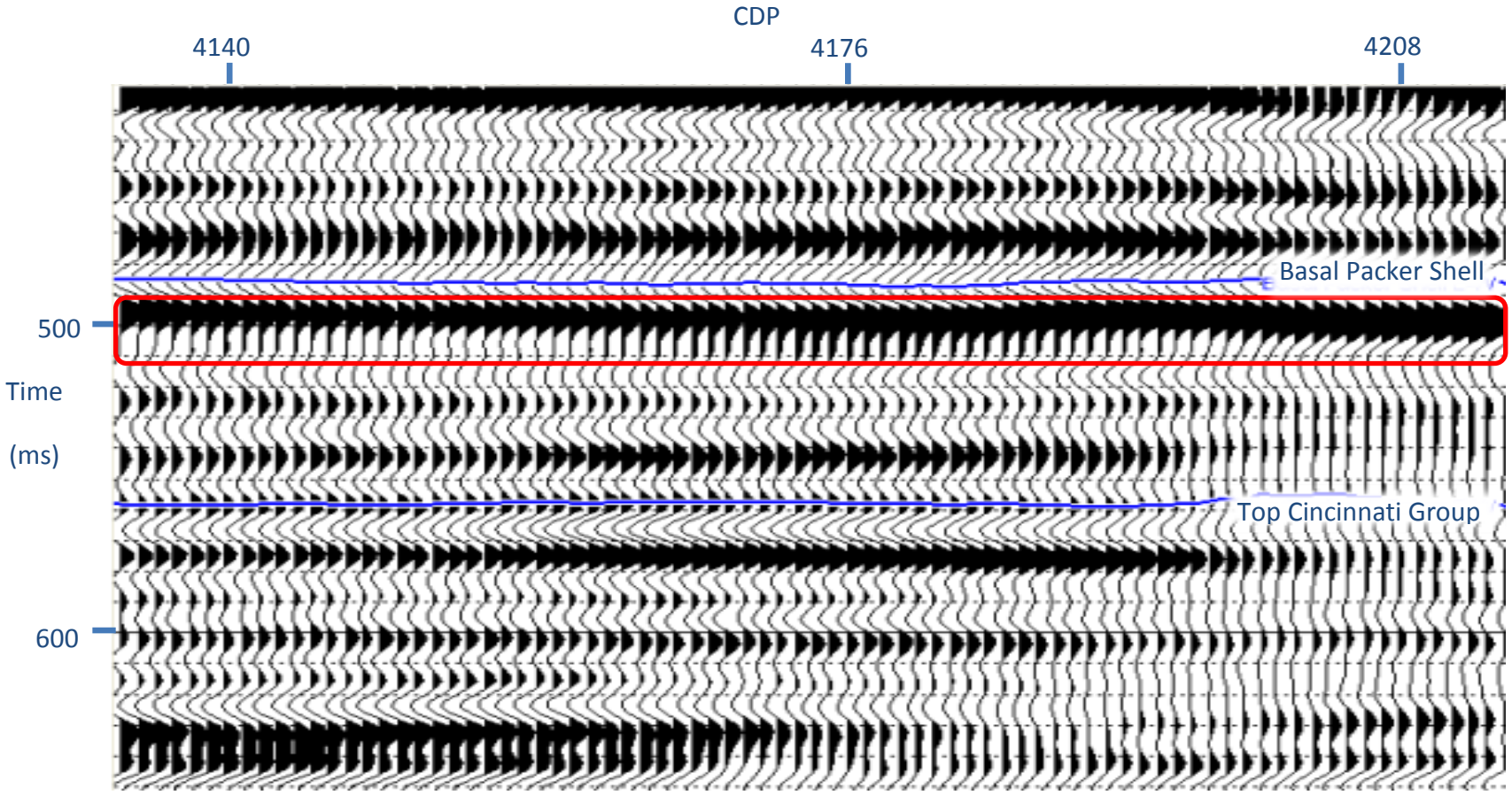

Figure 4. Above is a selection of the east-west trending seismic section. The basal Packer Shell reflection is highlighted just above 500 ms. The primary positive time sidelobe has been enclosed by a box at about 500 ms. The amplitude and shape of the sidelobe varies within the section. Note the broadening around CDP 4176 and CDP 4140.

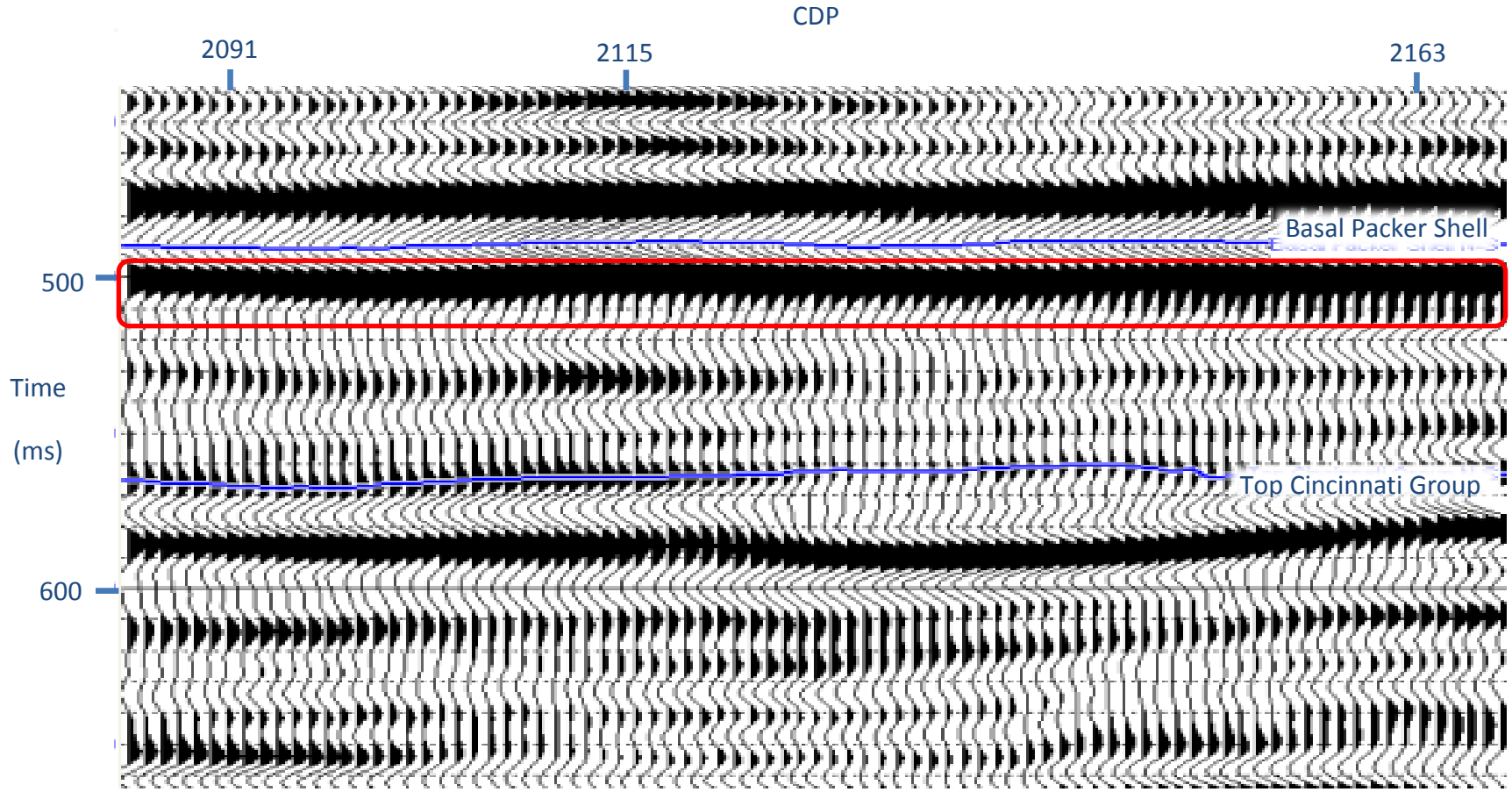

Figure 5. Above is a selection of the north-south trending seismic section. The basal Packer Shell reflection is highlighted just above 500 ms. The primary positive time sidelobe has been enclosed by a box at about 500 ms. The amplitude and shape of the sidelobe varies within the section. Note the broadening of the sidelobe around CDP 2115 and CDP 2163.

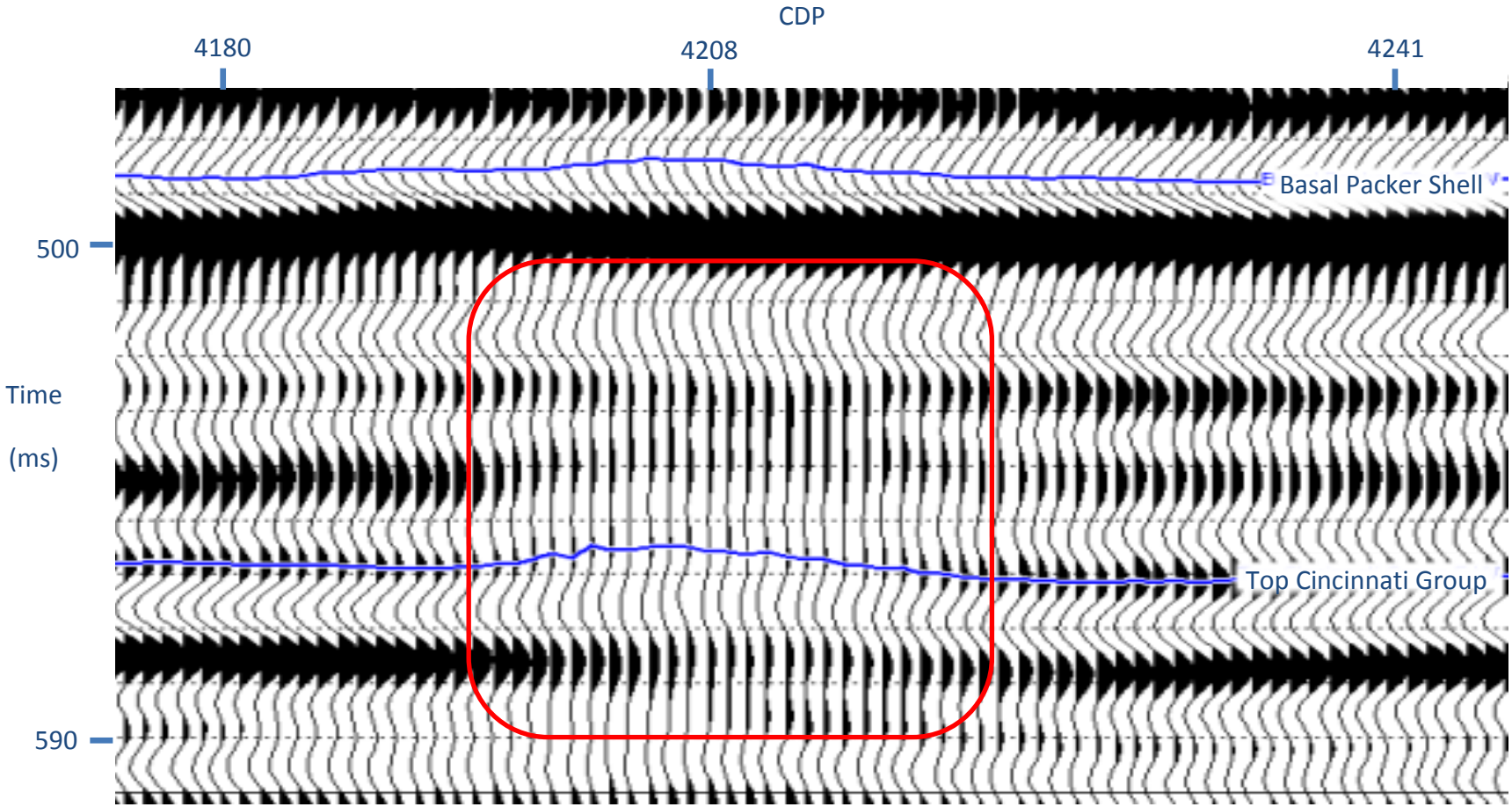

Figure 6. Above is a selection of the east-west trending seismic section. The basal Packer Shell reflection is highlighted just above 500 ms as well as the top of the Cincinnati Group at about 575 ms. Attenuation due to the gas shadow effect can be seen within the box centered at CDP 4208. The gas is attenuating the Cincinnati Group in addition to its sidelobes. Note the lack of broadening of the positive time sidelobe of the Packer Shell within the highlighted area.

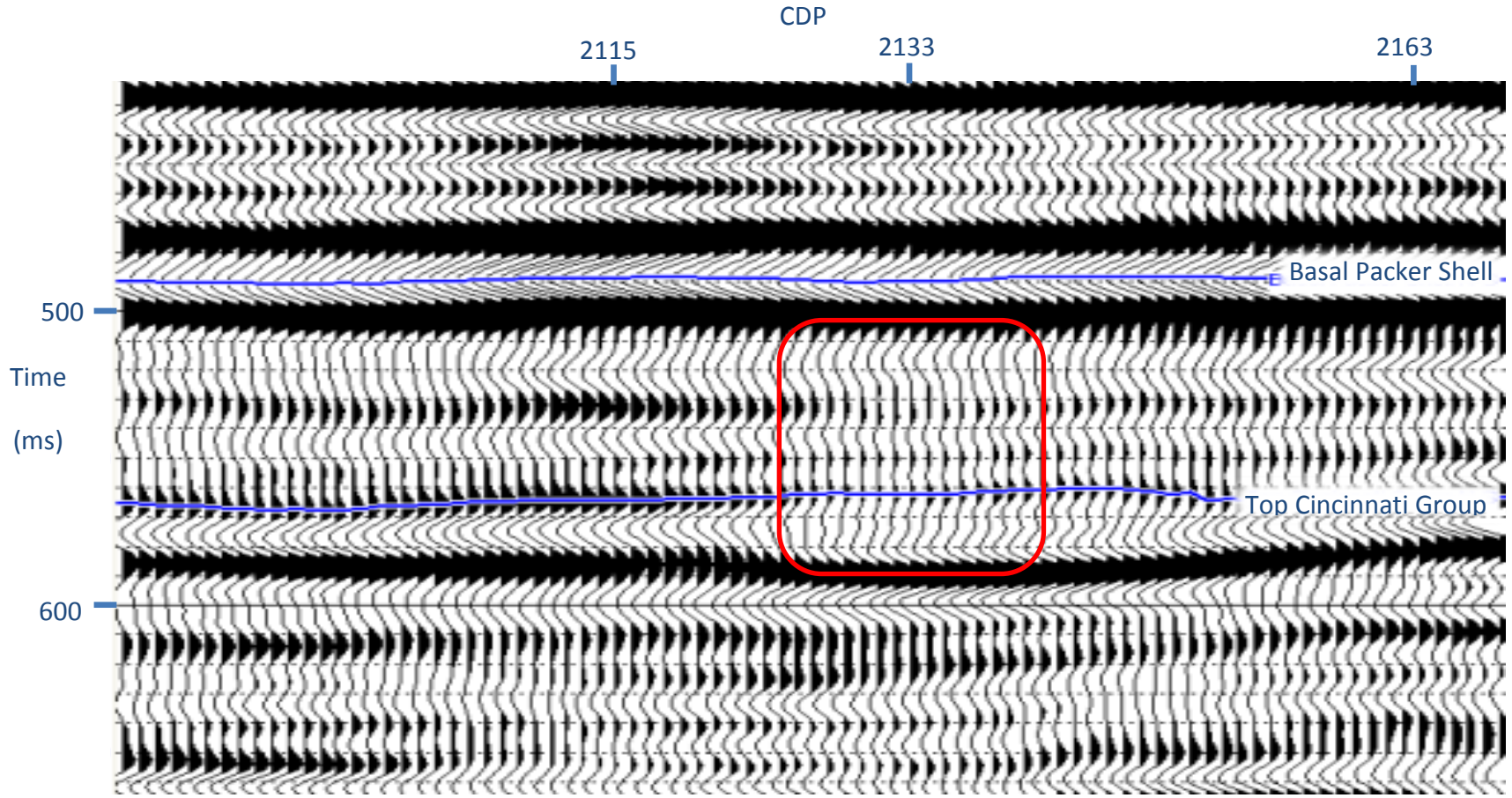

Figure 7. Above is a portion of the north-south trending seismic section. The basal Packer Shell reflection is highlighted just above 500 ms as well as the top of the Cincinnati Group at about 575 ms. Attenuation due to the gas shadow effect can be seen within the box centered at CDP 2133. The gas is attenuating the Cincinnati Group in addition to its sidelobes. Note the lack of broadening of the positive time sidelobe of the Packer Shell within the highlighted area.

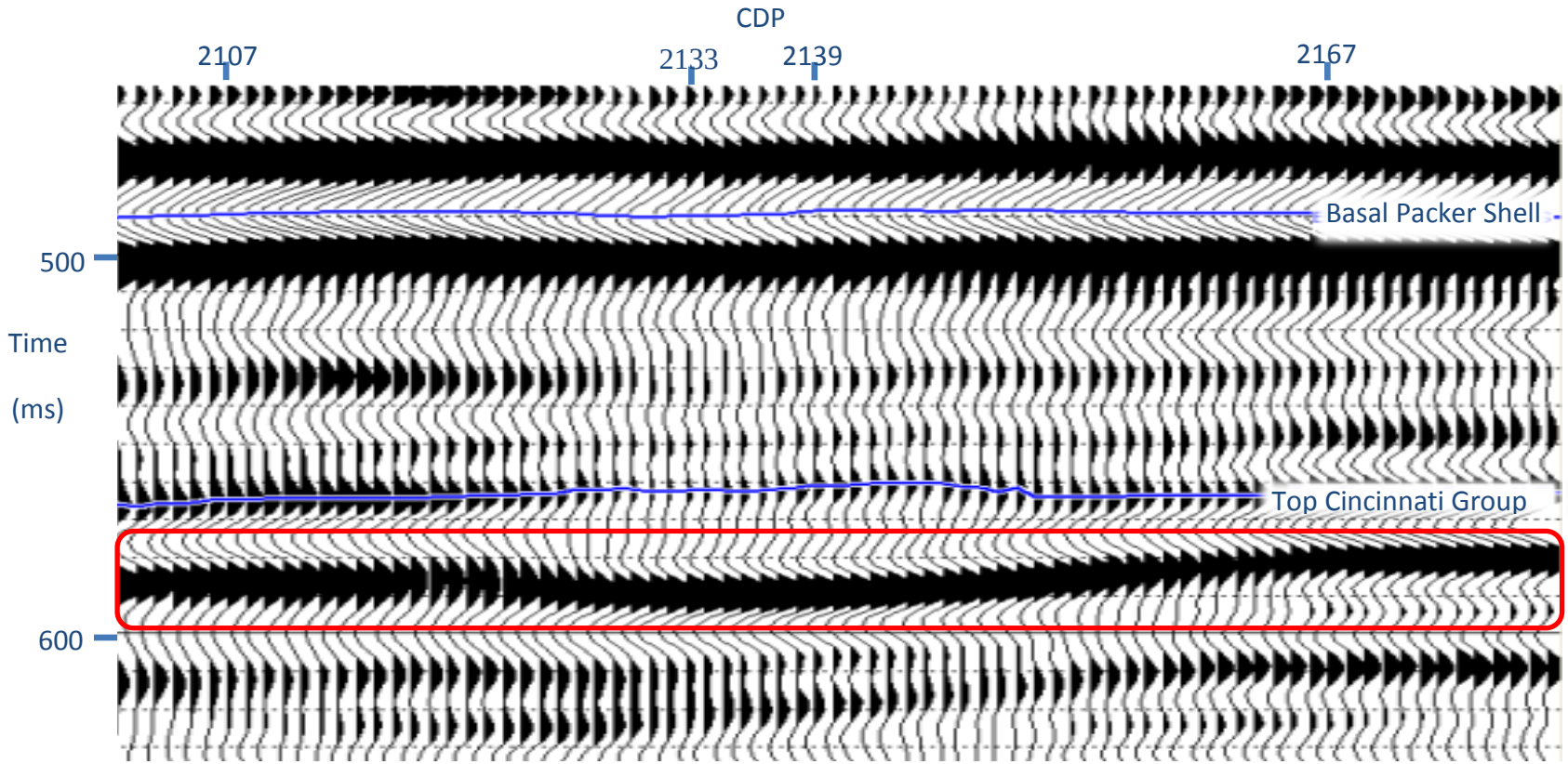

Figure 8. Above is a portion of the north-south trending seismic line. Highlighted at about 585 ms is an event within the Cincinnati Group that shows downward bowing structure. This structure appears nearly directly below the area of attenuation due to gas at CDP 2133. Gas effects are likely not the cause of this structure as underlying events would be clearly affected.

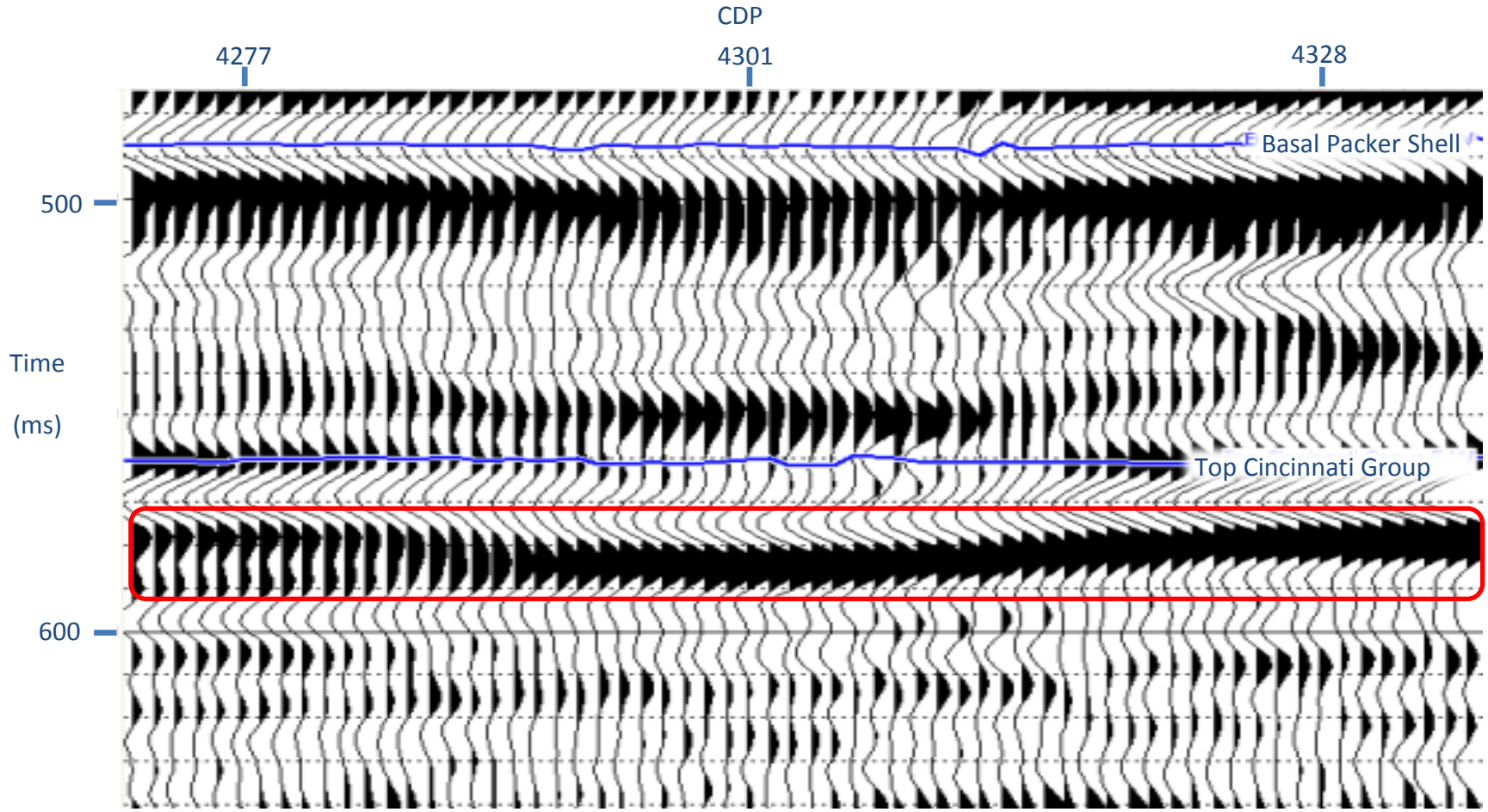

Figure 9. Above is a portion of the east-west trending seismic line. Highlighted at about 585 ms is an event within the Cincinnati Group that shows downward bowing structure. This structure does not show any indication of being associated with a gas reservoir and is likely true structure.

4.2 Average Frequency

Low frequency zones occur in both lines occur between 400 and 600 ms. In the east-west section the effect of the gas shadow reported by Bey (2012) is only seen in the same CDPs as the amplitude data, 4200 to 4217 (Figure 10). Next to these CDPs, from 4169 to 4196 there is another area of low average frequency that correlates with the broadening of the basal Packer Shell sidelobe. In the north-south section there is a much larger area of low average frequency (Figure 11). This area ranges from CDPs 2070 to 2175 at the same times. This area covers not only the area of the more apparent attenuation beneath the packer shell reflection, but also the less apparent areas of attenuation. In addition the modification of the positive Packer Shell sidelobe correlates with low frequency zones as well as in the east-west line. In both of the lines the areas of broadening are within zones of low average frequency, however the frequencies are about 4 or 5 Hz higher than those of the gas shadow attenuation.

The average frequency plot shows the average frequency localized in time and location. The effect of a gas shadow on average frequency will be to lower it dramatically as the high frequencies are those that are attenuated. The regions that were listed as potential gas shadows all correlated with zones of low average frequency. The other low frequency zones correlate with areas of broadening. If the broadening is happening as a result of velocity gradients within the interval, then the low average frequency can be explained with velocity transition zone frequency dependent filtering. Velocity transition zones cause destructive interference of the higher frequency components of a trace. In addition frequencies above this given frequency experience increasing amplitude decay (Liner, 2012).

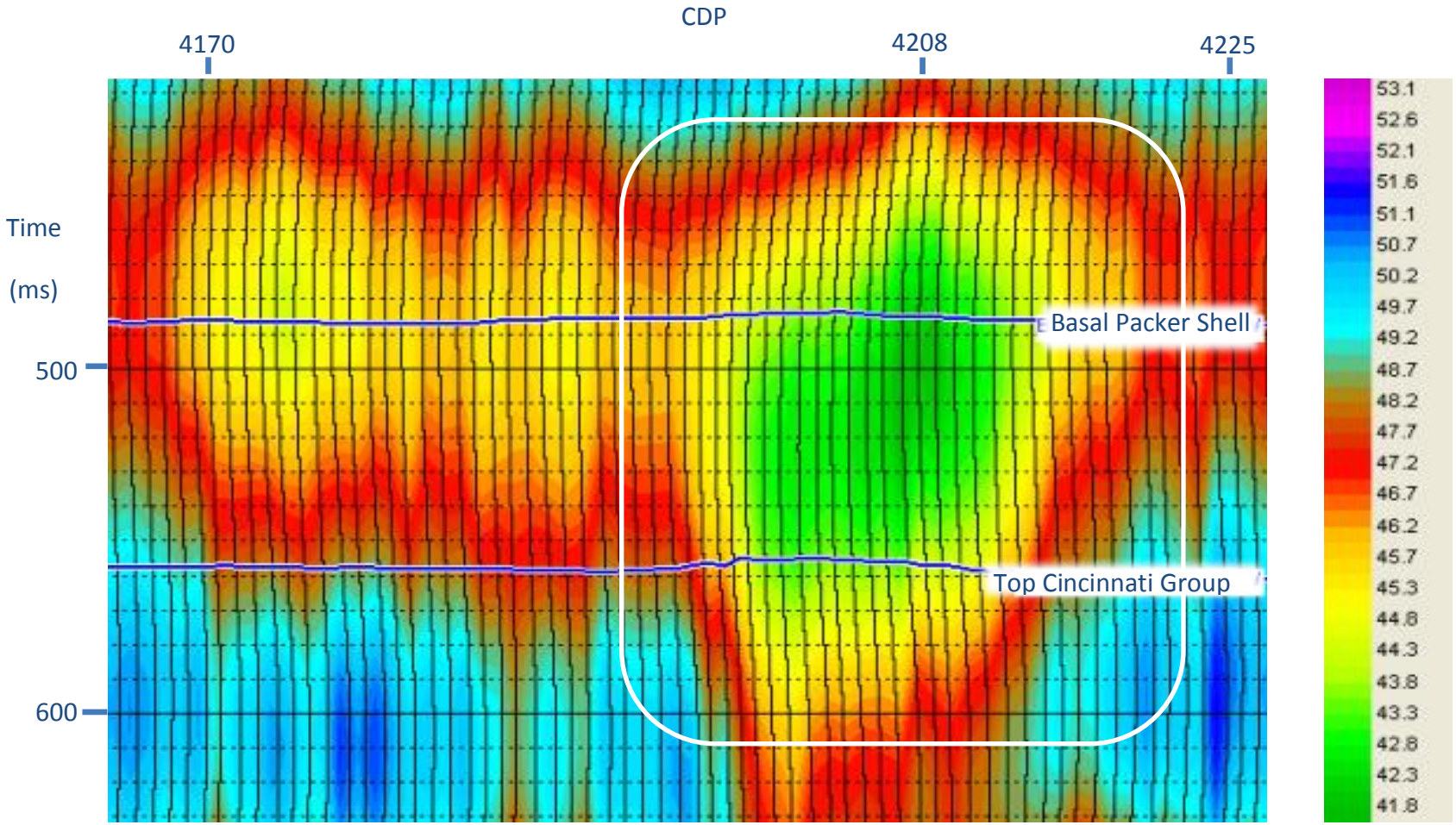

Figure 10. Above is a portion of the average frequency plot of the east-west trending seismic section. Highlighted is an area of low average frequency centered at CDP 4208. This area of low frequency is caused by attenuation from the Clinton interval gas reservoir, located just beneath the Packer Shell at about 500 ms.

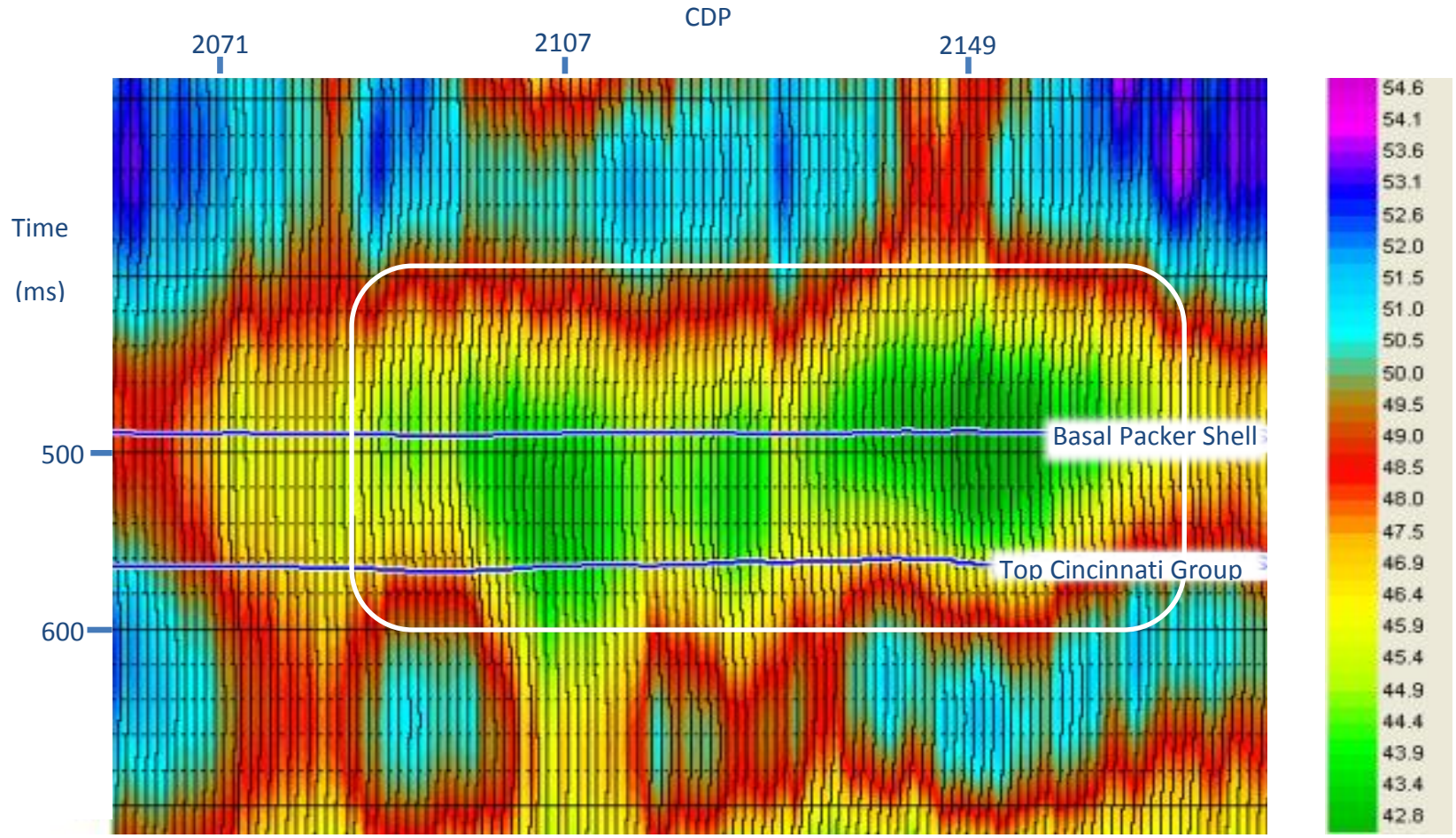

Figure 11. Above is a portion of the average frequency plot of the east-west trending seismic section. Highlighted are areas of low average frequency. The area around CDP 2149 is very close to an area of attenuation believed to be caused by gas within the Clinton interval. The other areas of low frequency have fewer indications of the presence of gas.

4.3 Instantaneous Frequency

The instantaneous frequency of the seismic lines show interruption of coherency below the basal Packer Shell in both seismic lines. In the east-west line there is interruption of the negative response at about 505 ms between CDPs 4200 and 4217 (Figure 12), correlating directly to the area of the gas shadow of Bey (2012) in both the amplitude and average frequency data of the east-west line. Likewise, there are responses in the north-south section at 505 ms between CDPs 2096 and 2108, as well as CDPs 2124 to 2143 (Figure 13). These areas match closely with the areas of attenuation in the amplitude data from the north-south line. On the other hand, there is little change of instantaneous frequency at the location of broadening of the basal Packer Shell sidelobe in either of the sections.

Instantaneous frequency is a complex trace attribute (Taner et al., 1979). Each trace is converted to an imaginary time series, in which the real part is the original trace, and the complex part is the complex number, *i*, times the Hilbert Transform of the original trace. The time derivative at which the complex trace vector is rotating through the complex plane is the Instantaneous Frequency. This measure is used as a proxy for the rate at which the character of a given trace is changing at any point in time. This attribute is commonly used to help trace a reflector across a section as, for example, a response like the basal Packer Shell reflection is very strong and continuous. Gas shadows can interrupt an otherwise coherent event as a whole in affected CDPs (Tanner, 1979).

The interruption of coherency of the negative instantaneous frequency event at 505 ms in the north south line matches nicely with the identification of gas shadows in

the section. Gas shadows cause a response in instantaneous frequency as underlying signals are attenuated. As the trace loses high frequencies through attenuation, I expect to see the instantaneous frequency get closer to zero.

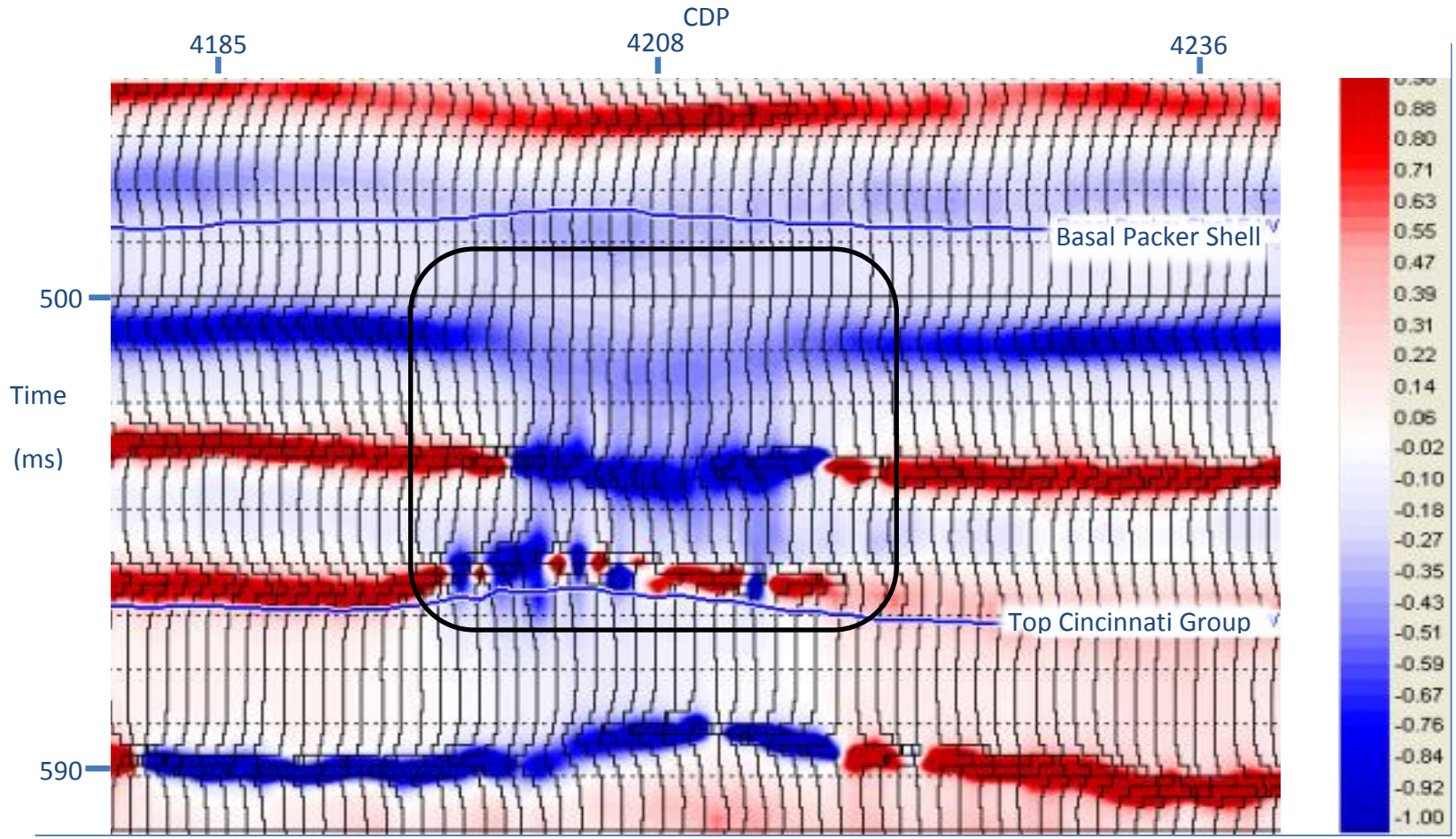

Figure 12. . Above is a portion of the instantaneous frequency plot of the east-west trending seismic section. Highlighted is an area where coherency is interrupted within the Clinton interval. This along with the complex behavior below is associated with the effects of gas.

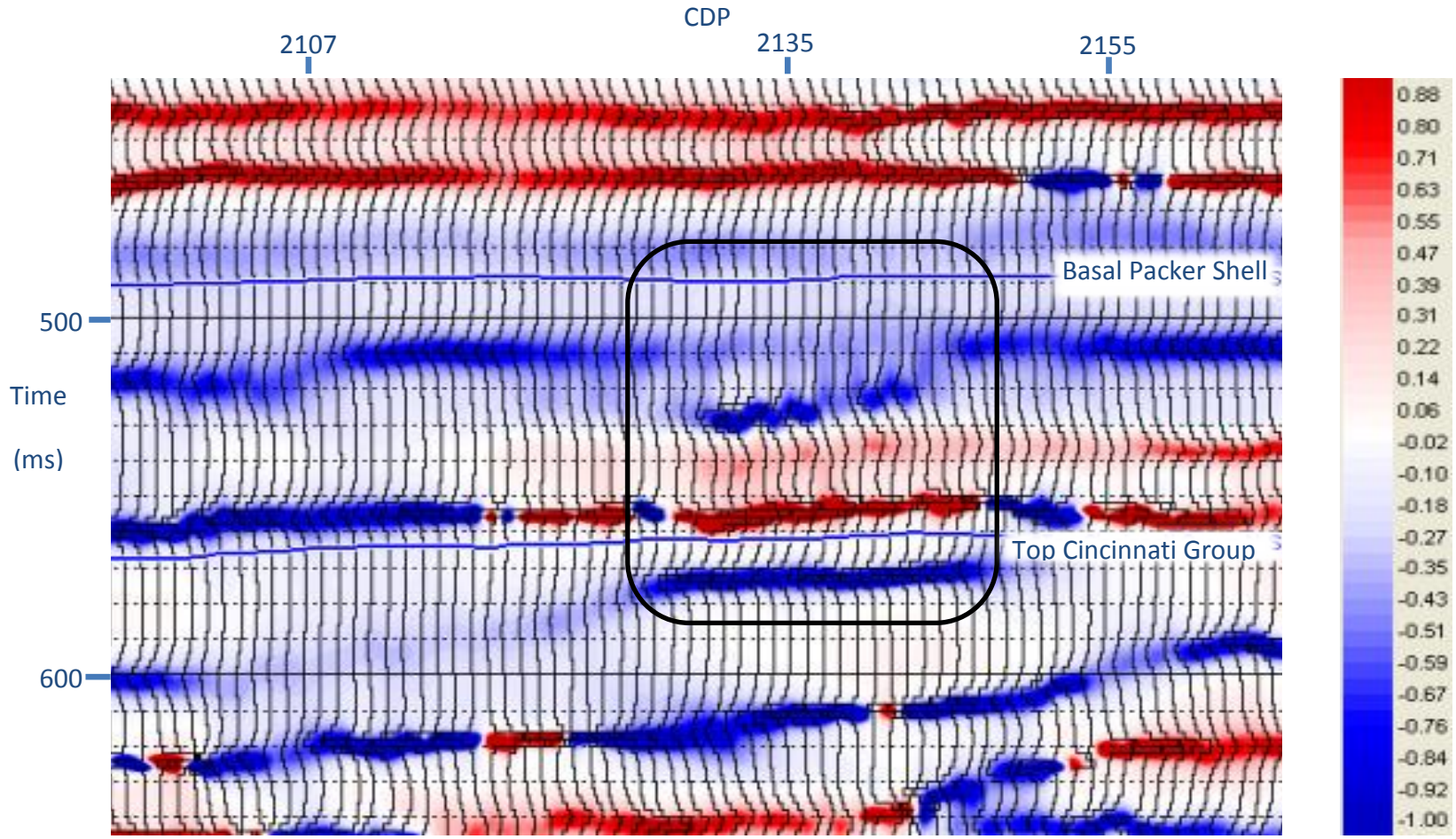

Figure 13. Above is a portion of the instantaneous frequency plot of the north-south trending seismic section. Highlighted is an area where coherency is interrupted within the Clinton interval. This along with the complex behavior below is associated with the effects of gas.

4.4 Wavelet Packet Transform

The plot shows the frequency content of the second scale of the wavelet packet transform where the frequencies that remain are centered around 70 Hz (Figure 14). High frequency attenuation can be seen starting sample 640 from CDPs 4205 to 4214 (Figure 15). On the other hand CDPs 4162 through 4192 do show variable character where sidelobe broadening is occurring.

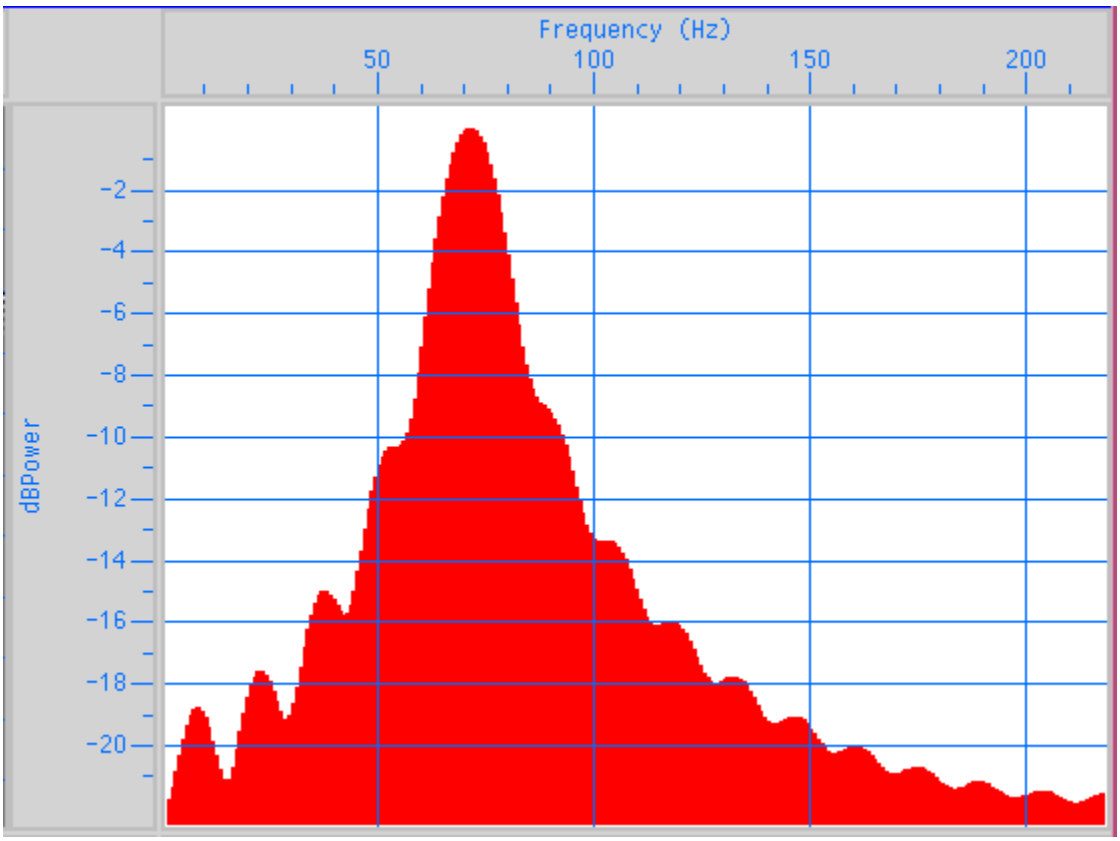

Figure 14. Frequency content of the second wavelet packet transform scale.

Applied to the area of interest in the north-south section (Figure 15), there does appear to be local high frequency attenuation occurring in the second scale of the wavelet packet transform, also filtering frequencies centered around 70 Hz.

The wavelet packet transform was applied to show frequency variations with time in the seismic sections to reveal the gas shadow. In looking at the second scale of the wavelet packet transform, particularly in the east-west line, it is clear that the frequencies around 70 Hz are the frequencies that are attenuated by the gas shadow.

The areas where these frequencies in the north-south line have been largely removed correlate with the areas in the amplitude, average frequency, and instantaneous frequency data that show hints of gas related attenuation. However, the evidence in the north-south line is all less convincing than that in the east west line because the areas are smaller and the extent to which the effects are seen is somewhat diminished. I suspect the effects of gas are there, they are all just significantly less dramatic.

Although the wavelet packet transform is very good for finding frequency localization with time it has not revealed any clear effects in regards to the Packer Shell sidelobe broadening. Areas correlating with the broadening in the wavelet packet transform are little different in frequency content across the north-south section.

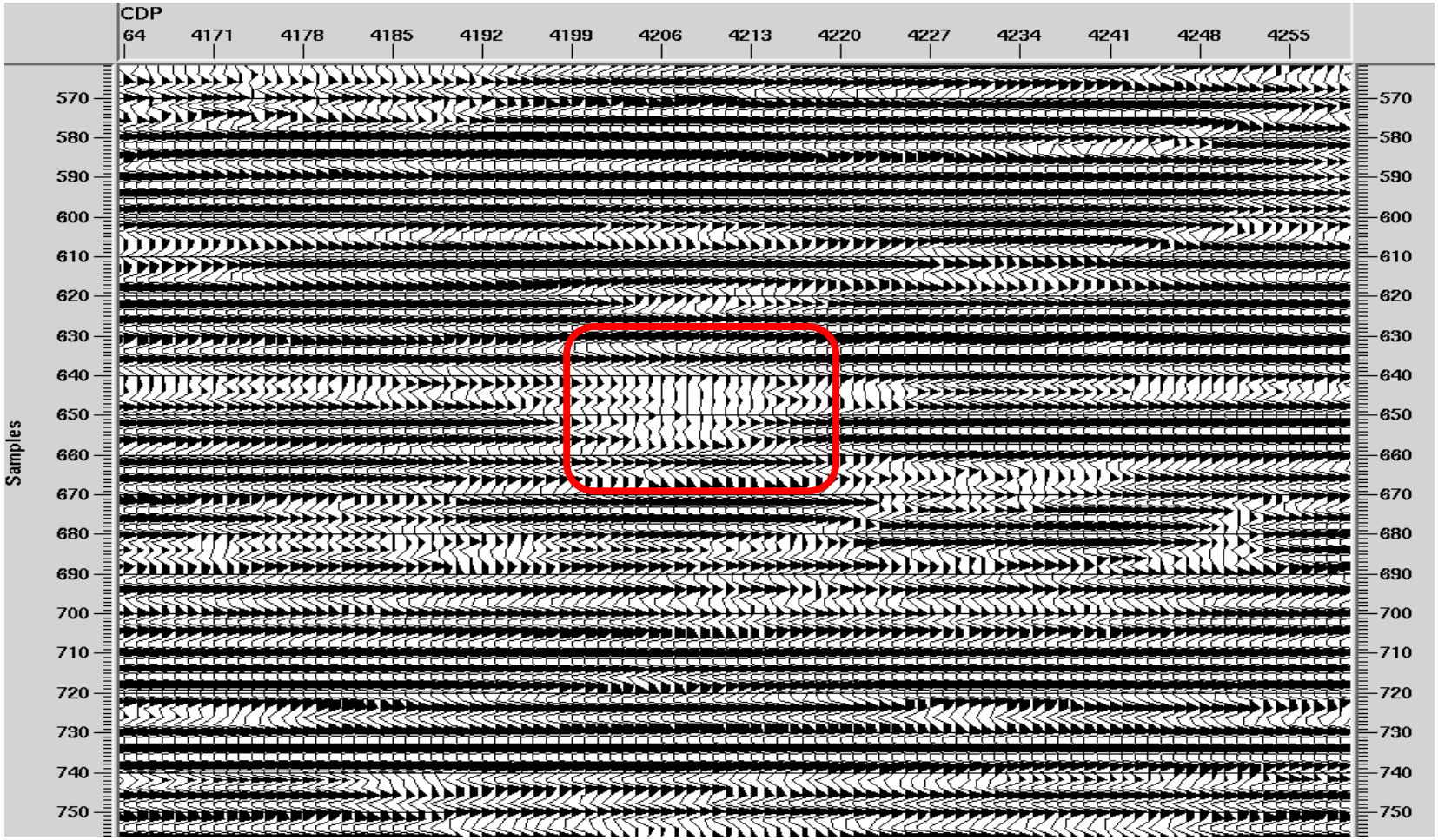

Figure 15. Above is a portion of the wavelet packet transform of the east-west trending line. The removal of frequencies centered around 70 Hz associated with a gas reservoir within the Clinton interval is highlighted.

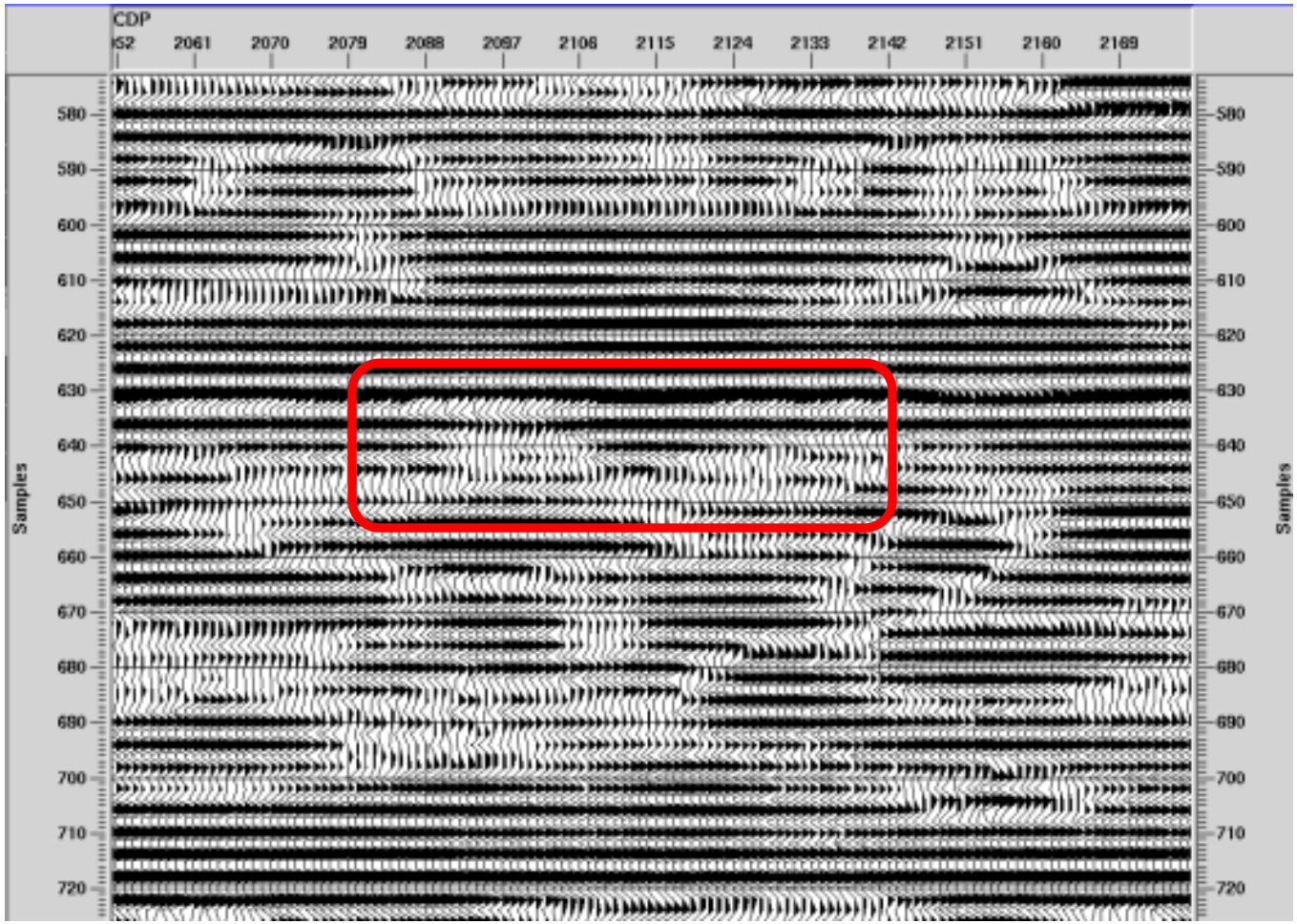

Figure 16. Above is a portion of the wavelet packet transform of the north-south trending line. The removal of frequencies centered around 70 Hz associated with a gas reservoir within the Clinton interval is highlighted.

4.5 Well Log Modeling

4.5.1 Well API# 3407525308

Well API# 3407525308 (Figures 17—21) is 25 miles from the center of the seismic survey and has a good gamma ray signature for the entire Clinton interval and surrounding units (Figure 1). Within the Queenston below, the shale baseline is at about 90 API Units. This well does show a relativly high gamma ray spike at 3631 ft where there is potentially a slightly more organic rich area within the Queenston Shale. Deeper within the Queenston, from about 3850 ft to 3950 I see an area where the gamma ray response is significantly lower than the shale baseline.

In the density log I find a very low density portion of the log that is at the boundary of the Stray Clinton and the upper Cabot Head. Likewise the upper sandstone of the Red Clinton is also relativly low density. On the other hand the upper sand of the White Clinton is a very high density unit. The log reads nearly 2.9 g/cc here. This is apparently even more dense than the PackerSshell. In the Queenston, the density fluctuates from a general baseline around 2.6 g/cc to about 2.4 g/cc. This instablility continues into the interval of the Queenston where the gamma ray log decreases significantly. At about 3866 ft. the density is slightly higher and very stable.

Seismic velocity within this well mimics the density log wit ha few exceptions. Within the low density upper sandstone of the Red Clinton the velocity is relatively high. Within the Queenston, the velocity does not track the density. Here the density fluctuations appear to have no relationship with the very steady 15,500 ft/s

velocity of the shale. This steady velocity extends deeper to about 3866 ft where I see the density increase and gamma ray decrease at the top of the Cincinnati Group. Here the velocity increases as well until about 3950 where the velocity returns to the steady shale baseline once more.

The synthetic traces, resulting from the sonic and density logs, show the Packer Shell reflection clearly with the primary sidelobe extending to the top of the Queenston. Past here there is a small positive amplitude event that occurs where the gamma ray high spike occurs in the Queenston at 3631 ft. The reflection coefficients here are small and negative.

The interval of well API# 3407525308 where the gamma ray response is significantly lower than the Queenson Shale baseline is interpreted as the interbedded limestones and shales that are creating the primary reflection that is experiencing attenuation from the gas shadows. The density log has highly variable readings from the Queenston. The Queenston is not known for variable readings in the subsurface of Ohio. The caliper logs indicate widening of the diameter of the borehole in areas that correlate to the variable readings. These widened areas must be washouts. The washouts persist until the top of the Cincinnati Group where thin limestones interbedded with calcareous shales provide a more stable borehole wall.

The results do not provide insight into the broadening of the positive Packer Shell sidelobe. The small positive amplitude event is likely not related to the gamma ray high spike as there are no significant reflection coefficients corresponding with it. It is unclear as to whether or not the small positive amplitude is related to the gamma ray high spike.

A more likely cause is variations in velocity and density from within the Packer Shell and the interbedded limestones at the top of the Cincinnati Group. The spike in gamma ray may be the result of slightly higher organic content at this depth.

The isolation model of the Packer Shell (Figure 20) shows the large trough created by the basal Packer Shell to Upper Cabot Head interface. The sidelobe continues through the Clinton interval (Figure 21). The isolation model of the Clinton interval and surrounding Silurian strata, shows a separate negative amplitude even occuring at the Stray Clinton with a positive amplitde event at the lower portion of the modeled interval. In this instance the strata between the Packer Shell and the Queenston appear to be dampening the negative response from the basal Packer Shell, and shortening the sidelobe.

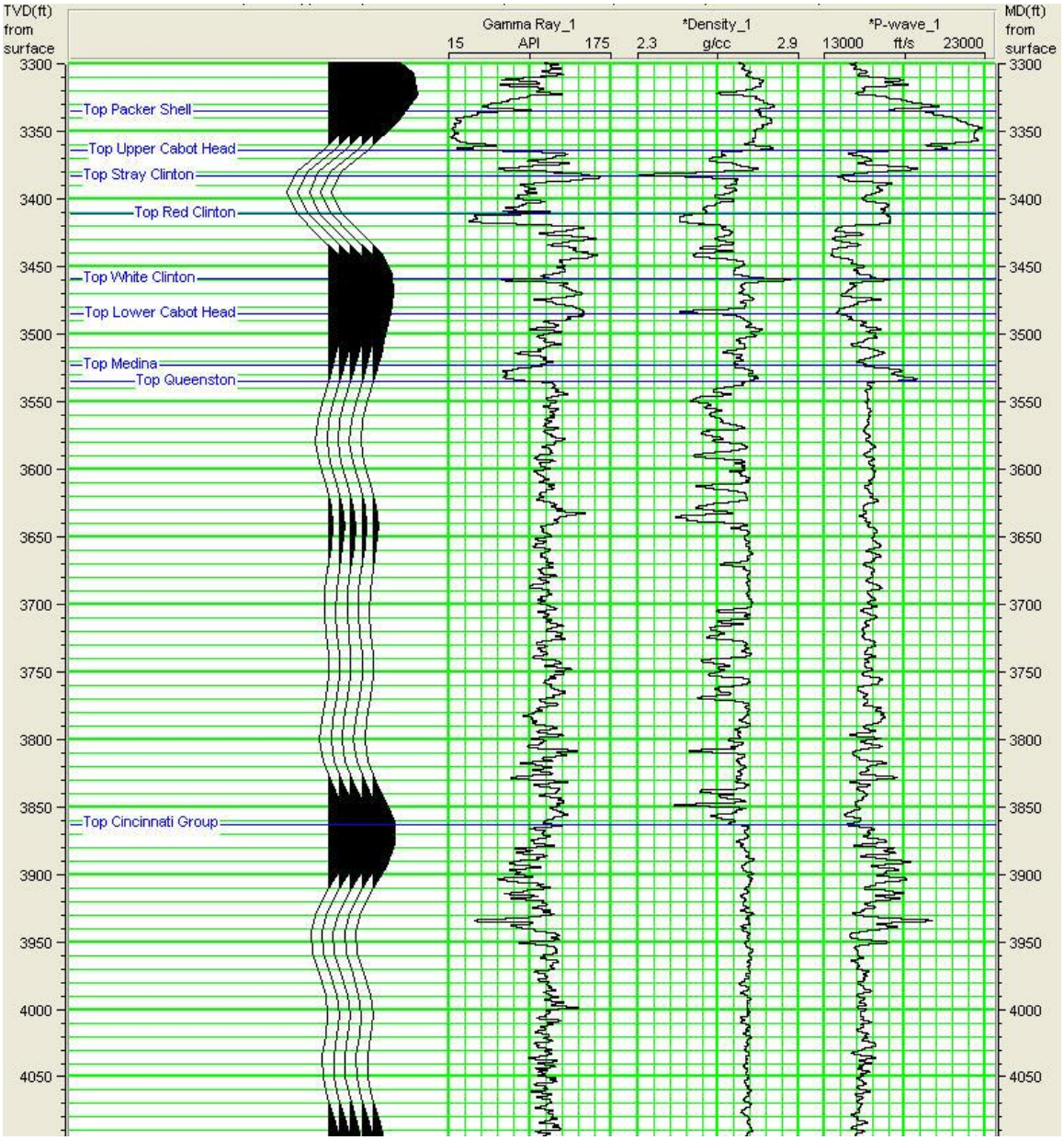

Figure 17. Above is a section of well API# 3407525308. The synthetic trace is unreliable due to the poor quality of the desnity log within the Queenston.

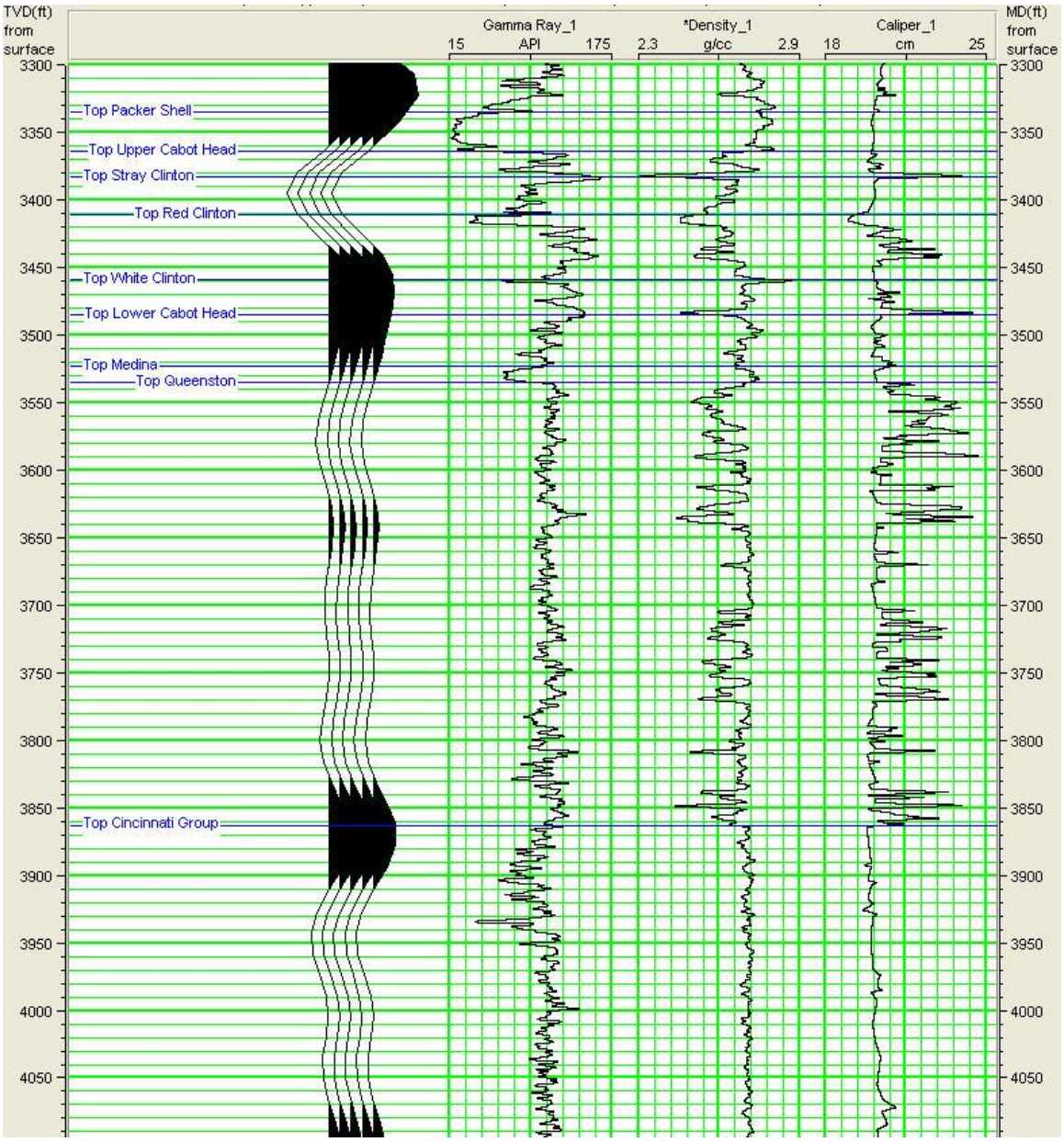

Figure 18. Above is a section of well API# 3407525308 with synthetic traces, gamma ray log, density log, and caliper log. Variablility in the caliper log within the Queenston indicates washouts from drilling. These washouts correlate with low spikes in the density log that are skewing the synthetic traces.

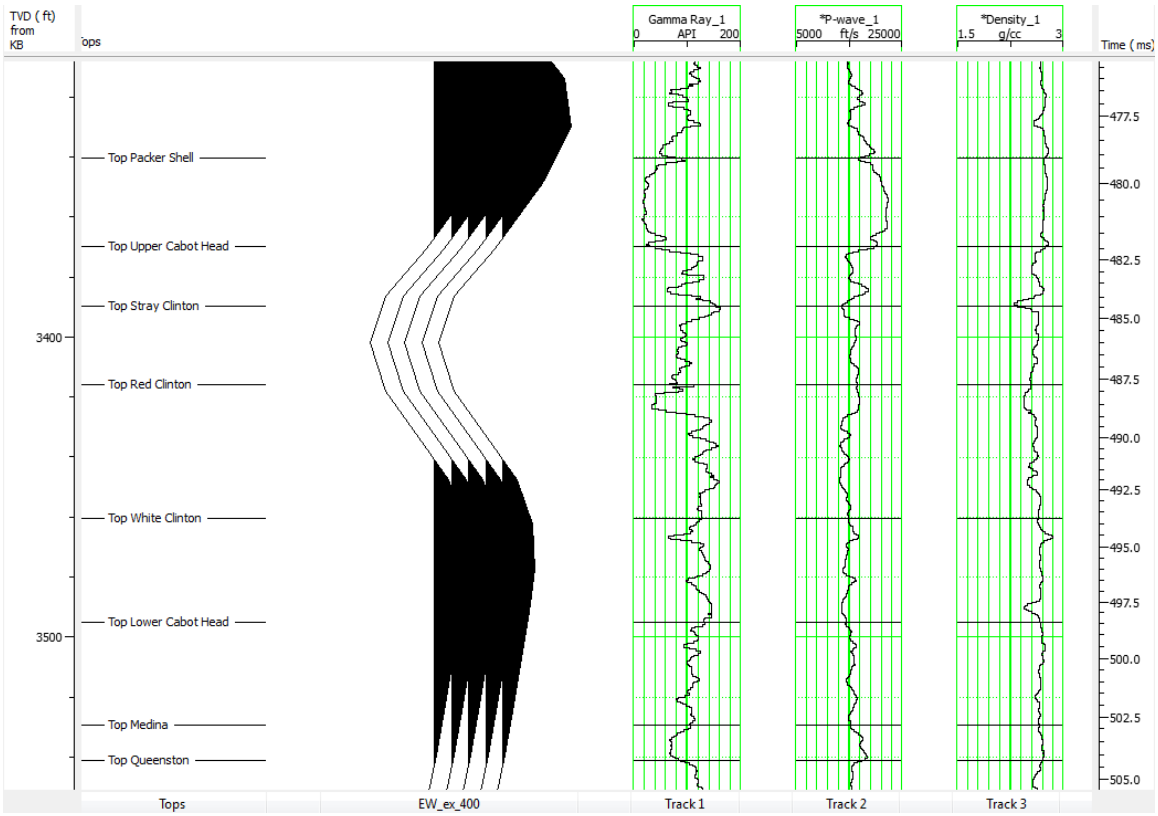

Figure 19. Above is the Packer Shell through the Medina in well API# 3407525308. Shown from left to right are the synthetic traces, gamma ray log, seismic velocity log, and density log.

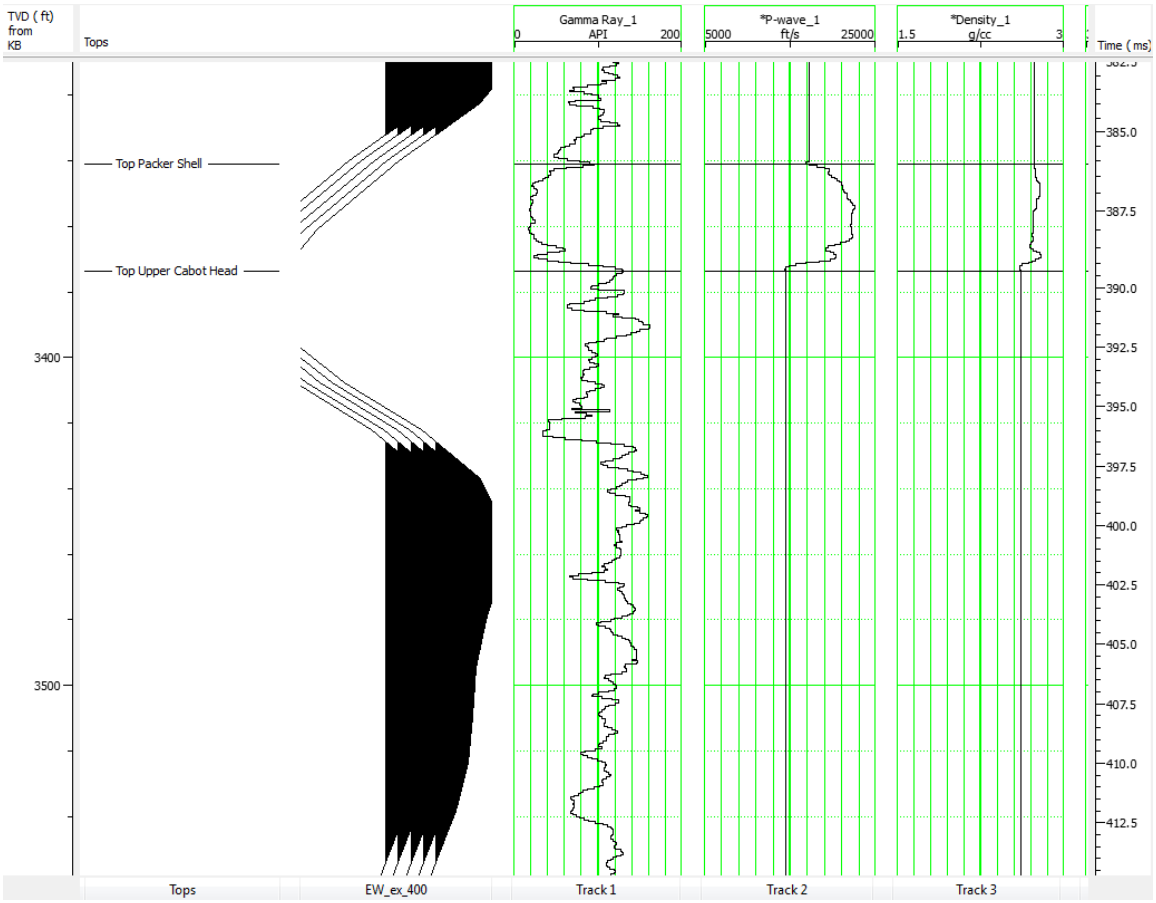

Figure 20. Isolation model of the Packer Shell in well API# 3407525308. The high amplitude through from the basal Packer Shell is present along with the sidelobe.

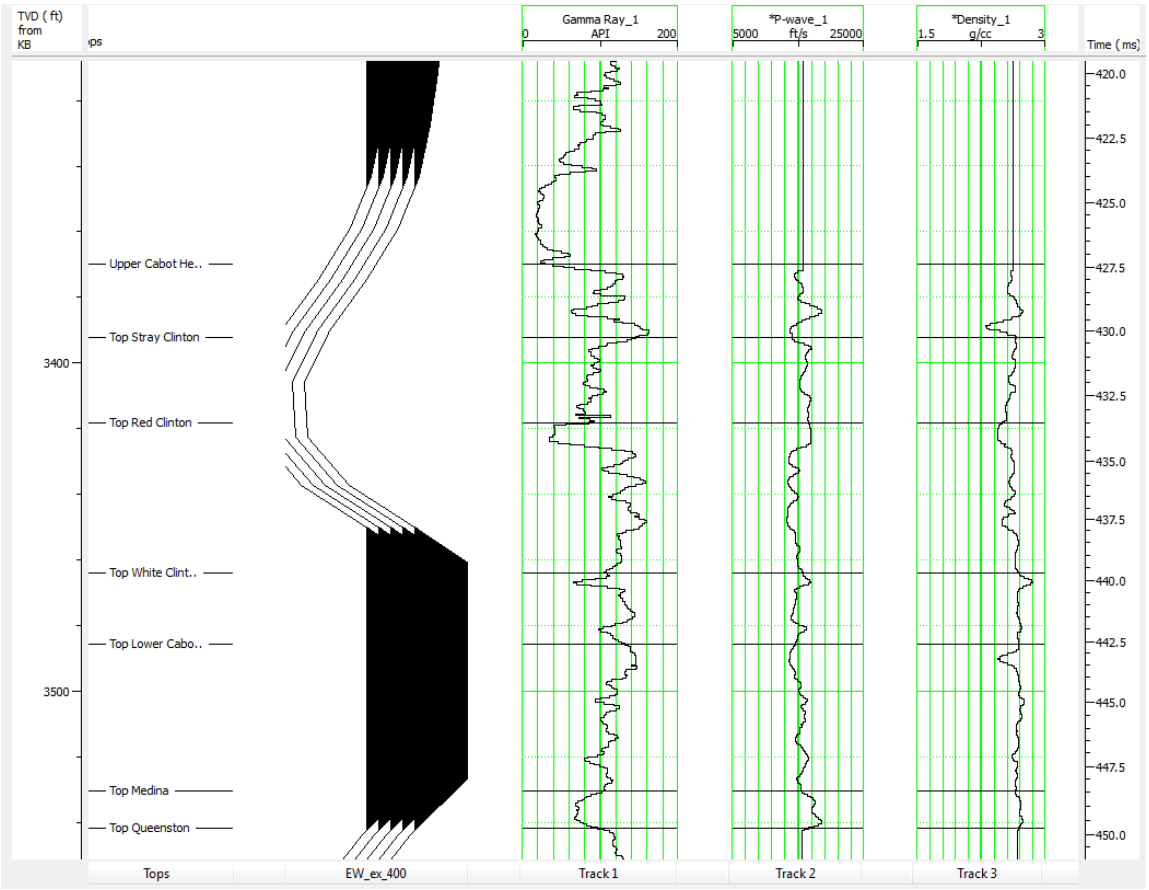

Figure 21. Isolation model of the Upper Cabot Head through Medina Sandstone in well API# 3407525308. A trough is made in the upper portion of this interval and a peak is made in the lower portion.

4.5.2 Well API# 3415125102

Well API# 3415125102 (Figures 22—25) is about 9 miles from the center of the seismic survey (Figure 1) and has a similar gamma ray response to well API# 3407525308 with the exception of the high gamma ray spike between the Medina and the Cincinnati Group. On the other hand well API# 3415125102 differs from API# 3407525308 in that there are not washouts within the Queenston. Here it is very steady, all of the way down to the interbedded limestones where the density increases slightly.

In well API# 3415125102, the basal Packer Shell, as always, has a prominent negative amplitude reflection. In this well, the positive sidelobe extends just past the

Medina Sandstone, and it begins later in relation to well API# 3407525308. The top of the Stray Clinton has a high reflection coefficient, but again their responses are cancelled out due to thin bed effects. The White Clinton on the other hand does not have any high relative reflection coefficients. There is a significant negative reflection coefficient within the Red Clinton at about 4200 ft. Interference from the Clinton interval in addition to interference from Medina Sandstone reflections are mitigating the basal Packer Shell sidelobe. Within this interval the synthetic trace has a low amplitude positive signal similar to well API # 3407525308. In this well, however, there is not significant variation in any of logs, at or even near this depth. From here deeper to about 4872 feet, the gamma ray fluctuates from under 50 API units to the shale average for the previous 400 feet. After 7872 feet the gamma ray log gets steady again around the typical Queenston Shale baseline. Within this interval of higher gamma ray response, at the top of the Cincinnati Group, there is little change in density but there is a significant increase in the seismic velocity.

Well API# 3415125102 has the positive sidelobe of the basal Packer Shell reflection slightly deeper than in well API# 3407525308. This could the the result of the high negative amplitude reflection coefficient within the Red Clinton. This appears to be the result of a high velocity unit within the Red Clinton at about 400 ft. Interference from this could be shifting the positive event associated with the positive sidelobe of the Packer Shell to later times. In addition there is a low positive amplitude event within the Queenston. The is likely the result of small reflection coefficients at this location with interference from a small negative reflection coefficient at the top of the Queenston.

In the isolation model of the Packer Shell, the large negative trough is represented, but the sidelobe extends past the Clinton interval. There is a notch in the Packer Shell that may be contributing to this extension. The isolation model of the Clinton interval shows the same pattern, wither by repllication or the model includes the lower portion of the Packer Shell-Upper Cabot Head interface. The latter appears to be the largest contributing factor in this case. The Medina Sandstone also apppears to be creating a positive amplitude event at the bottom of the model.

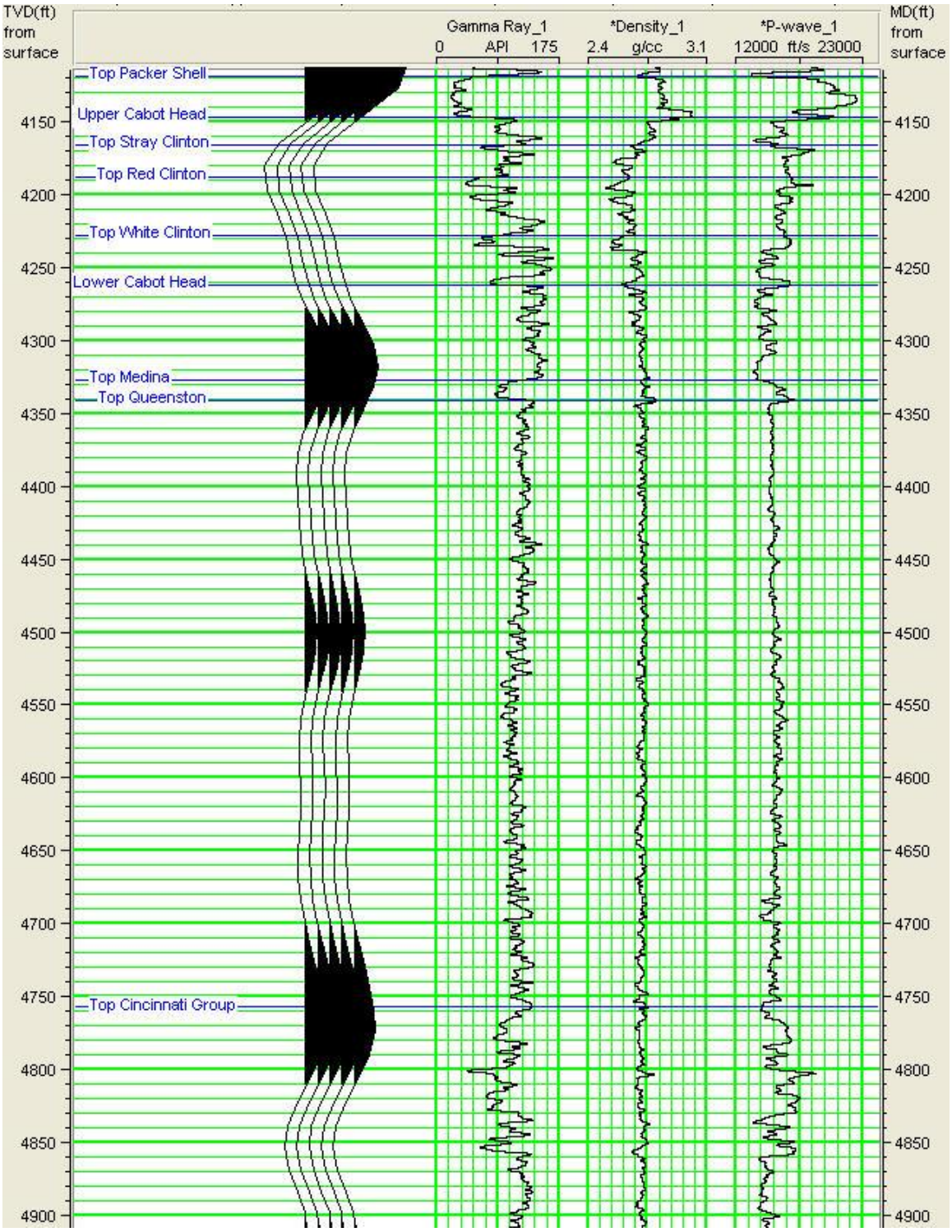

Figure 22. Above is a section of well API# 3415125102 with synthetic traces, gamma ray log, density log, and velocity log. There is no sign of broadening of the positive time basal Packer Shell sidelobe.

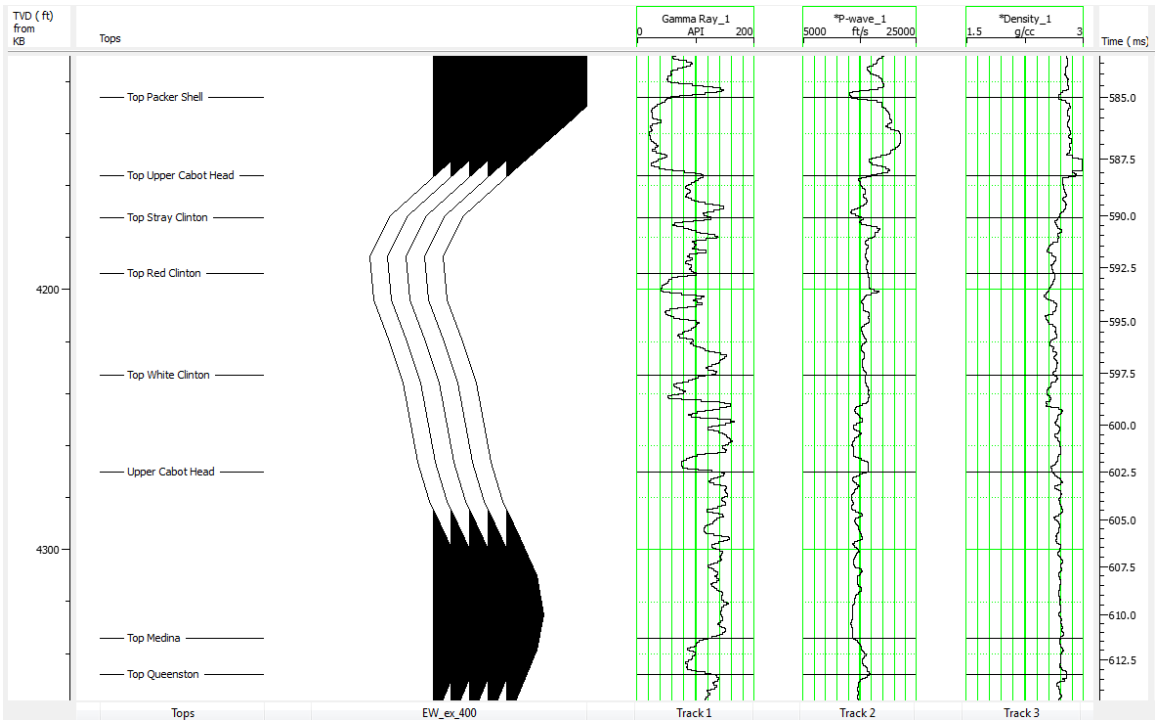

Figure 23. Above is the Packer Shell through the Medina sandstone in well API# 3415125102. Shown from left to right are the synthetic traces, gamma ray log, seismic velocity log, and density log.

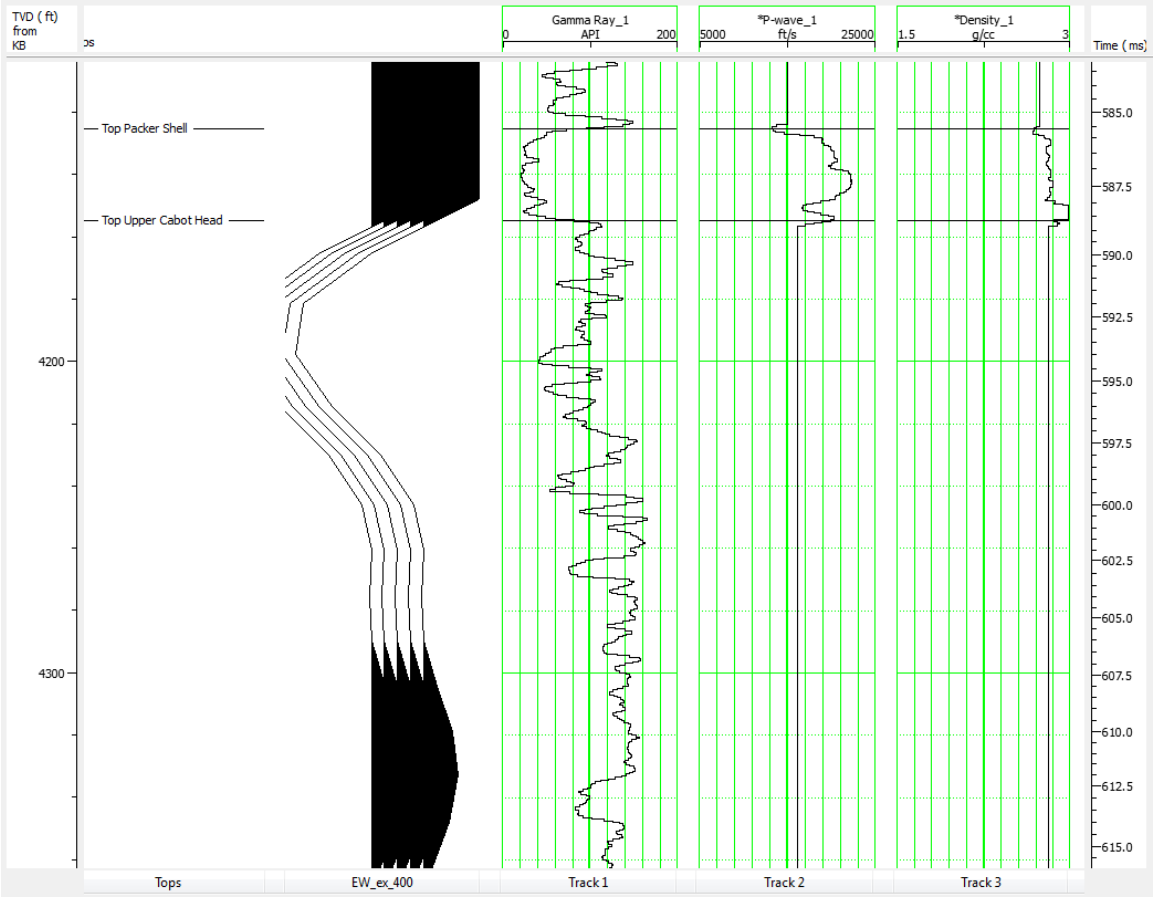

Figure 24. Isolation model of the Packer Shell in well API# 3415125102. The high amplitude through from the basal Packer Shell is present along with the sidelobe.

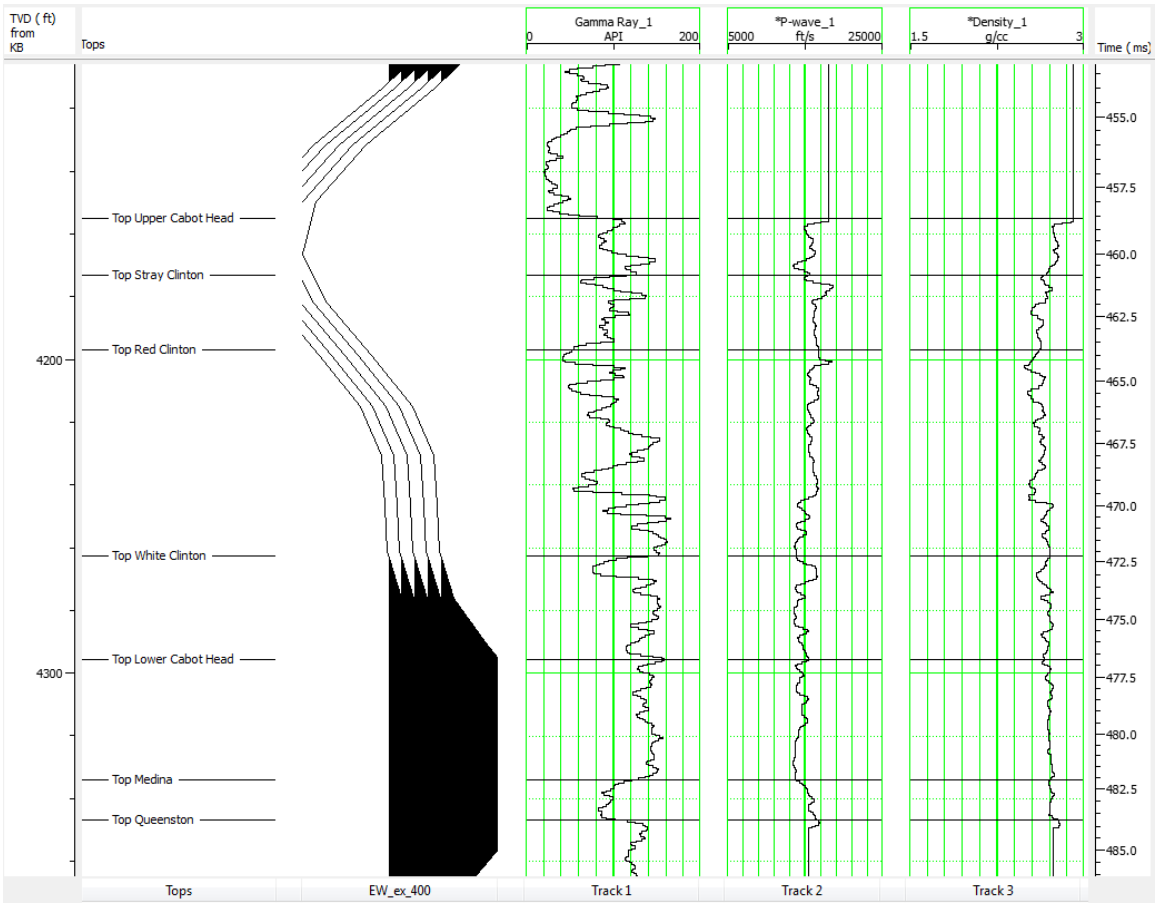

Figure 25. Isolation model of the Upper Cabot Head through Medina Sandstone in well API# 3415125102. A trough is made in the upper portion of this interval and a peak is made in the lower portion.

4.5.3 Well API# 3416925010

Well API# 3416925010 (Figures 26–31) is 4 miles from the center of the seismic reflection survey (Figure 1). Its synthetic traces show Packer Shell positive sidelobe modification similar to that seen in the seismic amplitude data. At the depth of broadening, the well indicates a high bulk density, high seismic velocity zone within the top of the White Clinton. No other wells showed the broadening of the sidelobe as in API# 3416925010. This well also displays three very low velocity intervals in the Queenston. These low velocity zones begin at 3910 ft. and the other two occur soon thereafter. The zones correlate with washouts indicated by the caliper log in Figure 27

and also correlate with large reflection coefficients. The effect of the intervals can be seen in the synthetic trace as it has a trough just below the Medina Sandstone.

The modification of the positive Packer Shell sidelobe is likely influenced by the high velocity, high density zone in the White Clinton. As the porosity is apparently low here, this could mean the formation has been cemented more than in other wells. This seems to represent a formation that would not be a good traditional reservoir. These high values yield a high enough reflection coefficient that broadening may be caused by the White Clinton directly. This well targeted a deeper formation and the Clinton interval was not reported to show oil or gas.

The intervals of low seismic velocity are suspect in the same ways as the density log from well API# 3407525308 was. It is evident that this is playing a role in the modification of the positive Packer Shell sidelobe modification. In addition it is acting to add more event before the effect of the interbedded limestones in the Cincinnati Group.

In the isolation model of the Packer Shell (Figure 29), the large negative trough is represented, but the sidelobe extends only to the White Clinton. The response of the Clinton interval and surrounding units (Figure 30) creates a negative amplitude event with a positive amplitude event both above and below. This signature interacts with the Packer Shell events by dampening the basal Packer Shell trough and sidelobe. The lower positive amplidude event from the Clinton interval and surrounding units is what is responsibe for the broadening of the Packer Shell sidelobe. An additional model of the Packer Shell-Medina Sandstone (Figure 31) shows the strong negative basal Packer Shell

event with a very large and broadened sidelobe. This is independent of the washouts that occur within the Queenston.

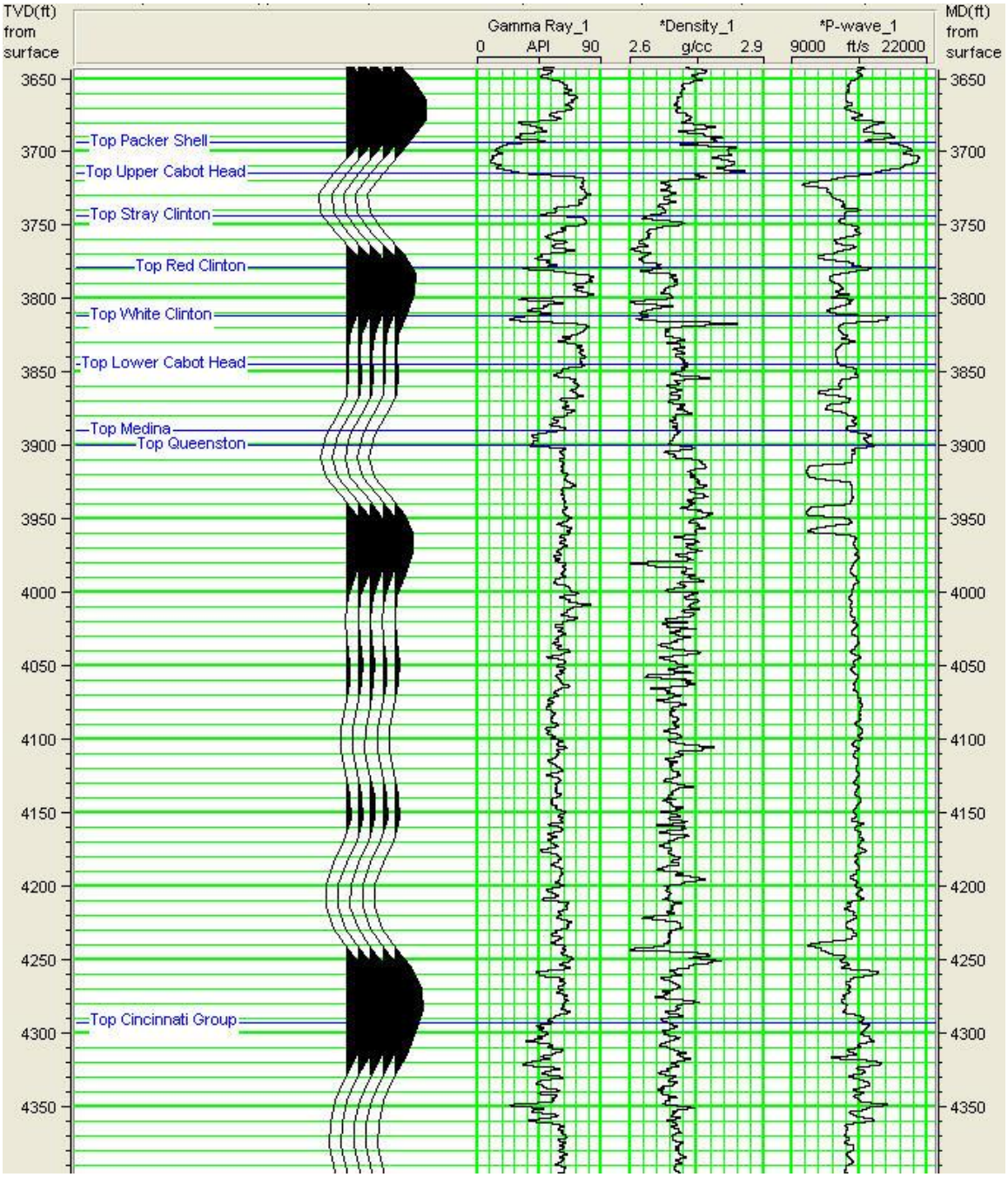

Figure 26. Above is a section of well API# 3416925010 with synthetic traces, gamma ray log, density log, and velocity log. This log does show broadening of the positive time basal Packer Shell Sidelobe possibly caused by the Clinton interval.

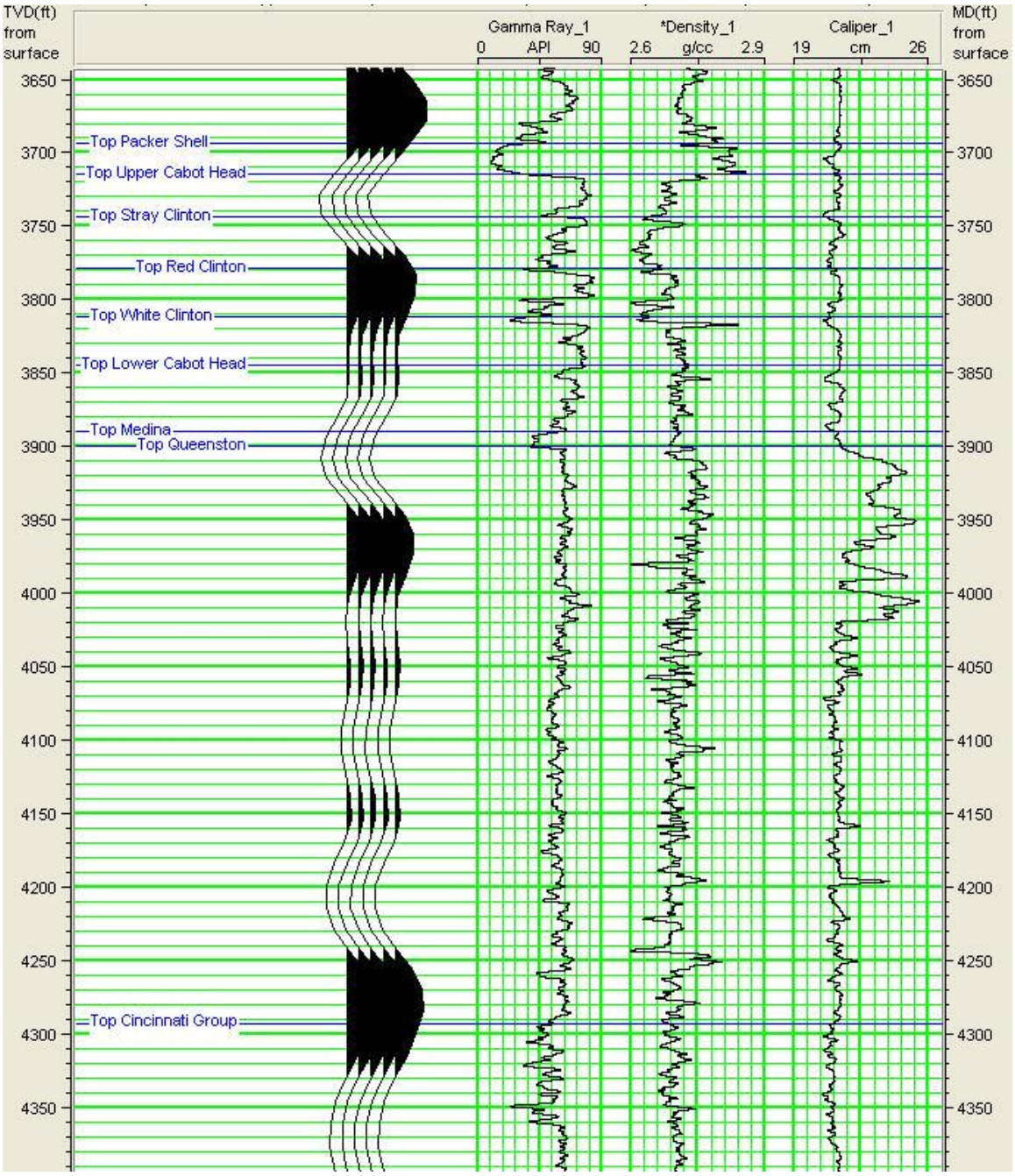

Figure 27. Above is a section of well API# 3416925010 with synthetic traces and gamma ray, density, and caliper logs. Variablility in the caliper log within the Queenston indicates washouts from drilling. These washouts correlate with low spikes in the density and velocity logs that are skewing the synthetic traces.

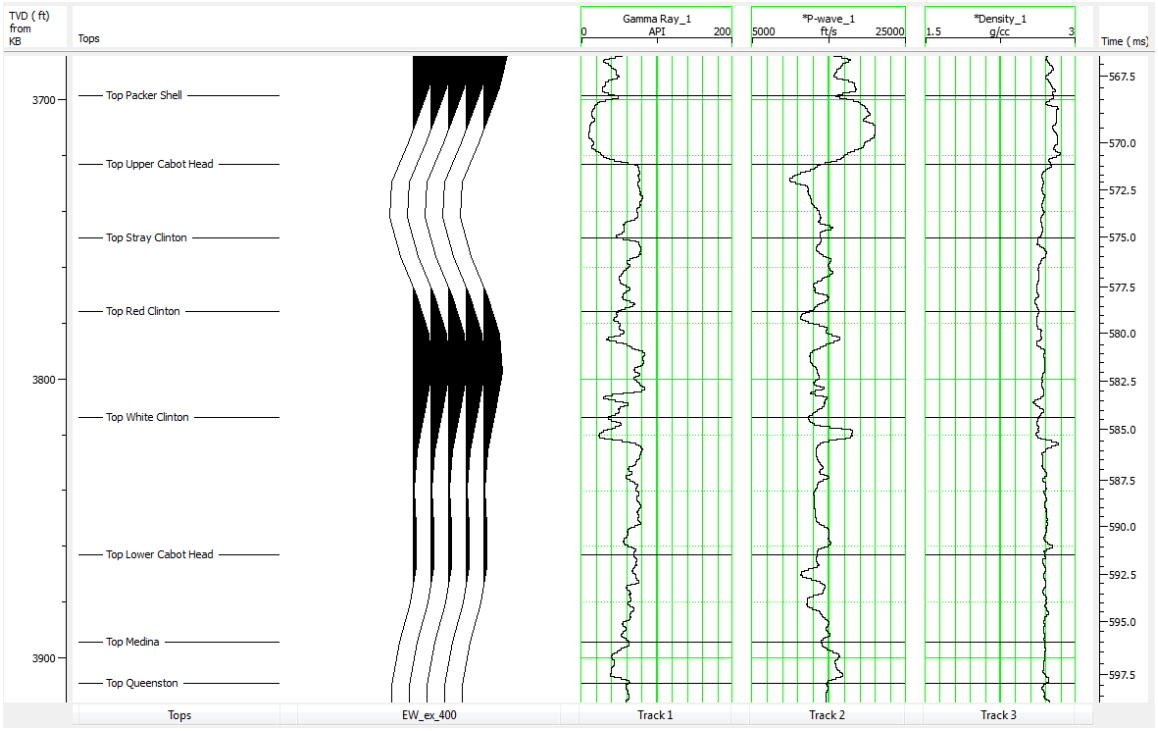

Figure 28. Above is the Packer Shell through the Medina Sandstone in well API# 3416925010. Shown from left to right are the synthetic traces, gamma ray log, seismic velocity log, and density log. Broadening of the Packer Shell sidelobe can be seen extending past the surface of the Lower Cabot Head.

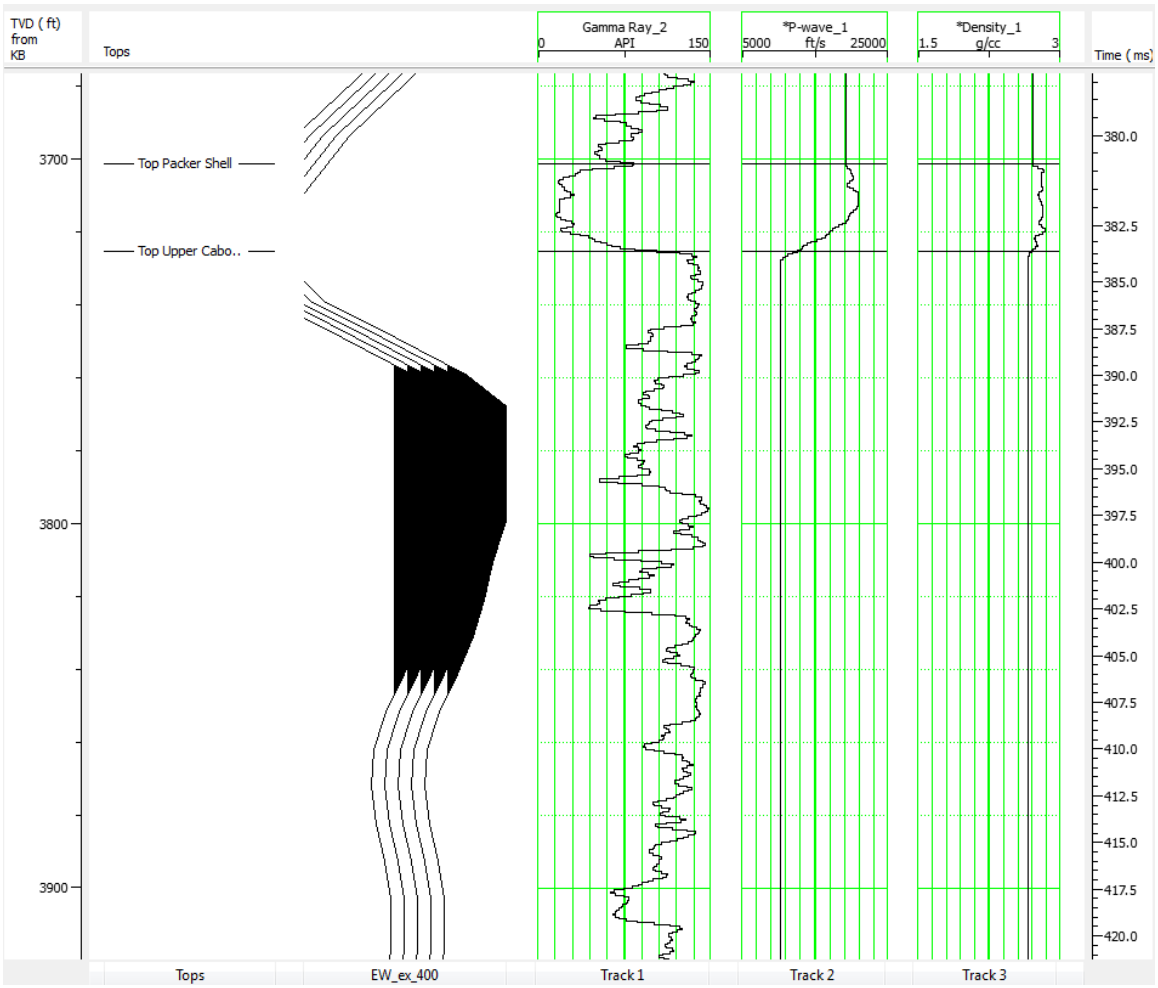

Figure 29. Isolation model of the Packer Shell in well API# 3416925010. The high amplitude through from the basal Packer Shell is present along with the sidelobe.

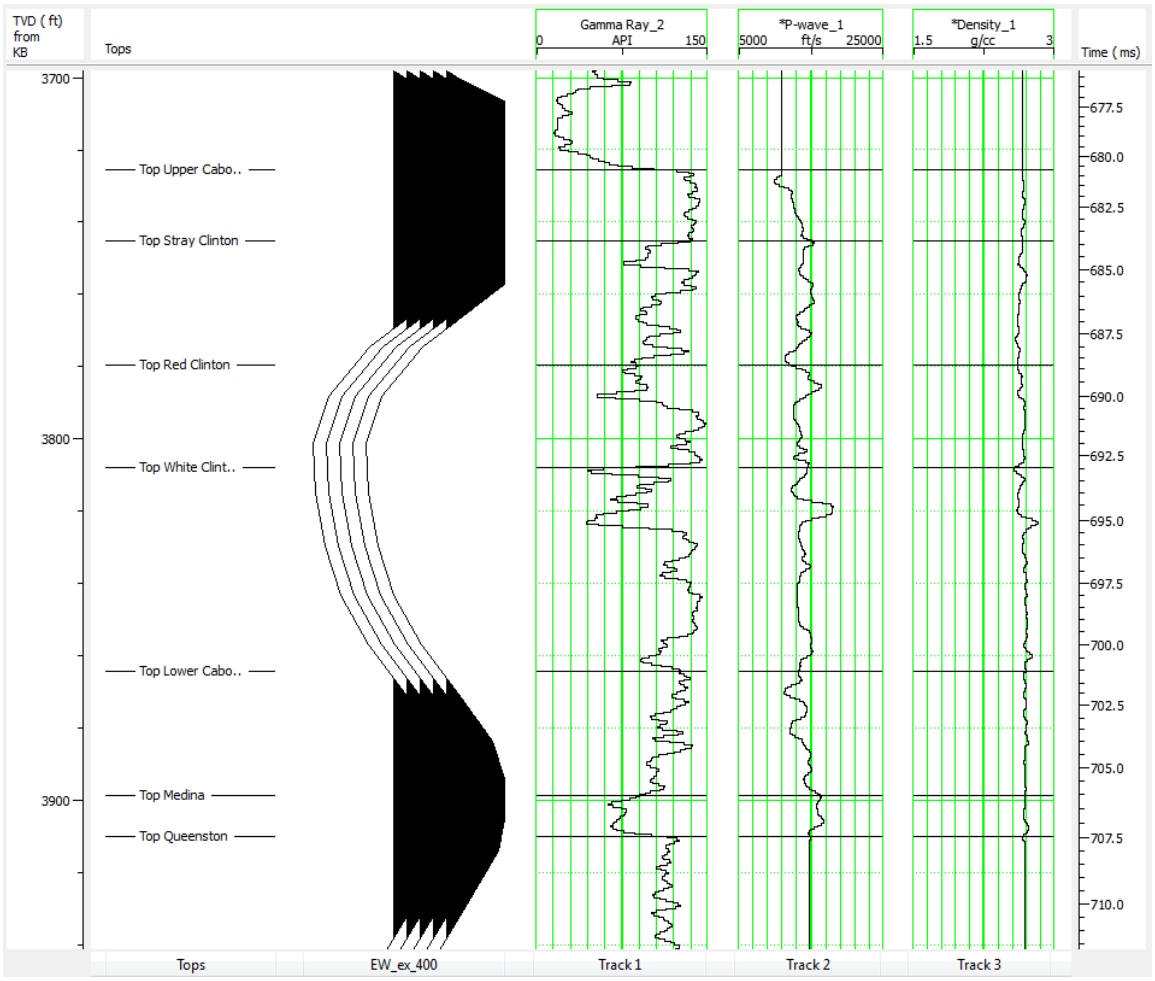

Figure 30. Isolation model of the Upper Cabot Head through Medina Sandstone in well API# 3416925010. This interval creates a trough in the middle with positive events at the top and bottom.

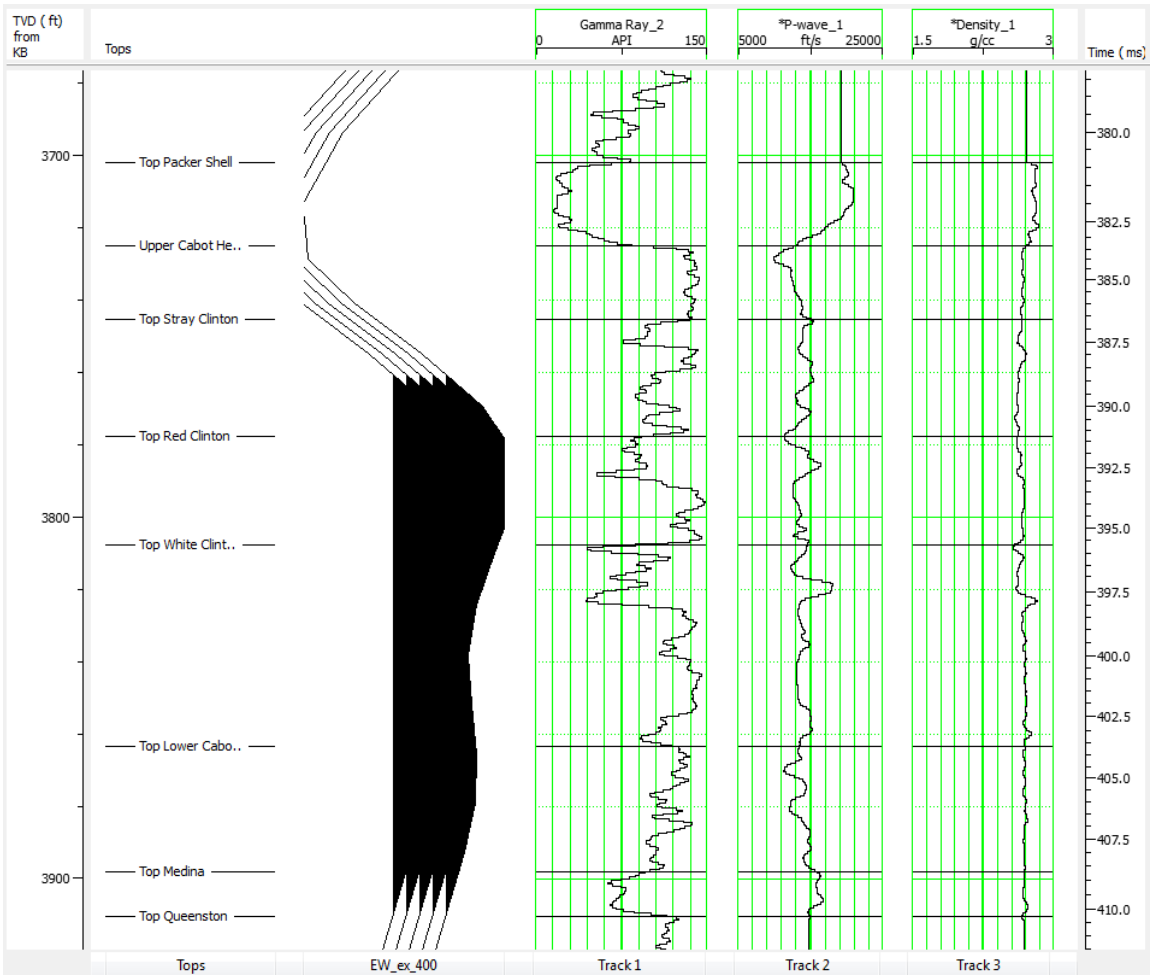

Figure 31. Isolation model of the Packer Shell through Medina Sandstone in well API# 3416925010. This interval creates a trough in the middle with positive events at the top and bottom.

4.5.4 Well API# 3415123662

Well API# 3415123662 (Figure 32) is 19 miles east of the center of the seismic reflection survey (Figure 1). The gamma ray signature of the whole Clinton interval is present. The gamma ray log also shows two very sandy sections within the Red Clinton. The density log shows the White Clinton as a low density zone as opposed to the high density zone shown in the previous well. Velocity in the upper sandstone of the White Clinton is also very low. The rest of the Clinton interval has a very steady velocity near 15000 ft/s.

Well API# 3415123662 does not extend far past the Medina. The sidelobe of the Packer Shell extends past the medina and further to the bottom of the well. Each section of the Clinton interval has relative high amplitude reflection coefficients, but adjacent coefficients of opposite polarity may cancel. Although thin bed effects play a large role in thin reflectors there is a net negative reflection coefficient at the top of the White Clinton again.

The net negative reflection at the top of the White Clinton may be the driving force in moving the positive sidelobe of the packer Shell past the Medina in well API# 3415123662. The extension of the sidelobe could also be the result of the lack of data below the Medina. If there were to be data from deeper there could be interference from the negative sidelobes of other events, especially the interbedded limestones of the Cincinnati Group.

In the isolation model of the Packer Shell (Figure 33), the large negative trough is represented, but the sidelobe doesn't begin until the White Clinton. The response of the Clinton interval and surrounding units (Figure 34) creates a negative amplitude event with a positive amplitude event both above and below. This signature interacts with the Packer Shell events by broadening the basal Packer Shell trough. Much of the sidelobe is summed out and any remaing effects of the sidelobe can only be seen at the Medina Sandstone.

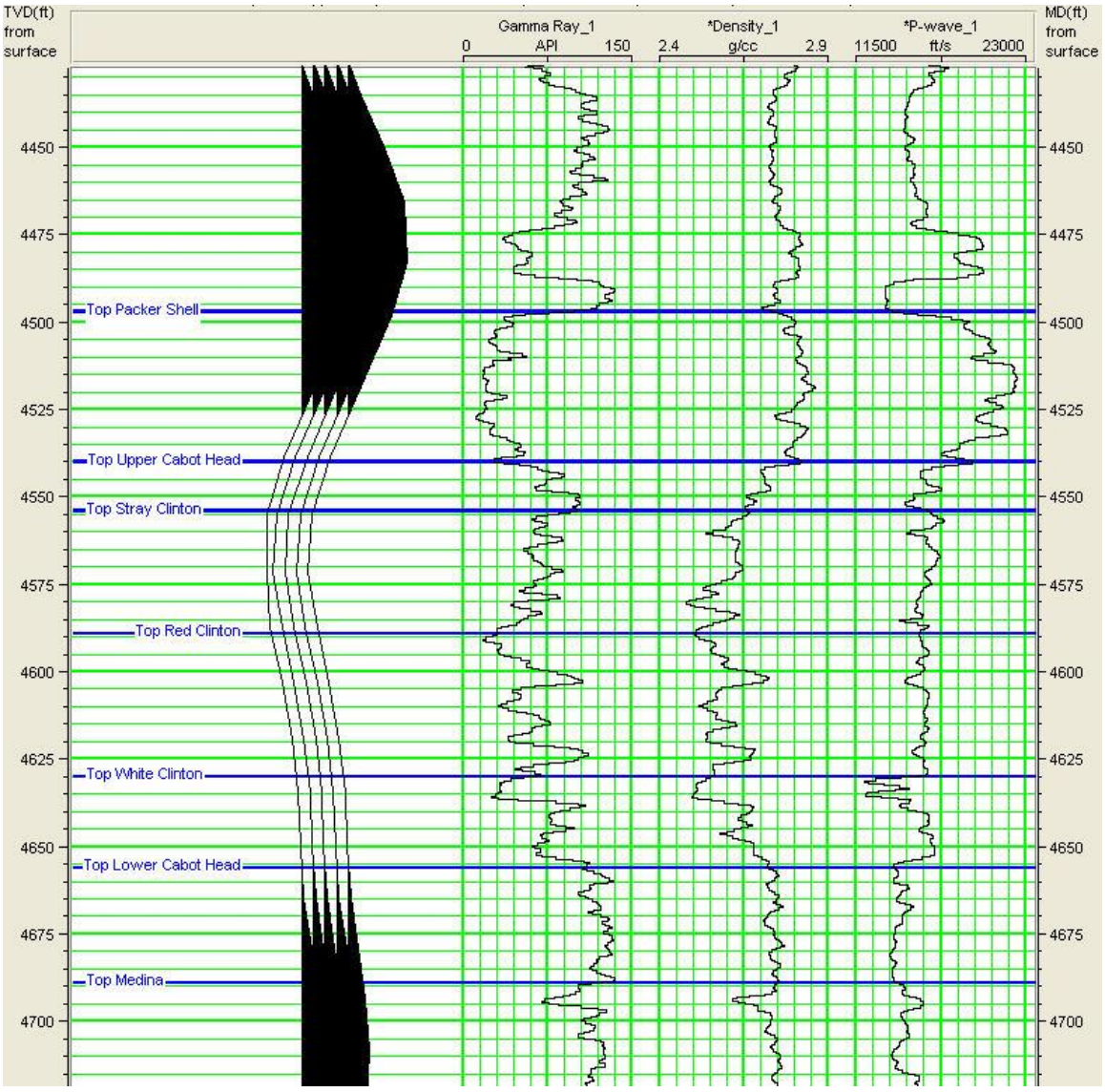

Figure 32. Above is a portion of the synthetic traces and gamma ray, density and velocity logs from well API# 3415123662. This well does not extend deep enough to reveal the effects of the Cincinnati Group. This well does not show signs of broadening in the positive time Packer Shell sidelobe.

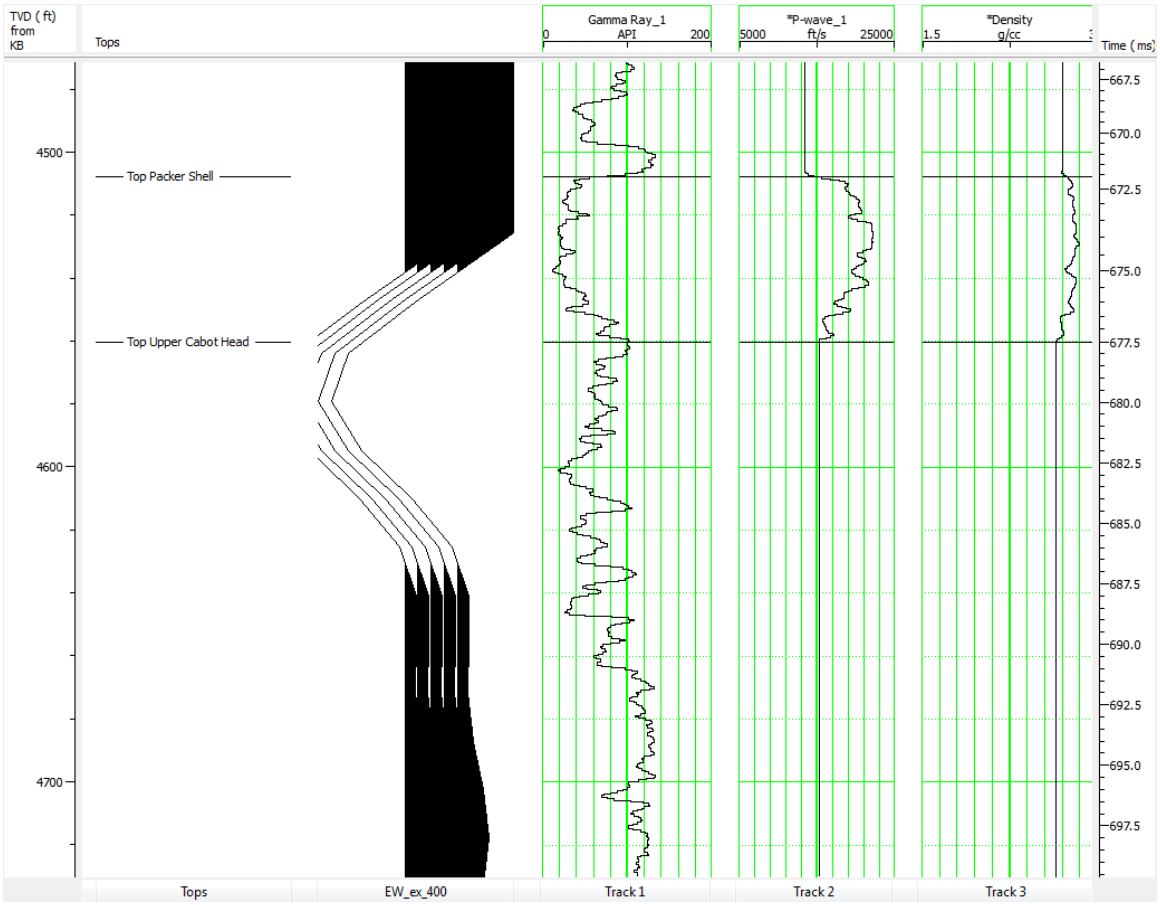

Figure 33. Isolation model of the Packer Shell in well API# 3415123662. The high amplitude through from the basal Packer Shell is present along with the sidelobe.

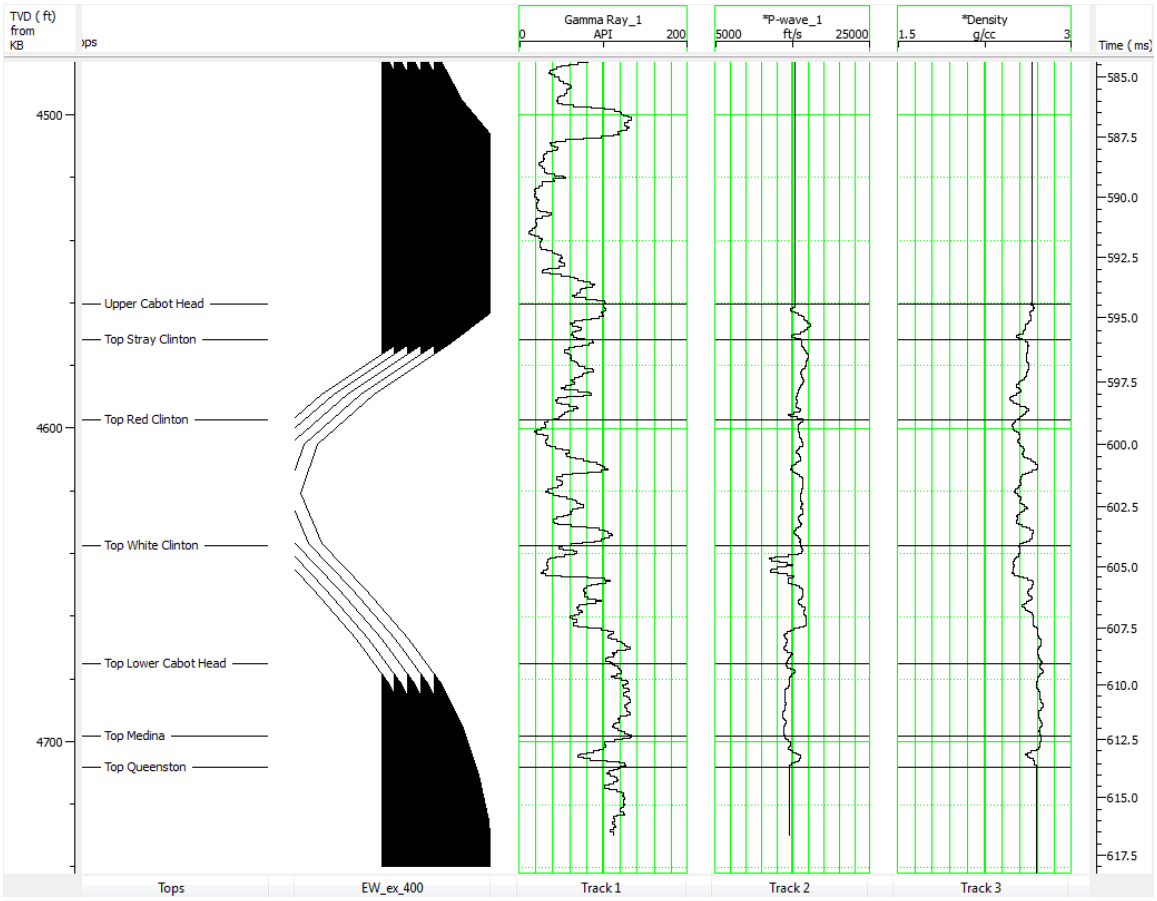

Figure 34. Isolation model of the Upper Cabot Head through Medina Sandstone in well API# 3415123662. This interval creates a trough in the middle with positive events at the top and bottom.

4.5.5 Well API # 3416923438

Well API # 3416923438 (Figure 35) is 11 miles south of the center of the seismic reflection survey (Figure 1). This well is very similar to API# 3415123662. Both of the wells do not extend more than 30ft into the Queenston. In addition the logs all look very similar in each well. One of the biggest differences lies in the synthetic traces. In API # 3416923438 the sidelobe of the Packer Shell does not appear to extend much farther than the Medina, whereas API# 3415123662 does.

The signal from basal surface of the Packer Shell is the dominant component of the synthetic trace in this in this portion of the well. In addition to this there is little

interference from any of the other units. The only other interference that is significant is from the bottom of the White Clinton. This well appears to be one of the more pure wells because of the small amount of interference. This well appears to be free of major velocity transition zones and it also is not under the influence of reflectors below.

In the isolation model of the Packer Shell (Figure 36), the large negative trough is represented with the sidelobe beginning at the Red Clinton. The response of the Clinton interval and surrounding units (Figure 37) creates a negative amplitude event with a positive amplitude event both above and below. This signature interacts with the Packer Shell events by broadening the basal Packer Shell trough. Much of the sidelobe is summed out and any remaing effects of the sidelobe can only be seen at the Medina Sandstone. In contrast to well API# 3415123662, the Packer Shell in this well does not have a broadened trough. This is likely a result of the Packer Shell in API# 3415123662 not being as homogenous as the Packer Shell in API # 3416923438.

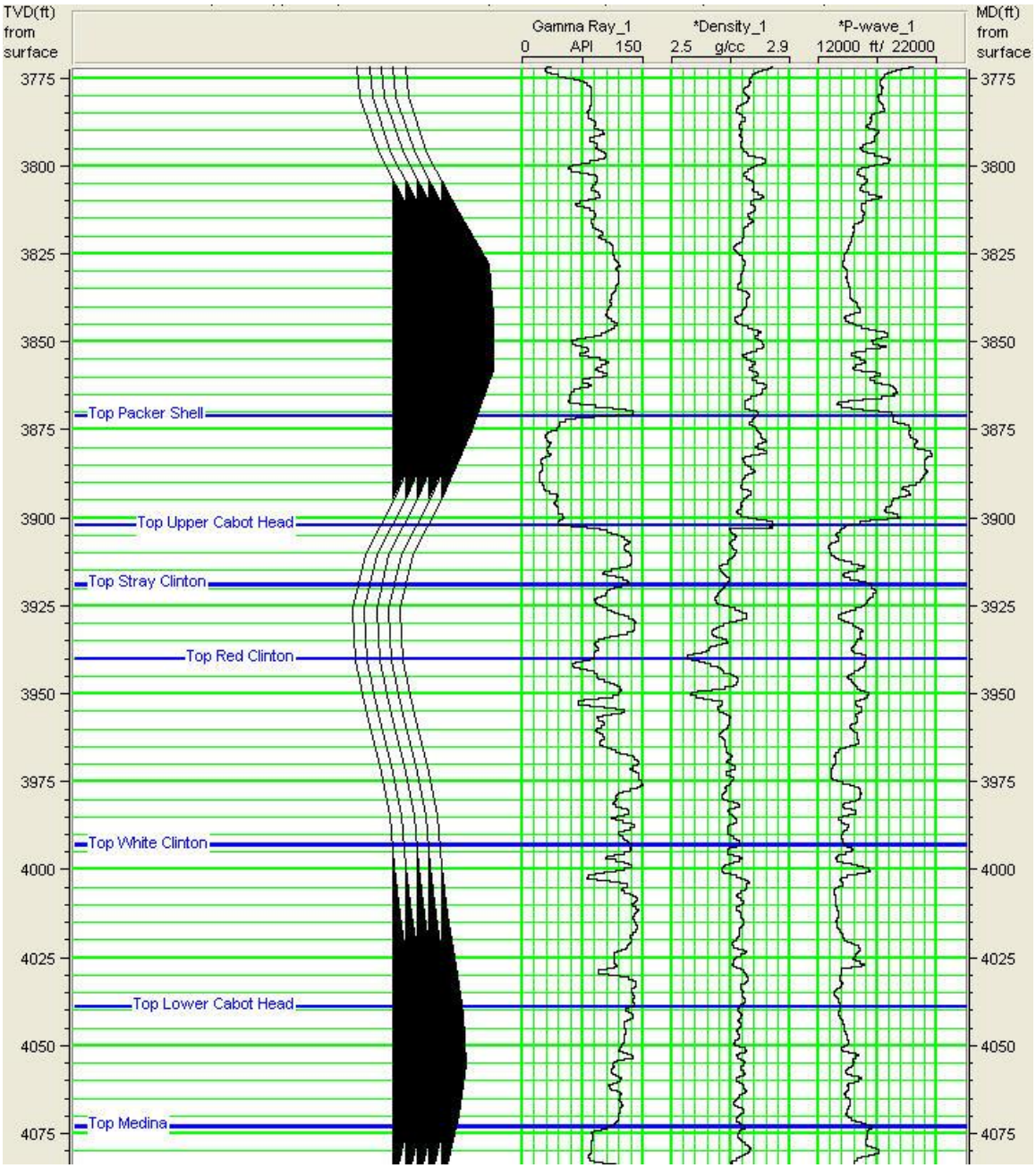

Figure 35. Above is a portion of the synthetic traces and gamma ray, density and velocity logs from well API # 3416923438. This well does not extend deep enough to reveal the effects of the Cincinnati Group. This well does not show signs of broadening in the positive time Packer Shell sidelobe.

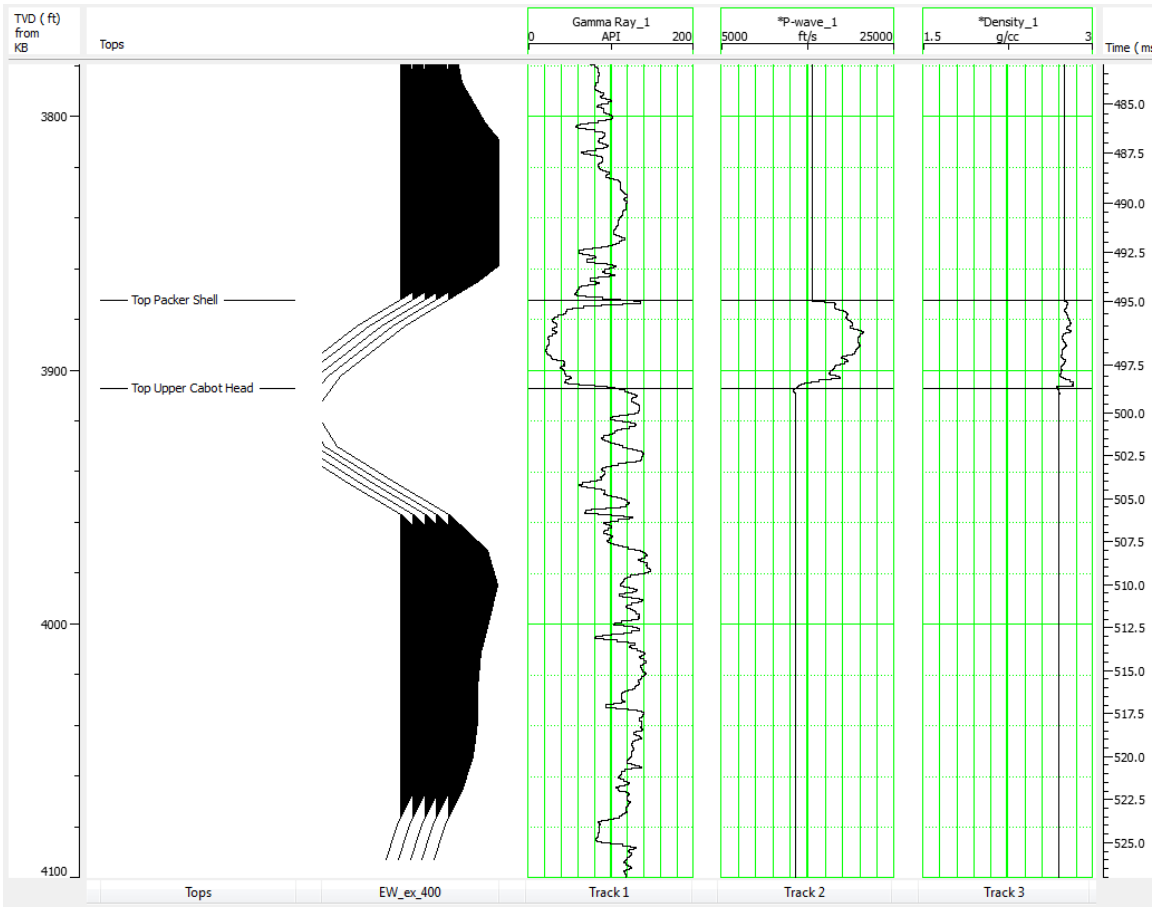

Figure 36. Isolation model of the Packer Shell in well API# 3416923438. The high amplitude through from the basal Packer Shell is present along with the sidelobe.

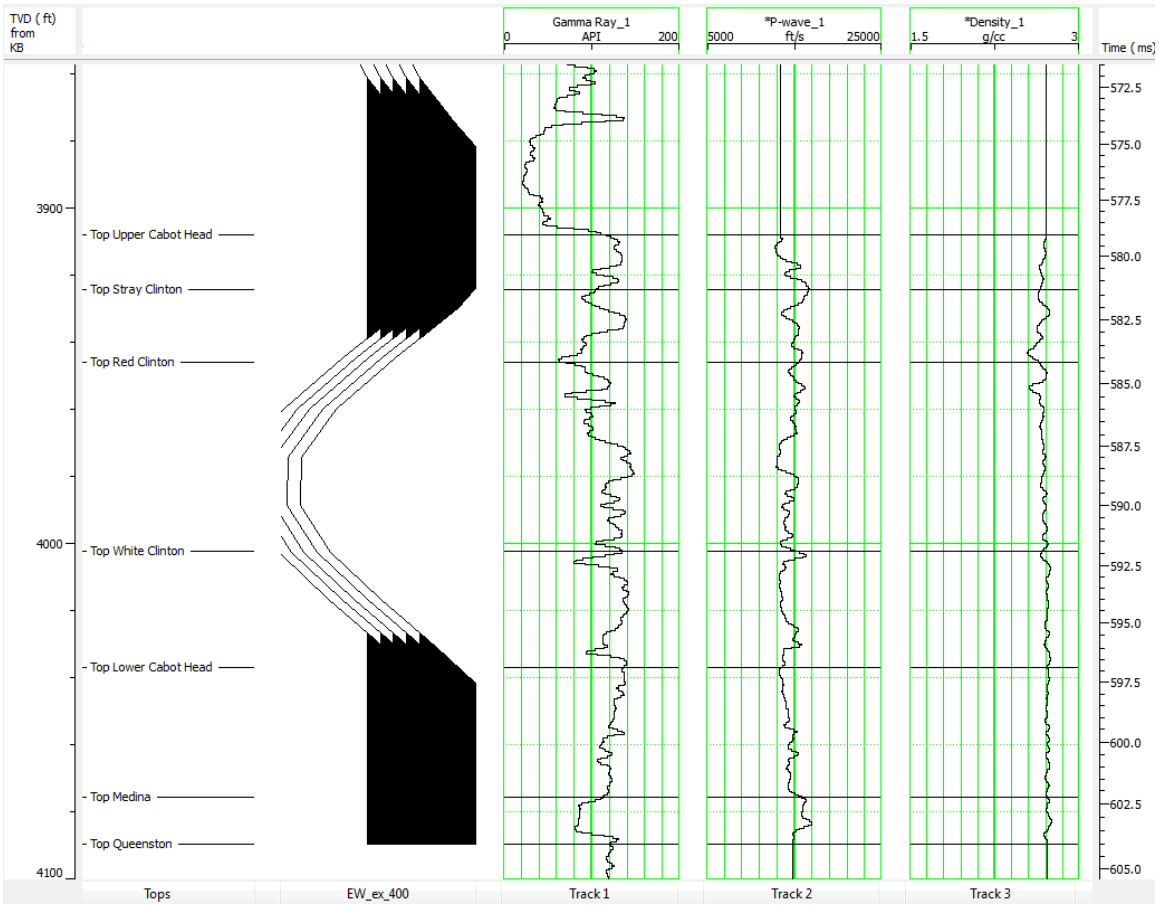

Figure 37. Isolation model of the Upper Cabot Head through Medina Sandstone in well API# 3416923438. This interval creates a trough in the middle with positive events at the top and bottom.

4.5.6 Well API# 3416923437

Well API# 3416923437 (Figure 38) is about 11 miles south of the center of the seismic reflection survey (Figure 1). It appears to have some high density high velocity zones in the Red Clinton. This is occurring at a portion of the logs that the synthetic trace, although similar to API #'s 3416912438 and 3415123662, appears a more elongated. This is the effect of the Medina Sandstone. There is also a large negative reflection coefficient in the Upper Cabot Head corresponding to a relatively high velocity and low density. This is occurring at the trough of the basal Packer Shell reflection.

The gamma ray log indicates extra sandstones within the Red Clinton. These additional sandstones correlate with large reflection coefficients. These spikes in reflection coefficient may be responsible for creating interference leading to the apparent elongation of the Packer Shell signature. This could also be contributing to the extension of the sidelobe past the Medina Sandstone. On the other hand, this is a well that does not penetrate deep enough for us to see any interference effects from reflectors within the Queenston.

In the isolation model of the Packer Shell (Figure 39), the large negative trough is represented with the sidelobe beginning at the Red Clinton. In this case the sidelobe of the Packer Shell is broadened. The response of the Clinton interval and surrounding units (Figure 40) creates a negative amplitude event with a positive amplitude event both above and below. This signature interacts with the Packer Shell events by cancelling the upper portion of the Packer Shell's broadened sidelobe. This interaction results in a broadened trough associated with the Packer Shell and a sidelobe that has been shifted downward in the well.

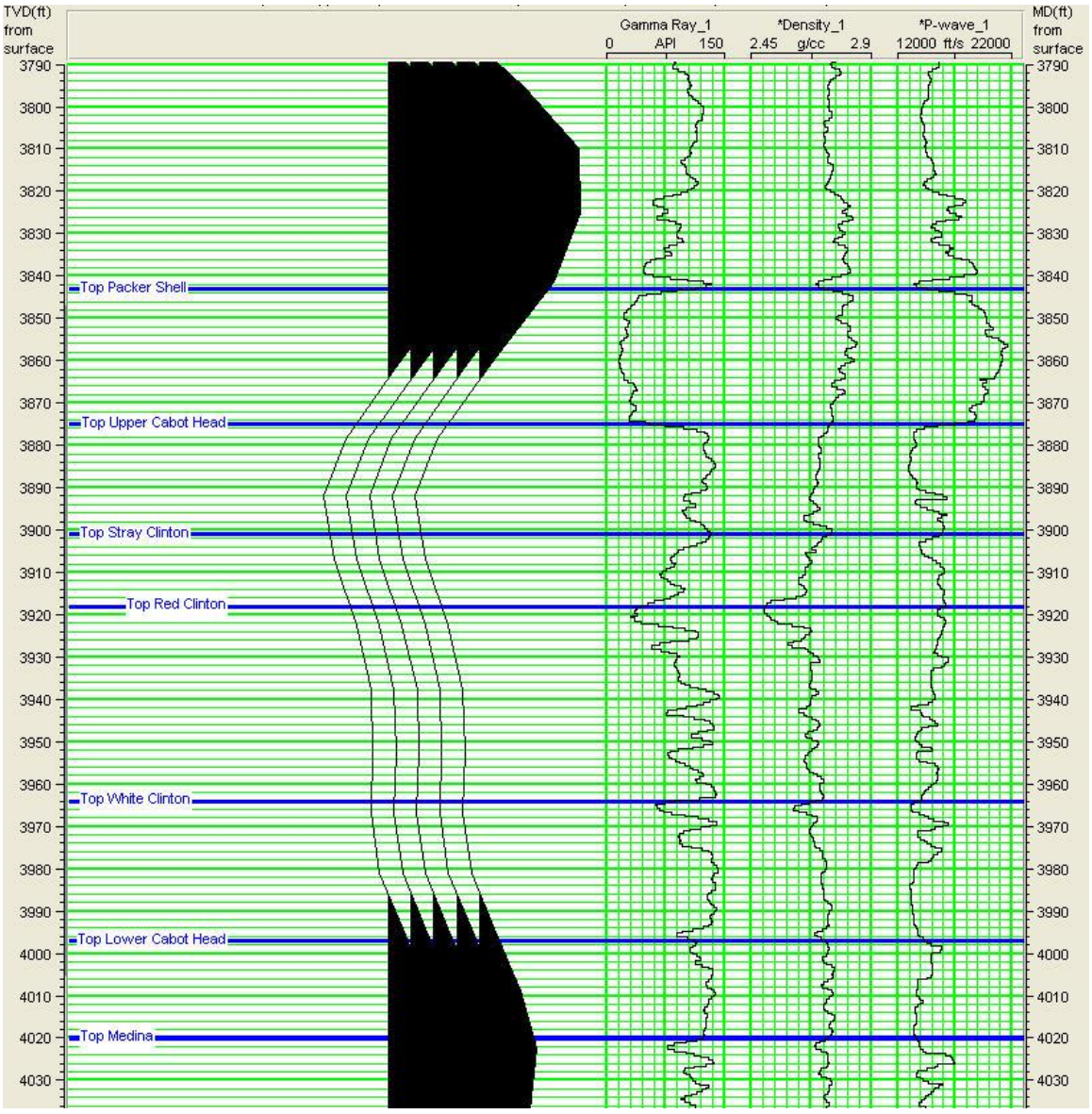

Figure 38. Above is a portion of the synthetic traces and gamma ray, density and velocity logs from well API# 3416923437. This well does not extend deep enough to reveal the effects of the Cincinnati Group. This well does not show signs of broadening in the positive time Packer Shell sidelobe.

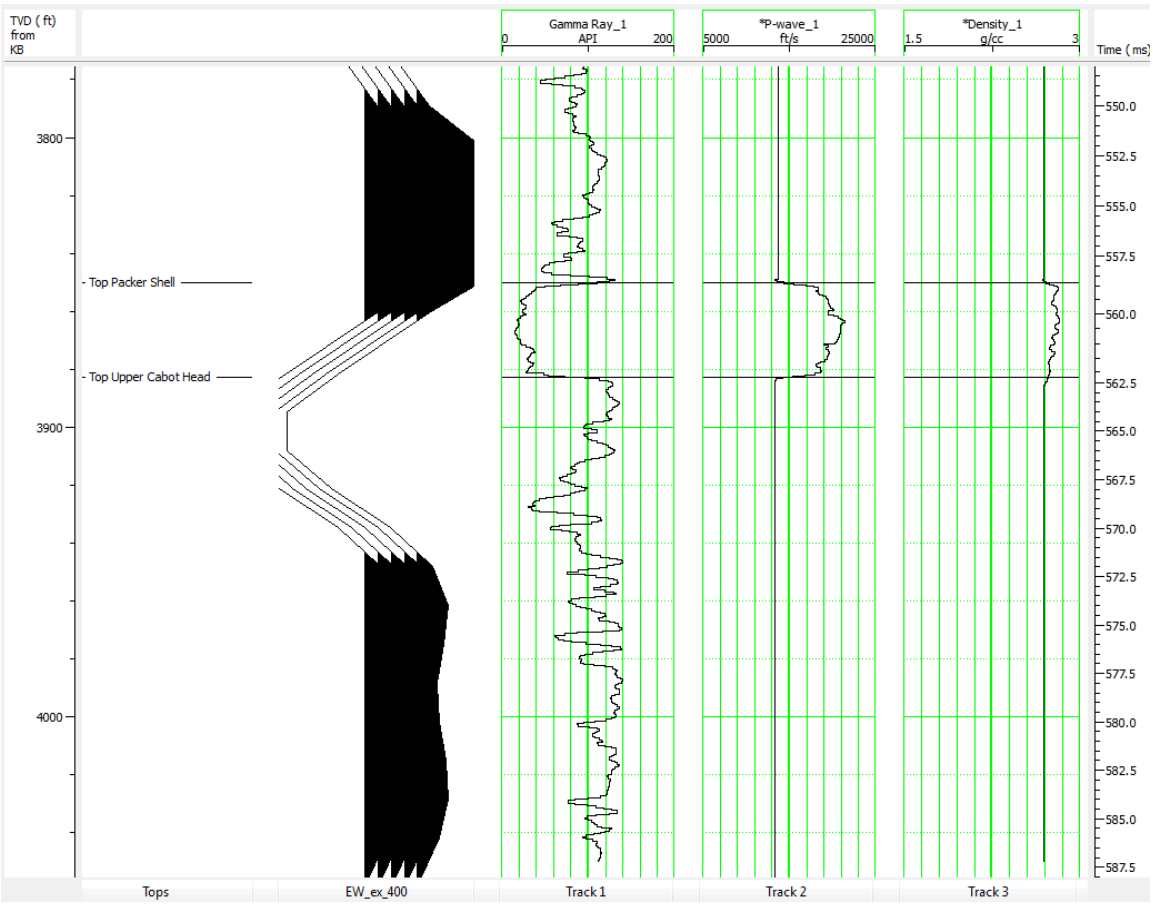

Figure 39. Isolation model of the Packer Shell in well API# 3416923437. The high amplitude through from the basal Packer Shell is present along with the sidelobe.

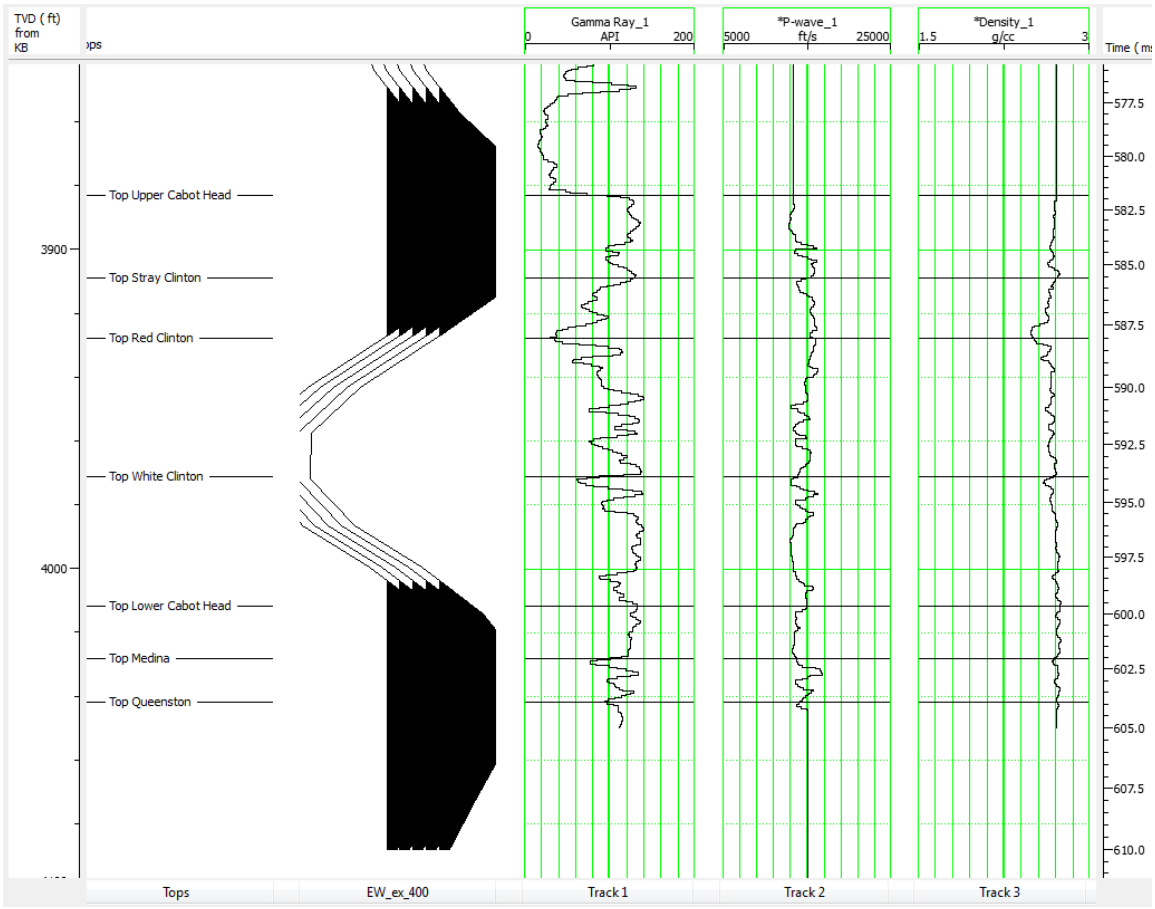

Figure 40. Isolation model of the Upper Cabot Head through Medina Sandstone in well API# 3416923437. This interval creates a trough in the middle with positive events at the top and bottom.

4.5.7 Well API# 3416923352

Well API# 3416923352 (Figure 41) is about 11 miles south of the center of the seismic survey (Figure 1). It does not fully penetrate the Queenston. Unlike well API #3415123662, this well shows the sidelobe of the Packer Shell extending only to the top of the Queenston. There is an additional, although very small positive amplitude event before the primary sidelobe of the Packer Shell. This event seems to occur at the same depth as a high velocity portion of the coarsening upward sequence within the Red Clinton. The sandstone intervals of the Clinton are shown as low density, yet high velocity zones.

The unexpected positive amplitude event may indicate interference from sandstone intervals in the Clinton. This could be a direct signal from the Clinton but, I do not see this behavior in the seismic sections collected. If this alteration of the Packer Shell sidelobe was observed in the seismic data, it would be reasonable to interpret this as the Clinton interval.

In the isolation model of the Packer Shell (Figure 42), the large negative trough is represented with the sidelobe beginning at the Red Clinton. In this case the sidelobe of the Packer Shell is broadened. The response of the Clinton interval and surrounding units (Figure 43) creates a negative amplitude event with a positive amplitude event both above and below. This signature interacts with the Packer Shell events by nearly completely canecelling the upper portion of the Packer Shell's broadened sidelobe. This interaction results in a broadened trough associated with the Packer Shell and a sidelobe that has been shifted downward in the well.

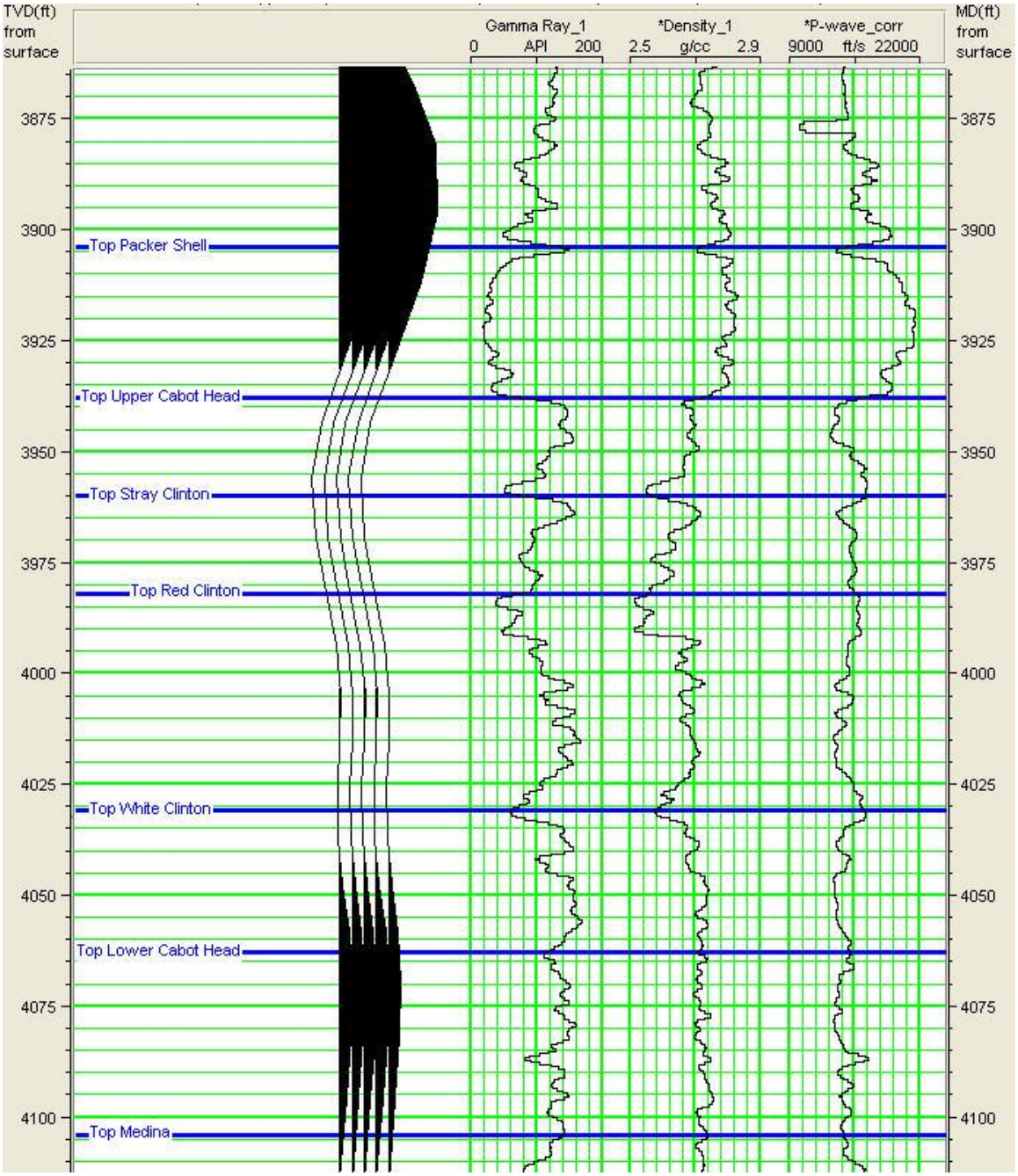

Figure 41. Above is a portion of the synthetic traces and gamma ray, density and velocity logs from well API# 3416923352. This well does not extend deep enough to reveal the effects of the Cincinnati Group. This well does not show signs of broadening in the positive time Packer Shell sidelobe.

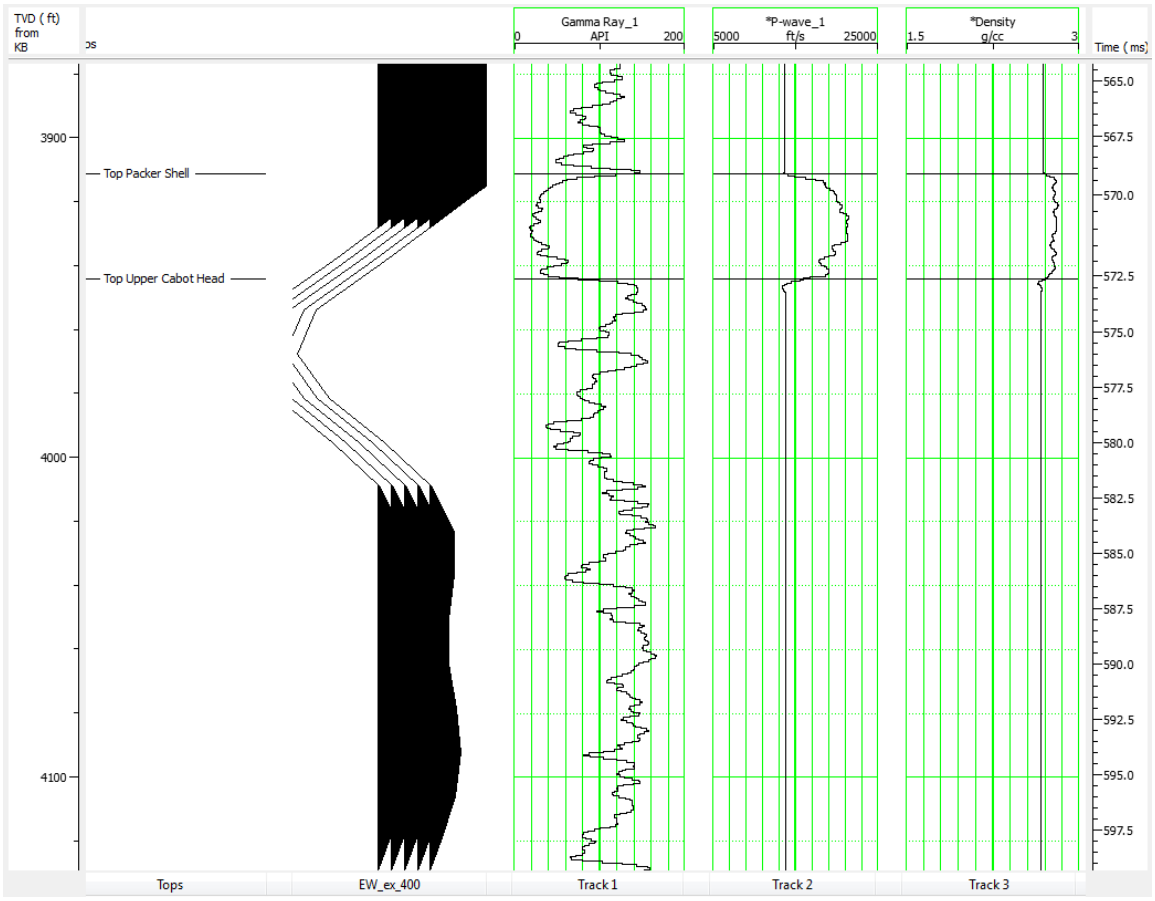

Figure 42. Isolation model of the Packer Shell in well API# 3416923352. The high amplitude through from the basal Packer Shell is present along with the sidelobe.

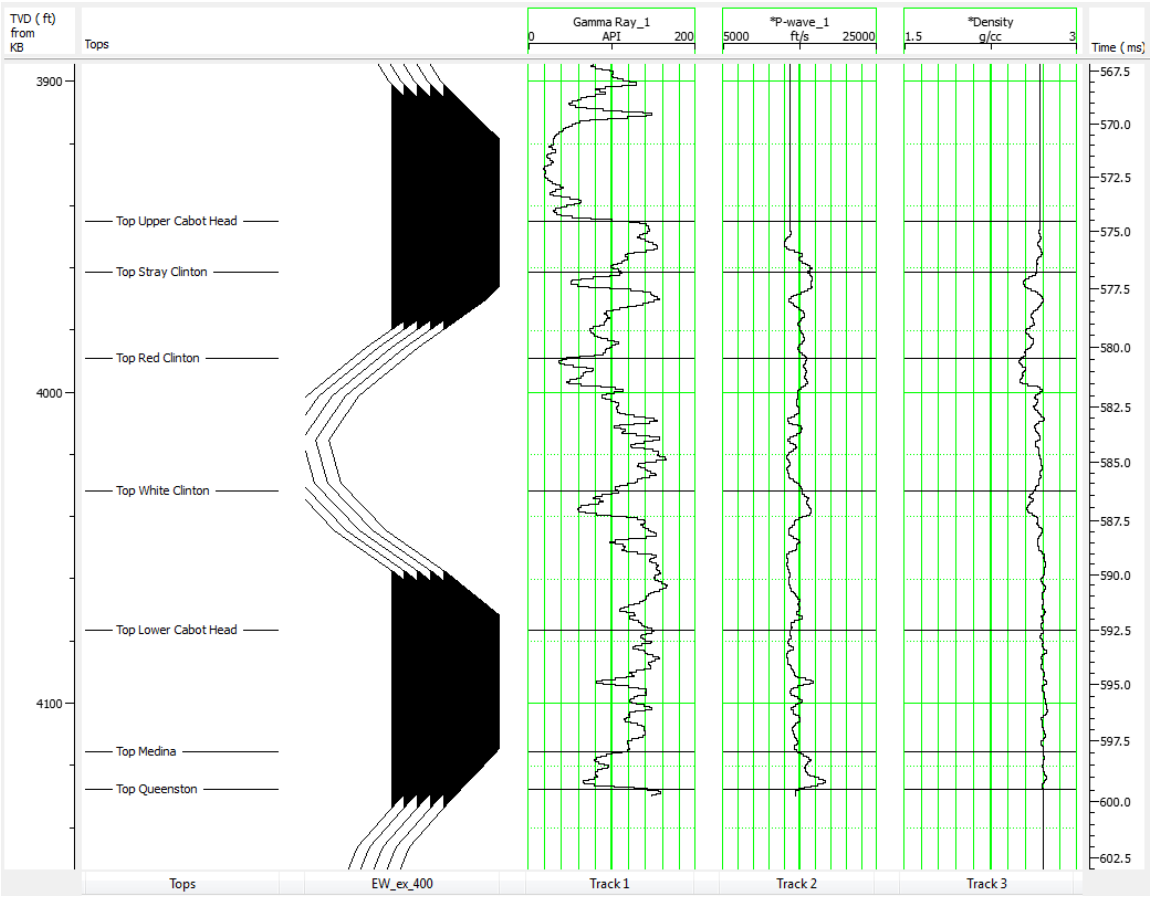

Figure 43. Isolation model of the Upper Cabot Head through Medina Sandstone in well API# 3416923352. This interval creates a trough in the middle with positive events at the top and bottom.

4.5.8 Well API # 3416924931

Well API # 3416924931 (Figures 44—46) this well is 13 miles west of the center of the seismic reflection survey (Figure 1). This well does extend into the Queenston but it also shows the same extra positive event before the primary sidelobe of the Packer Shell. In API# 3416923352 there are high density, and high velocity zones in the Red and White Clinton. On the other hand in API # 3416924931 there is a similar zone only in the White Clinton. There is an extra positive amplitude event occurring before the traditional sidelobe of the Packer Shell.

The presence of only one high density, high velocity event in the Clinton may reduce interference of the extra positive amplitude event making it appear much larger in this well. In addition the caliper log (Figure 45) shows washouts correlating with the extra event, suggesting data in the density and/or velocity logs could be affected. Well API # 3416924931 also shows the interbedded carbonates creating a reflection that correlates with those that are being attenuated by gas shadows in the seismic sections.

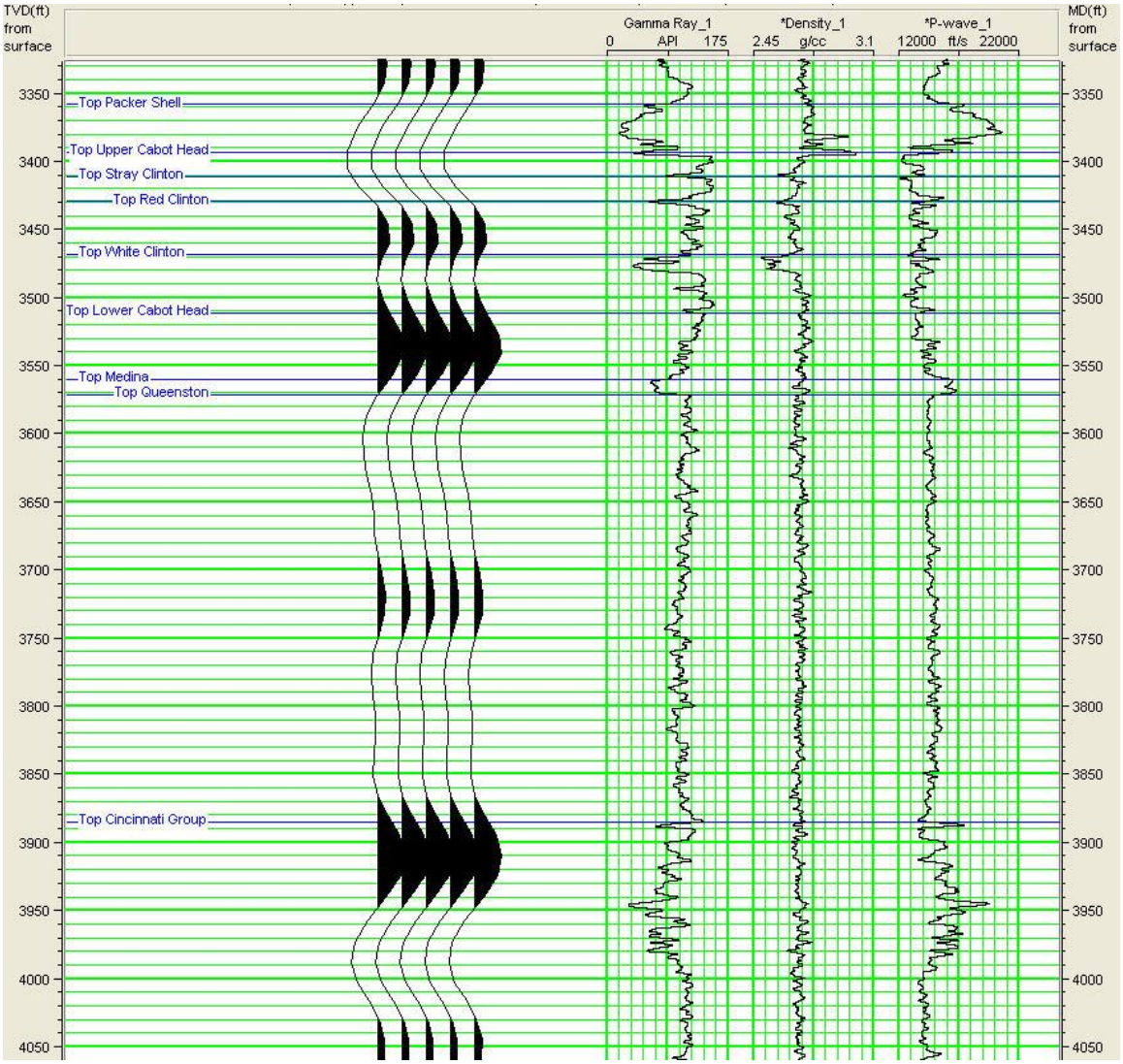

Figure 44. Above is a section of the synthetic traces and gamma ray, density and velocity logs from well API # 3416924931. The synthetic traces show unusual behavior in the Packer Shell-Clinton interval.

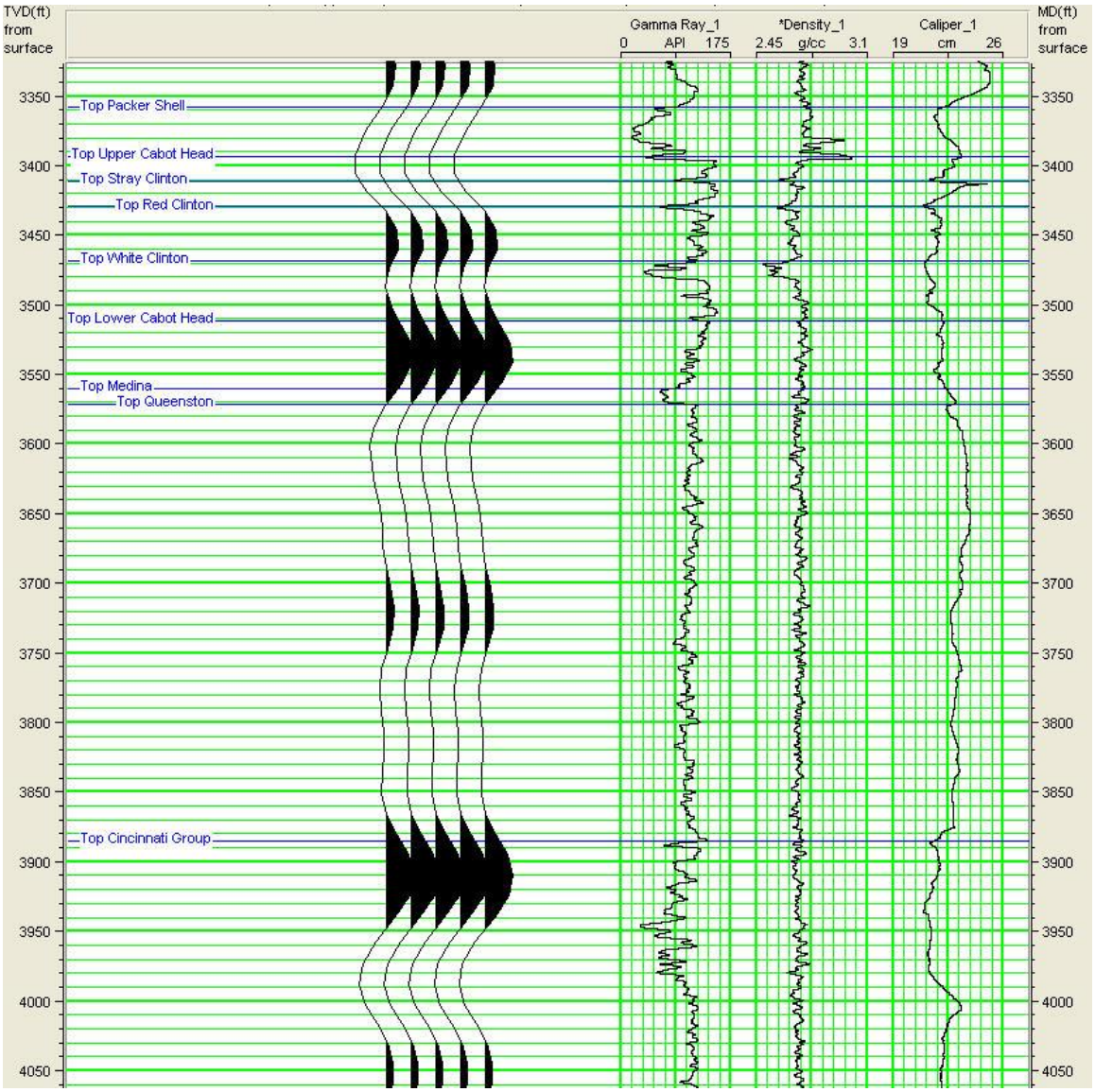

Figure 45. Above is a section of the synthetic traces and gamma ray, density and caliper logs from well API # 3416924931. Variability in the caliper log indicates washouts. Washouts cause bad readings in the density and velocity logs. This is likely causing the unusual behavior in the synthetic trace from the Packer Shell-Clinton interval.

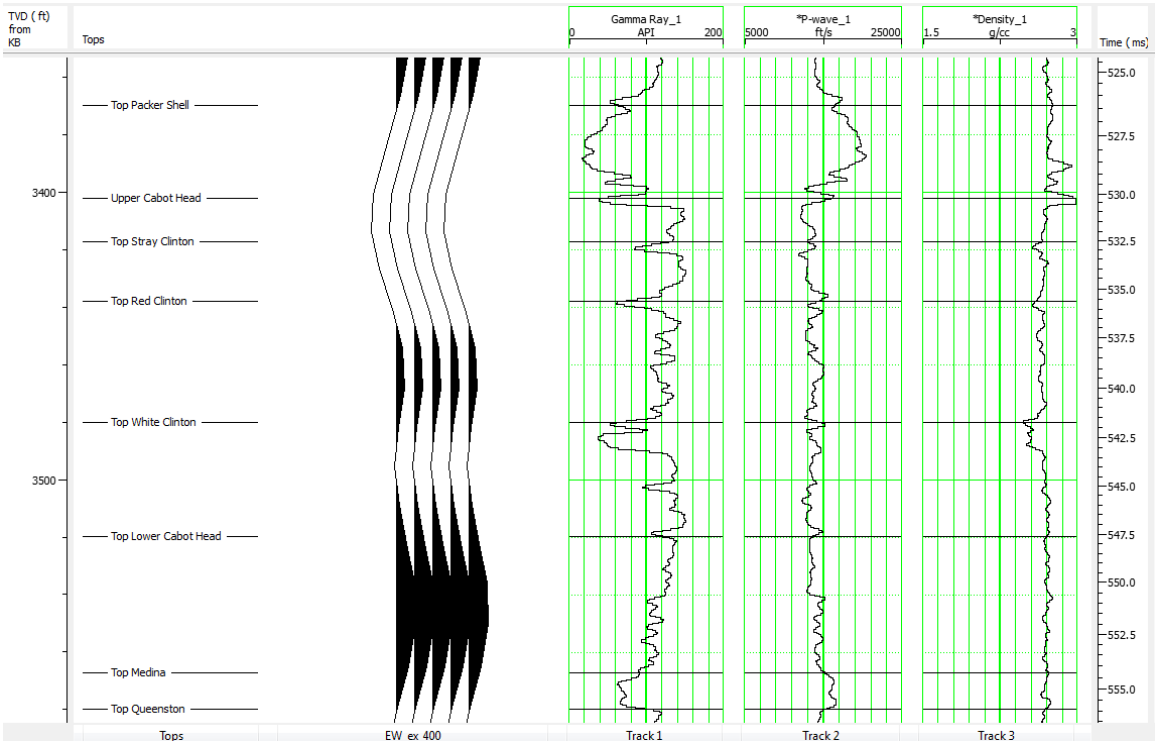

Figure 46. Above is the Packer Shell through the Medina Sandstone in well API# 3416925010. Shown from left to right are the synthetic traces, gamma ray log, seismic velocity log, and density log.

4.6 Velocity Transition Zones

It is difficult to interpret the seismic response of the Clinton interval with the standard convolutional model. The interval's deltaic nature provides a level of intricacy that complicates the stratigraphy. In response to relative sea level, depositional environments are shifted leading to sometimes gradual changes in lithology. One of these complexities includes velocity transition zones. Alfred Wolf pointed out that reflections do not only occur from sharp discontinuities, but also from transition layers (Wolf, 1937). In the time since Wolf's work, research has found that transition layers produce frequency filtering effects (Liner, 2012).

Although the velocity transition zones are thinner than the examples of Liner, 2012, there still may be a frequency filtering effect by stacking these smaller velocity transition zones, modeling of complex reflection coefficients could be integral in learning new things about the seismic response of the Clinton interval. Additional processing of the seismic data could make a frequency analysis more meaningful through deconvolution and frequency enhancement.

Chapter 5: Conclusions

The seismic attributes of the Clinton interval in conjunction with the map of initial production give me confidence that I am observing a gas shadow on both seismic lines collected over the Gabor gas storage field. The attenuation of amplitudes, low average frequencies, instantaneous frequency anomalies, and wavelet packet transform anomalies all correspond to areas on or near high initial production. Sidelobe modification appears to correlate with high initial production and gas shadows. Although gas shadows occur in or very near to zones of high initial production, and lack of sidelobes is only found near gas shadows, a clear link or explanation has not been established between the two.

Broadening of the basal Packer Shell sidelobe appears to be a separate effect from the gas shadows based on the seismic attributes. The average frequencies are slightly higher, there is no instantaneous frequency anomaly, and wavelet packet transform has variable character, always different from the gas shadows. Traces modeled with well log data show broadening could be a direct result of variations within the White Clinton. Another possible cause of the broadening could be velocity transition zones and complex reflection coefficients yielding the broadened response directly. This behavior is only observed adjacent to gas shadows in the data. If the data were to have been taken while the reservoir was empty, it is possible that this broadened behavior would fill the zones that would otherwise be attenuated by gas.

It is unclear, however, if the broadening is associated with the gas shadow. Although they do occur adjacent to each other, this analysis does not prove a relationship. I am limited with 2D data collected only over a fully charged gas storage field. With additional processing, some 3D coverage may be able to be achieved near the intersection of the lines. Given a full 3D volume over a fully charged and empty gas storage field, different conclusions could be reached. In addition, detailed modeling of frequency dependent complex reflection coefficients related to velocity gradients could give insight into the reservoir potential of these zones. In future exploration efforts in the Clinton interval perhaps broadening of the Packer Shell sidelobe should be investigated further for the effect of a known gas filled reservoir to determine if the broadening disappearance is diagnostic.

Synthetic traces of nearby wells show a variety of signals surrounding the Clinton interval. The Packer Shell response, above the Clinton interval, is common to each log. Below the Clinton interval, the Cincinnati Group is the next major reflector and it has been determined to be the event that is attenuated by the gas shadows. Between the Packer Shell and the Cincinnati Group, washouts caused problems in wells that penetrated the Queenston.

The isolation models containing synthetic traces for the Packer Shell only, or the Upper Cabot Head through the Medina Sandstone show distinct patterns. The Packer Shell creates a large negative amplitude response with a broad sidelobe which generally extends to the Medina Sandstone. The Upper Cabot head through the Medina Sandstone create a negative reflection with the trough around the Red and White Clinton. This response is also associated with positive sidelobes above and below.

One well showed broadening of the Packer Shell sidelobe that appears to be caused by a high velocity high density spike in the White Clinton. The isolation models show these spikes lead to a smaller negative amplitude created by the interval from the Upper Cabot Head to the Medina Sandstone. When added to the Packer Shell response the sidelobe was broadened. This broadening resembles the broadening of the Packer Shell sidelobe near the gas shadow in the seismic data. In addition, the well logs indicate the White Clinton also has very low porosity implying this response my not be conducive to a good hydrocarbon reservoir.

Another response that was observed was the development of the Medina Sandstone reflector at the bottom end of the Packer Shell sidelobe. This too could be a contributing factor to the sidelobe modification. The well logs do provide some mechanisms for broadening of the Packer Shell sidelobe. It remains unclear however, what effects the presence of gas has had on this response.

References

BARNES, A. E. (2007) Redundant and useless seismic attributes. *Geophysics.* 72 (3). p.33–38.

BEY, S. M. (2012) *Reservoir Characterization and Seismic Expression of the Clinton Interval over Dominion's Gabor Gas Storage Field in North-East Ohio.* Master of Science Thesis. Wright State University.

BRETT, C. E.; GOODMAN, W. M.; LoDUCA, S.T. (1990) Sequences, cycles, and basin dynamics in the Silurian of the Appalachian Foreland Basin. *Sedimentary Geology.* 69. p. 191–244.

BROWN, A. R. (1996) Seismic attributes and their classification. *The Leading Edge.* October. p. 1090.

CASTAGNA, J.P.; SUN, S.; SIEGFRIED, R.W. (2003) Instantaneous spectral analysis: Detection of low-frequency shadows associated with hydrocarbons. *The Leading Edge.* February, p. 120–127.

CASTLE, J. W. (1998) Regional sedimentology and stratal surfaces of a Lower Silurian clastic wedge in the Appalachian Basin foreland basin. *Journal of Sedimentary Research.* 68 (6). p. 1201–1211.

CASTLE, J. W. (2001) Appalachian basin stratigraphic response to convergent-margin structural evolution. *Basin Research*. 13. p. 397–418.

CHEN, Q.; SIDNEY, S. (1997) Seismic attribute technology for reservoir forecasting and monitoring. *The Leading Edge.* May.

COIFMAN, R.R., MEYER, Y., QUAKE, S. and WICKERHAUSER, M.V. (1989) Signal processing and compression with wave packets: Proceedings of the International Conference on Wavelets, Marseille, Meyer, Y. Ed., Masson, Paris.

COOGAN, A. H. (1996) Ohio's surface rocks and sediments. Feldmann, R. M.; Hackathorn, M. (Eds). In: *Fossils of Ohio.* Ohio Division of Geological Survey Bulletin 70.

DEIGHAN, A. (1997) *Applications of wavelet transforms to the suppression of coherent noise from seismic data in the pre-stack domain*, PH. D Dissertation. University of Glasgow.

GOERTZ, A.; CIEŚLIK, K.; HAUSER, E; WATTS, G; McCROSSIN, S.; ZBANIK, P. SEG Technical Program Expanded Abstracts 2011. p. 1488-1492.

KELTCH, B. (1985) Why I use geology for Clinton Exploration? *The new Clinton collection, 1985*.p. 19–42

LINER, C. L. (2012) Elements of seismic dispersion: A somewhat practical guide to frequency-dependent phenomena. *2012 Distinguished Instructor Short Course.* 15.

PEPPER, J. F.; deWITT, W.; EVERHART, G. M. (1953) The "Clinton" sands in Canton, Dover Massillon, and Navarre Quadrangles, Ohio. *Oil and Gas Geology of the "Clinton" Sands of Ohio.* U.S. Geological Survey Bulletin 1003–A

RYDER, R. T.; TRIPPI, C. S.; CRANGLE, R. D. JR.; HOPE, R. S.; ROWAN, E. L.; LENTZ, E. E. (2012) Geologic cross section *C–C'* through the Appalachian basin from Erie County, north-central Ohio, to the Valley and Ridge province, Bedford County, south-central Pennsylvania: U.S. Geological Survey Scientific Investigations Map 3172, 2 sheets, 70-p. pamphlet.

SHERIF, R. E. (2002) *Encyclopedic Dictionary of Applied Geophysics*, ed. Scherrer, E. F. Society of Exploration Geophysicists, Tulsa, OK.

TANER M. T.; KOEHLER, F.; SHERIFF, R. E. (1979) Complex seismic trace analysis. *Geophysics.* 44 (6). P. 1041–1063.

TANER, M. T. (2001) Seismic attributes. *CSEG Recorder.* September . p. 48-56.

WOLF, A. (1937) The reflection of elastic waves from transition layers of variable velocity. *Geophysics.* 2 (4). p.357–363.

WYTOVICH, D. A. (2010*) Reservoir analysis of the Clinton interval in Stark and Summit Counties, Ohio*. Master of Science Thesis. Wright State University.